Title: Development of sensor systems for application in cryopreservation

Name: Jahanbeen Jahangir

Development of Sensor Systems for Application in Cryopreservation

by

JAHANBEEN JAHANGIR

A thesis submitted to the University of Bedfordshire in partial fulfilment of the requirements for the degree of Doctor of Philosophy

Institute of Biomedical and Environmental Science and Technology

University of Bedfordshire Luton

250 Butterfield Great Marlings

Luton Bedfordshire UK

LU2-8DL

December 2014

Development of Sensor Systems for Application in Cryopreservation

JAHANBEEN JAHANGIR

Abstract

This work describes the development, validation and application of sensor systems to monitor phase transition events of cryoprotectant mixtures in samples and cryopreservation profiles and post-thaw recovery of *Lactobacillus delbrueckii* subsp. *bulgaricus* CFL1.

Ice nucleation and glass transition (Tg) temperatures influence cell viability during cryopreservation. Knowledge of these phase changes for cryoprotectant mixtures is an essential step in optimising cryopreservation protocols for cell survival. Differential scanning calorimetry (DSC) is used to determine Tg, but the expensive nature of such instrumentation limits its widespread use. Cost-effective sensor systems have been designed to monitor ice-initiation and Tg events in small volume samples of cryoprotectants solutions. Tg values were measured for glycerol, sucrose and Me_2SO (with and without NaCl supplement and ice-nucleators) in cryotubes and cryostraws, using temperature and screen-printed impedance sensors. The effect of changes to ice-initiation temperature on Tg was also investigated at different cooling and warming rates by using a Grant Asymptote (EF600) controlled rate freezer. The resulting Tg values obtained by single-channel transition monitoring system (TMS 1) were not significantly different from the values obtained by DSC reported in the literature. However multiple channelled transition monitoring system (TMS 2) requires further circuit modification and multiple screen-printed temperature probes to study the phase-change temperatures and to determine transition events in more than one sample at a time.

The lactic acid bacterium (LAB) *Lactobacillus delbrueckii* was investigated as a model system to monitor the effect of different cryopreservation protocols on post-thaw cell metabolic activity. An important parameter for monitoring the post-thaw quality of LAB for starter culture preparation is the change in pH of the culture medium during incubation at 40 ^{o}C. Glass pH combination electrodes are the most common and widely used sensors. However, they are fragile, must be conditioned before use and are not disposable. An alternative to conventional glass electrodes are screen-printed carbon-metal electrodes. Different percentage mixtures of ruthenium and antimony pastes were tested and 54.5% carbon-antimony electrodes gave the best sensitivity and consistency in potentials at fixed pH with a screen-printed salt-bridged Ag/AgCl reference. LAB cultures were cryo-preserved at very rapid, moderate and very slow cooling rates and their post-thaw metabolic activity after overnight incubation in MRS broth was determined using screen-printed pH electrodes. Back to back testing with conventional glass pH sensors was performed to compare responses. Results indicated that early ice-initiation (by means of nucleators) prevents the cells from extensive dehydration (during cooling) and enables maximum post-thaw recovery after incubation (due to equilibrium ice formation and ice melting). In future, screen-printed pH sensors require development with integrated salt-bridged Ag/AgCl reference to make it robust in signalling response.

The availability of low cost, disposable, non-fragile sensors and sensor systems to monitor transition events allows the determination of Tg of cryopreservation media during both cooling and warming cycles. A combined screen-printed (impedance + temperature) sensor is proposed for this purpose. A combined screen-printed (pH + reference) sensor would allow the monitoring of metabolic activity in post-thaw and fresh starter cultures of LAB. At present the salt-bridged pH reference is manually attached to the screen-printed pH working electrode but it requires further modifications to the method of attachment. The two sensor systems would enable optimisation of cryopreservation protocols for LAB and could enable such measurements to become routine at commercial scale.

ACKNOWLEDGEMENTS

All praise to Almighty Allah, who is extremely kind and humble to all human beings. My gratitude is attributed to Almighty Allah.

I wish to thank Professor David Rawson, my director of studies, for his valuable criticisms, suggestions, constant encouragement and freely devoting his time to discuss and develop this work with me. His guidance has made me fulfilling my dream of becoming a research scientist and a happy person.

I am especially grateful to Dr. Barry Haggett and Dr. Roberto Andres my supervisors, for their incredible guidance and support in sensor design.

As well as, I owe a big thanks to John Morris my external supervisor a St .John's Innovation Centre UK. Also, my humble recognition to Fernanda Fonseca at INRA France, for her initial guidance in cell culturing and providing me freeze-dried samples of LAB cultures.

Most importantly, I am grateful to my loving husband Dr. Muhammad Nabeel Asghar who has always supported me, helped me and stood beside me through thick and thin.

I am thankful to my dearest mother and father, who are the true inspiration of my life, who offer me ample of opportunities to enable me to learn extensively and purposefully. I am thankful to my whole family especially my siblings, maternal uncles, aunts, cousins and in laws who always worried about me and took special care of me.

In the end, I want to mention about my dearest friends who were always with me whenever I need them. Thanks a lot all of you for being the inspiration, motivation and the beacon of hope for me.

DECLARATION

I declare that this thesis is my own unaided work. It is being submitted for the degree of Doctor of Philosophy at the University of Bedfordshire.

It has not been submitted for any degree or examination in any other University.

Name of candidate: Jahanbeen Jahangir Signature:

Date: 14 December 2014

DEDICATION

I dedicate this work to my beloved father

Dr. Jahangir Shuja (Late)

His love, guidance and appreciation has made me able to fulfil my dream of becoming a scientist and a better person.

LIST OF CONTENTS

LIST OF CHAPTERS

CHAPTER 1

CHAPTER 2

CHAPTER 6

LIST OF FIGURES

LIST OF TABLES

LIST OF APPENDIX

LIST OF ABBREVIATIONS

AC	Alternating Current
AI	Artificial Insemination
BNC	Bayonet Neill–Concelman
CMC	Cryoelectron Microscopy
CPA	Cryoprotectant Additive
CV	Cyclic Voltammetry
DC	Direct Current
DEA	Dielectric Thermal Analysis
DMTA	Dynamic Mechanical Thermal Analysis
DNA	DeoxyriboNucleic Acid
DSC	Differential Scanning Calorimerty
DSC	Differential Scanning Calorimeter
DTA	Differential Thermal Analysis
ER	Electrical Resistance
ETA	Electrical Thermal Analysis
IIF	Intracellular Ice Formation
IMS	Impedance Monitoring System
IVF	In Vitro Fertilisation
LAB	Lactic Acid Bacteria
Me_2SO	Dimethyl Sulfoxide
MRS	De Man, Rogosa and Sharpe
NB	Nutrient Broth
NMR	Nuclear Magnetic Resonance
PC	Personal Computer
PCB	Printed Circuit Board
Pt-RTD	Platinum Resistance Temperature Detector
RCF	Relative Centrifugal Force
RNA	RiboNucleic Acid

RPM	Revolutions Per Minute
RTD	Resistance Temperature Detector
Tg	Glass Transition
TMS	Transition Monitoring System
USB	Universal Serial Bus

Chapter 1

Introduction

1 Statement

Cryopreservation is widely used to preserve biological samples in the presence of suitable cryoprotectants (CPAs). During cryopreservation, the solution of CPAs undergoes thermodynamic changes, altering the state of the solution from liquid to solid (ice) or glass (amorphous solid) phase. These phase changes vary with modifications of cooling rates and ice nucleation temperatures, and are important as they can influence survival of biological samples.

1.1 Background to cryopreservation

Low temperature biology plays an important role in the conservation of biological components such as stem cells, tissues, organs and organisms (Appelbaum et al., 2004, Nicolas et al., 2007). Two principal freezing techniques, slow and rapid cooling, are adopted to cryopreserve living materials. Rapid cooling involves vitrification; where cells are treated with high concentrations of cryoprotectants and plunged into liquid nitrogen to form a glass without ice crystallisation; whereas during slow cooling in diluted concentrations of cryoprotectants at slow rates of temperature change, solutions form ice and glass mixture. In both cases different

morphologies of ice and glass mixtures are obtained due to different CPA concentrations and loading procedures.

Cryopreservation has been used to preserve cells without harming their functionality or genetic structure over 60 years. Protocols need to be optimised in order to recover viable cells and to avoid stresses leading to cell death. Cryopreservation is performed at sub-zero temperatures in the presence of cryoprotectants. Cryoprotectants tend to perform their function at extremely low temperatures either by penetrating into the cells (permeating cryoprotectants) or protecting the cell surface (non-penetrating). Glycerol, dimethyl sulfoxide (Me_2SO), ethane diol and propane diol are the most common permeating cryoprotectants whilst lactose, raffinose, trehalose, sucrose and d-mannitol are non-permeating in nature. The use of high concentration of cryoprotectants increases the chance of osmotic and toxic damage. Therefore, it is necessary to develop reliable procedures to characterise phase behaviour of cryoprotectants and to reduce their toxicity effects. Phase behaviour refers to the determination of the viscosity encountered by the cells during freezing in the presence of cryoprotectants (Morris et al., 2006). Phase change allows the determination of the point of ice and glass formation in the mixture of CPAs. Determination of phase change events allows cell damage during prolonged cell storage at lower temperatures and post-thaw osmotic shock during warming of the sample to be minimised. Two key issues during cryopreservation are: (I) the avoidance of intracellular ice; and (II) the control of extracellular ice formation during freezing, which increases the solute concentration, resulting in osmotic imbalance. Intracellular ice crystals can cause membrane damage or puncture the cells; however extracellular ice crystals can cause mechanical stresses to membrane surfaces if cells are densely packed and ice crystals are formed inside the channels formed between the cell and ice crystals

(Parks and Graham, 1992). To avoid or control intracellular and extracellular ice-formation during cryopreservation, seeding process is sometimes introduced, either manually or by means of ice-nucleators, to control ice crystallization by inducing early ice formation in the CPA sample (before the sample is spontaneously nucleated) (see Section 1.5).

1.2 Phase changes in a liquid

A liquid or mixture of liquids may be transformed into supercooled, states at lower temperatures. During supercooling the liquid temperature decreases below its equilibrium melting point while maintaining its liquid state. As temperature falls the liquid transforms into solid (ice) water sequestration occurs and the unfrozen fraction becomes highly viscous and turns into glass over a small temperature range (Roozen et al., 1991). It has been demonstrated that the rate of cooling, the size of ice crystals and the process of recrystallization all have an impact on cell survival (Fonseca et al., 2006). The size of ice crystals and the degree of dehydration are both dependent on Tg (Morris et al., 2006). Tg is a point where water stops freezing and discontinuous change in the specific heat takes place (Roozen et al., 1991).

Factors affecting Tg

The concentration of cryoprotectants, sample volume, ice nucleation temperature and cooling and warming rates are key factors affecting Tg shifts (Morris et al., 2006, Fonseca et al., 2006).

1.3 Background to freezing mechanism

The timing and temperature of ice crystallization and glass formation are influenced by cooling rate and solute concentration. Viscosity plays an essential role during cryopreservation of cells, e.g. spermatozoa or red blood cells. Higher concentration of cryoprotectants and slow cooling rates make ice and glass mixtures that increase the diffusion distance. Diffusion distance allows determining the diffusion of water in freeze concentrated matrix at different linear cooling rates. The diffusion distance is increased due to uncontrolled solidification of the solution in extracellular matrix allowing the formation of isolated unfrozen matrix channels causing cells to face hyperosmotic conditions leading to cryoinjury. Thus rate of cooling (i.e. slow or fast) and ice nucleation temperature are important steps to be optimised in order to prevent cryoinjury of the cells (Fig 1.1). Rapid cooling can result in micro-ice crystals populating the glass (Morris et al., 2006). This is thought to result in a lowering of the Tg, and possibly leads to osmotic shock, due to the differences in cryoprotectant concentration between the cooling and warming periods, experienced by the cells. During cooling the concentration of CPAs is increased due to ice formation returning to its initial concentration during warming.

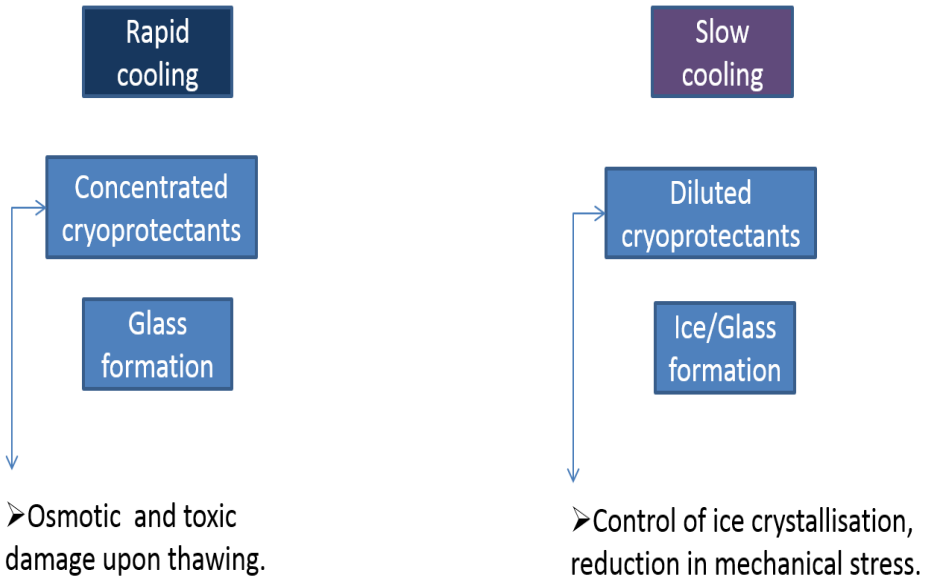

Figure 1.1: Slow and rapid cooling phenomenon. Arrows indicate the kinds of damage caused by concentrated and diluted forms of CPAs

Ice formation, ice nucleation and ice recrystallization are three different phenomena in the freezing mechanism of cryoprotectants mixtures. During slow cooling water starts to freeze extracellularly, increasing the viscosity of the mixture of cryoprotectants. A hypertonic condition is initiated causing cell dehydration. Water passes out the cells as non-frozen channels are created outside the cell membrane which controls diffusion rate of water and cryoprotectants (Morris et al, 2006). Further temperature reduction causes glass formation of non-frozen channels (Fig. 1.2). The reason for monitoring Tg temperatures of cryoprotectant mixtures (with/without seeding and additive) is to investigate: (a) point of ice initiation, glass formation and ice melting; (b) influence of cooling rate and seeding temperatures on ice/glass formation (Parks and Graham, 1992); (c) degree of cell dehydration (Morris et al., 2006) and; (d) identification of mechanism of cryoinjury and optimal preservation temperatures in the mixtures of cryoprotectants for

maximum cell survival (Smith et al., 2010, Appelbaum et al., 2004, Morris et al., 2006).

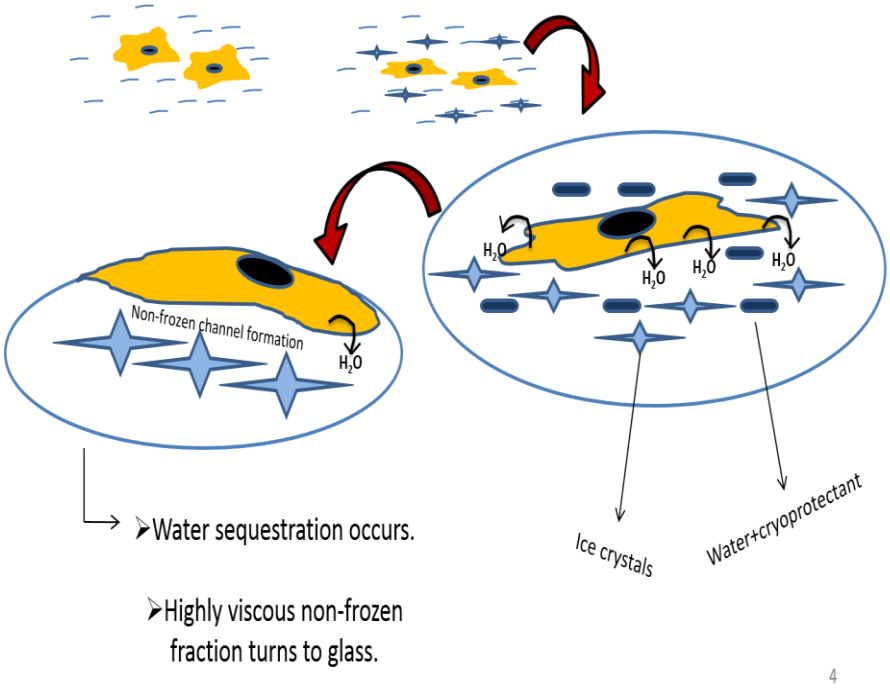

Figure 1.2: Phenomenon of slow cooling during cryopreservation of cells. : (Top left) Schematic showing cells bathed in aqueous matrix containing cryoprotectant. (Top right) initiation of ice crystals in the matrix during slow cooling. (Bottom left) formation of non-frozen channels and initiation of hypertonic environment due to water sequestration. (Bottom right) cell dehydration due to hypertonic conditions during slow cooling.

1.4 Fundamentals of freezing injury and action of CPAs

Metabolic activity of cells decreases at lower temperatures. Cryopreservation is a method of protecting the cells from freezing injuries and permitting long-term cell storage at ultra-low temperatures. In order to minimise cryoinjury, cells are treated with cryoprotectants and stored in liquid nitrogen. This process is used in many scientific, research and medical applications such as blood transfusion, in vitro fertilisation (IVF) and artificial insemination (AI) etc.

Cryopreservation process can be explained in following steps (Gao and Critser, 2000):

1) Addition of cryoprotective agents (CPAs) to biological sample (cells or tissues) before cooling;

2) Cooling the sample to a lower temperature and cold storage (e.g., cooled to −100 °C, at the rate of 5 ˚C min^{-1} and then cold storage in liquid nitrogen at a pressure of 1 atm);

3) Warming of the sample; and

4) Removal of CPAs from the sample after thawing.

Key issues

An important research question in cryobiology is: how to explore the physical and biological mechanisms related to injury of cells at lower temperatures particularly cryoinjuries caused by phase change in both intra-and extracellular environment. The contradiction stays between experimental findings and concept of the process of preservation steps stated by Gao and Crister 2000. Cellular injury is either caused by each step or a combination of the steps

stated above. By exploring the mechanism of freezing injury; optimal procedures, devices or biophysical and mathematical models will be created to allow long-term cryopreservation and minimal cryoinjury.

1.4.1 Mechanisms of cryoinjury

Cryoinjury during slow cooling

During cell dehydration in slow cooling, cells maintain an equilibrium state with outer solution and avoid intracellular ice formation (IIF) but damage can occur due to solute toxicity and physical changes due to excessive cell shrinkage during osmotic stress (Lovelock, 1953b, Lovelock, 1953a, Meryman, 1970, Meryman, 1974).

Solute toxicity: Due to the formation of external ice, the concentration of extracellular and intracellular solutes increase resulting in water efflux from the cells (Mazur, 1963a). Molecular mechanism by which solutes effect membrane permeability is still unclear however, changes in chemical equilibrium results in several biochemical and biophysical changes causing cell death. Excessive shrinkage of cells is one of the damaging factors which cause membrane fusion due to membrane dehydration. Membrane surface area reduction reduces the magnitude of expansion that a cell can tolerate when it is exposed to an isotonic environment (Wiest and Steponkus, 1978).

Excessive cell shrinkage due to exposure to hypertonic environment results in a cell death during slow cooling. A more recent hypothesis proposed by (Muldrew et al., 2000) stated that in hypertonic environment in the extracellular matrix, the dissolved ions interact with fixed charges on cytoplasmic protein

and form salt bridges. On thawing (dilution to isotonic) these ions are brought back into the cell cytoplasm causing cells to swell above their elastic limit.

Cryoinjury during rapid cooling

Cryoinjury also depends upon the cooling rate. If the cooling rate is very rapid intracellular water does not have time to leave the cells and, the reduction in water activity levels through dehydration is not enough to avoid the formation of intracellular ice as the cells become supercooled.

During rapid cooling intracellular water is not lost fast enough to achieve equilibrium and the cytoplasm becomes highly supercooled resulting in the formation of intracellular ice causing cryoinjury to the cell organelles.

Temperature effect: (Mazur 1963a, 1963b) stated that it is not long-term storage but the intermediate zone i.e. (-15 to -60 °C) during cryopreservation which is lethal to the cells. This zone is faced twice by the cells during cryopreservation once during cooling and again at warming. At -5 ˚C the cell and its surrounding medium remain supercooled, at -15 ˚C ice forms (either abruptly or by introducing ice crystals) in the external medium; the cell contents remain unfrozen at this state because plasma membrane block the ice crystal growth in the cytoplasm resulted in creating a greater chemical potential inside the cells (due to supercooled water) than partially frozen extracellular solution (Mazur, 1965). The supercooled water can only form intracellular ice if the extracellular ice is formed under described conditions i.e. -5 to -15 ˚C. No recent studies have shown the formation of IIF in supercooled cytoplasm if extracellular matrix did not form ice in the temperature zones described by Mazur (Franks et al., 1983).

Three different hypothesis explain the formation of intracellular ice (IIF) but all of them support the statement that extracellular ice interacts with plasma membrane to form intracellular ice (Soleimani et al., 2013, Wiest and Steponkus, 1978).

1.4.2 Role of cryoprotectants in reducing freezing injury

The cryoprotective action of cryoprotectants depend upon their colligative properties (Glanc-Gostkiewicz et al., 2013). Penetrating CPAs such as glycerol and Me_2SO are widely used for cryopreservation. They prevent the cells from extensive dehydration during freezing and also protect the cells from intracellular ice formation during freezing and thawing. However CPAs change their concentrations during cooling and warming , and the change in concentration of a CPA mixture may exert cytotoxic effects on the biological samples during freezing (Fahy, 1986). The rates of cooling and warming also effect cell survival e.g. human red cells frozen very slowly i.e. 0.27 ˚C and 1.7 ˚C min^{-1} had higher survival when warming was slow (0.47 ˚C to 1 ˚C min^{-1}) as compared to when the warming was more rapid i.e. 26, 160 or 550 ˚C min^{-1} (Morris et al., 2006). Cooling and warming rates effect cell viability and controlling their rates enable the control of ice-nucleation, ice-melting and ice recrystallisation events.

1.5 Ice nucleators

Phase change involves the transformation of a matter from one state to another; e.g. from liquid to solid or gas. These changes take place due to the variations in external conditions i.e. temperature, volume, pressure etc. During phase transitions, a system absorbs or releases heat from the system and transforms matter from one state to another.

If a solution, undergoes a temperature reduction, it reaches a point (close to its melting point) supercooling or undercooling occurs prior to ice-initiation. Supercooling takes place when temperature of a solution is lowered below its freezing point without becoming a solid. Supercooling is the difference between ice-initiation and ice-melting temperatures. During ice-initiation the system absorbs heat from the environment until it reaches its melting point (θ^m) and remains at an equilibrium state unless temperature is reduced further. Continuous temperature reduction causes formation of ice nuclei resulting in more and more ice crystal formation due to the binding of water molecules with ice nuclei and transforms the water into solid state (ice).

***Action of ice nucleators*:** Ice nucleators have several nucleation sites or depressions on their surfaces allowing water molecules to bind and when temperature falls, ice nuclei are formed on the nucleation sites catalysing the ice formation in the system (Gurian-Sherman and Lindow, 1993).

Ice nucleators initiate the ice formation by promoting the binding of water molecules to the surface of initial ice-crystals that form in a liquid system (Kawahara, 2013). The growth of ice in the presence of nucleators help to control the event of flash freezing in a biological sample during cooling phase.

Asymptote nucleating beads and Snowmax, are minute ice nucleating particles chosen in this project to promote ice nucleation at higher temperatures.

The present work describes the analysis of the effect of ice-nucleators on transition temperatures of the cryoprotectants used. The ice nucleators promote the formation of ice crystals and growth of ice in the presence of nucleators that helps to control the events of flash freezing in a biological sample during cooling cycle. Ice-nucleation increase the growth rate of ice crystals during cooling and inhibits recrystalisation during warming of the solutions (Mizrahy et al., 2013).

1.5.1 Importance of controlling ice-nucleation temperatures

Regulating the temperature of ice formation is important in many applications e.g. production of pharmaceutical products, cryopreservation of biological materials or food preservation. Ice nucleation in the absence of an ice nucleating agent is an uncontrolled phenomenon that can result in cell damage and loss of viability (Teixeira et al., 1997). Nucleators control the formation of ice crystals by reducing the molecular motion of water molecules and allowing their binding with ice crystals formed in the matrix (Fonseca et al., 2003). Adherence of water molecules initiates ice formation in the sample before its expected flash freezing temperature. Early ice-initiation has the advantage of forming a maximum freeze concentrated matrix with equilibrium ice formation at different cooling rates protecting cells from mechanical damage by inhibiting non-equilibrium ice-formation.

Control of ice nucleation is a critical step during cryopreservation of biological components. Regulating this event would help to standardise cryopreservation

protocols and increase cell viability (John Morris and Acton, 2013). Ice nucleation can be controlled by several methods:

1) Seeding: introducing ice crystals to the undercooled solution, or cooled closed to its freezing point, by generating a cold spot manually.
2) Ice nucleating catalysts: addition of certain chemical nucleants into the cryoprotectant mixtures allowing ice nucleation in the sample.
3) Shaking or tapping: a mechanical method used to cause the undercooled sample to nucleate.

1.6 Optimisation of cooling profiles

It is necessary to optimise the freezing mechanism in order to achieve smaller ice crystals (reducing tissue damage), detecting the point of ice crystallisation during freezing and achieving a maximal freeze concentration to obtain the highest Tg possible for reducing the chances of delayed ice crystallisation (during warming) (Carrington et al., 1996, Luyet and Rasmussen, 1967, Blond and Simatos, 1991)

Excessive supercooling or undercooling causes a delay in ice crystallisation because the solution remains in its liquid state below the freezing point for long periods resulting in water plasticisation with cryoprotectant molecules. The supercooled water does not leave the CPA molecules in the plasticised state therefore, when the temperature is decreased further, partial or dilute ice/glass mixtures are formed within the matrix (Roos and Karel, 1991a, Roos and Karel, 1991b). This is undesirable as it requires the system to undergo several relaxation-recrystallisation events in order to form a maximally freeze-concentrated matrix. This phenomenon is termed as kinetic restriction causing non-equilibrium freezing.

During warming of such systems one or more lower transition temperatures may achieved due to ice crystallisation. This phenomenon is called devitrification or delayed crystallisation (Carrington et al., 1996, Luyet et al., 1966, Franks, 1985).

The addition of ice-nucleators can limit excessive undercooling, devitrification and delayed crystallisation initiating ice at higher temperatures and forming a maximally freeze concentrated matrix due to equilibrium ice formation in the CPA samples.

Mazur (1963a) used a numerical approach to conclude that slow cooling provides improved survival rates as it permits water to leave the cells rapidly, resulted in the reduction of intracellular ice formation. Slow cooling and rapid warming is considered to be the favourable approach to reduce recrystallisation of intracellular ice that could cause mechanical injury to the cells (Appelbaum et al., 2004, Rall et al., 1980, Sherman, 1962, Whittingham et al., 1979).

1.7 Methods of determining transition events of CPAs

Several methods have been adopted to monitor Tg. DSC (differential scanning calorimeter (Choi and Bischof, 2008), CMC (cryoelectron microscopy) (Morris, 2006), ETA (electrical thermal analysis) (Her et al., 1994), DEA (dielectric thermal analysis) (Laaksonen and Roos, 2000), molecular rotors (Heideker et al., 2005), DMTA (dynamic mechanical thermal analysis) and NMR (nuclear magnetic resonance) (Germond et al., 2003, Kalichevsky et al., 1992). The most common and widely used method is DSC, where the amount of heat released or absorbed by the system is measured to determine the phase transition. It is an expensive and time consuming method which determines change in heat flow in the test and reference sample when they are cooled or heated. DSC is used at an industrial

scale to test the crystalline and amorphous behaviour of the food, polymers, pharmaceutical products etc.

1.8 History of the conductivity and impedance analysis to monitor transition events

Greave (1954) was one of the first investigators to use thermal conductivity to observe crystallisation process. Electrical resistance (ER) measurements or freezing resistance analysis similar to Greave's work has been used to study eutectics in frozen solutions (Rey, 1960, Mackenzie, 1985, Deluca and Lachman, 1965). The ER process has often been termed as a "eutectic analyser". Rey (1999) observed that ER itself did not give a clear indication of the changes occurring in non-ionic, saccharides or polymers. In order to attain clear indications of significant transition events in non-ionic materials such as proteins, saccharides or polymers, a novel system was designed by (Rey, 1999, Louis Rey, 2004) where function of impedance ($Z \sin\phi$) provided detailed information of freeze dried solutes by monitoring the changes in ion mobility. (Louis Rey, 2004, Ward and Mateijtschuk, 2010, Cook et al., 2009) have introduced impedance measurements to freeze-dried pharmaceutical products containing complex formulations. Ward and Mateijtschuk (2010) correlated the impedance analysis ($Z \sin\phi$) with conventional instruments and described it as a useful tool for assessing the mobility changes in the region of a frozen matrix (that conventional instruments do not explain). This information was not only useful for the formulation development of pharmaceutical products, but also enable to development of freezing or freeze drying cycles according to the requirements of the product.

J.Morris and his co-workers explored the change in electrical resistance of a 2.5 ml sample of 10% Glycerol+0.15M NaCl using a eutectimeter cell (Morris et al., 2006). The cell determined the resistance and temperature at 1s interval. At slower rate of cooling (Fig. 1.3 A) their sample showed change in resistance at -65.7 ˚C. During warming, the electrical mobility was achieved at -63 ˚C (consistent with DSC measurements). At faster cooling rates, greater hysteresis was observed during cooling (Fig 1.3 B) i.e. -70 ˚C which was regained during warming to -63 ˚C. The Tg results obtained by conductivity results during cooling and warming complemented with the DSC studies. With DSC, it was not easier to observe Tg in both events i.e. cooling and warming (Schilder, 2003). Their measurements allowed monitoring Tg in both events.

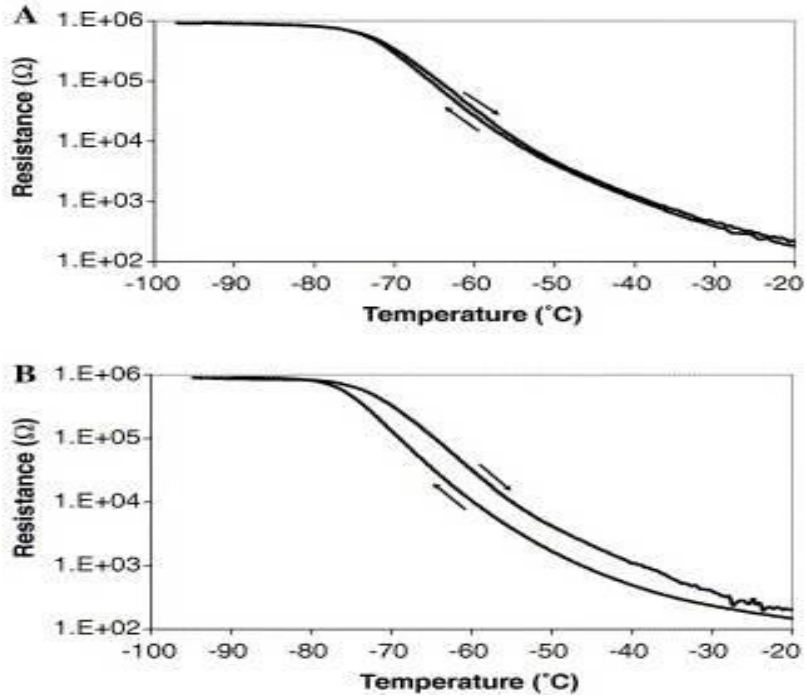

Figure 1.3: Resistance measurements (A) at cooling rate of 1 °C min^{-1} (B) at a cooling rate of 20 °C min^{-1}. Both samples warmed at 1 °C min^{-1}. Image from: Morris et al.,2006. Weblink: (http://dx.doi.org/10.1016/j.cryobiol.2006.01.003)

A multichannel impedance monitoring system was recently designed by (Smith et al., 2013) for monitoring freeze-drying or lyophilisation processes in sucrose samples. A multichannel analytical impedance monitoring system was designed which comprised planar electrodes (to monitor impedance) and a thermocouple to determine temperature change during freeze drying. The measurements were taken in glass freeze-drying vials.

The aim of the present study is to exploit the function of impedance by means of screen-printed sensors and a sensor system to evaluate transition events of cryoprotectant mixtures during cryopreservation.

Monitoring impedance may help to examine the transition events of complex cryoprotectant mixtures during cooling and warming and enable the development

of cryopreservation techniques according to the tolerable temperature (cooling rate) and cryoprotectant concentration for the biological product.

1.9 Model organism

Lactobacillus was chosen as a model organism due to its extensive dairy industrial applications and its sensitivity towards freezing or frozen storage stress (Teixeira et al., 1997, Fonseca et al., 2003 , Fonseca et al., 2001, Maurya et al., 2013)

A study has been undertaken in this project where post-thaw viability of LAB has been monitored after slow cooling and cryopreservation to liquid nitrogen temperatures for certain time periods, to identify the effect of cryopreservation on the viability of post-thaw cells.

Production of lactic acid via fermentation has had a renowned importance for thousands of years. The first culture was isolated in 1873 and the similarity between lactic acid bacterium and milk-souring bacteria was discovered in the early 1900s. Classification of lactic acid bacterium was described by Orla-Jenson (Orla-Jensen, 1919).

The Lactic acid bacterium is mainly connected with dairy products such as cheese, yoghurt and buttermilk. It also plays an important role in meat production, bread production and their preservation. Various strains have been used as probiotics to improve human and animal health.

The term Lactic Acid Bacterium (LAB) was accepted at the start of 20th century. The Lactic acid bacterium belongs to a group of bacteria having physiological, metabolic and morphological similarities as well as being phylogenetically related as well (van Reenen and Dicks, 2011).

1.9.1 Classification of LAB

At present LAB is comprised of 20 genera, of which 12 genera are considerably important for food–technology: *Aerociccus, Enterociccus, Carnobacterium, Lactococcus, Leuconostoc, Lactobacillus, Oenococcus, Pediococcus, Streptococcus, Tetragenococcus, Vagococcus and Wiesella*. *Bifidobacteroum* was once considered to be in LAB group. However, due to its significance in the gastrointestinal tract of both human and animals with few LAB, it was recently removed from the LAB group (Axelsson, 2009, Halász, 2009).

LAB are divided into certain genera of the basis of morphology, growth temperatures, mode of glucose fermentation, acid and alkaline tolerance and ability to grow at high salt concentrations.

LAB are subdivided into cocci and rod shaped. *Lactobacillus* and *Carnobacterium* are rod shaped while rest of the genera are cocci form.

Lactobacillus delbrueckii subsp. *bulgaricus* belongs to the *"Lactobacillus acidophilus group"* which is extensively used in the dairy industry. The group also *includes Lactobacillus acidophilus* and *Lactobacillus johnsonii* isolated from human gut (Nicolas et al., 2007).

1.9.2 General physiology of Lactobacillus

Lactobacillus is a gram-positive, rod like and filamentous organism which is non-motile, non-spore forming, anaerobic habit but aerotolerant in nature (Figure 1.4). Aerotolerant anaerobe means that the *lactobacillus sp*. can happily grow in both anaerobic and aerobic environments due to the presence of peroxidase which protects it from oxygen by-products (e.g. H_2O_2) (Stieglmeier et al., 2009).

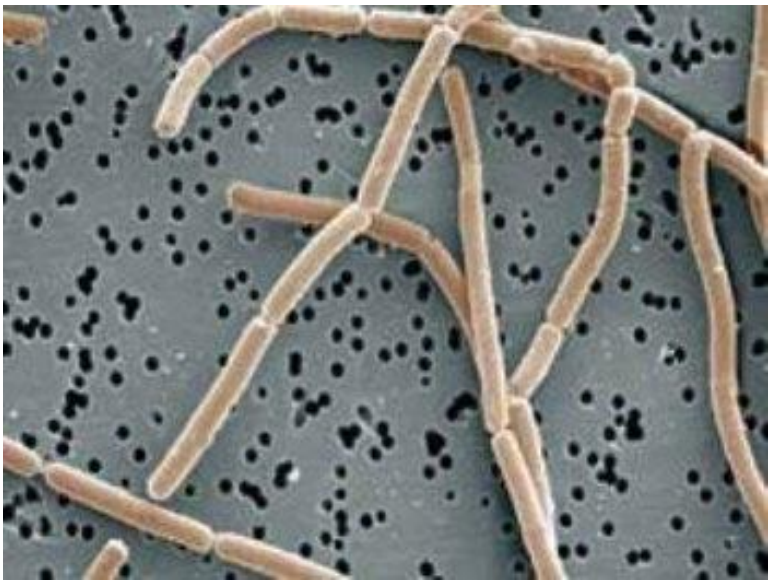

Figure 1.4: Rod shaped filamentous and non-motile cell structure of *Lactobacillus delbrueckii* subsp. *bulgaricus.* (Photo from: Jeff Broadbent, Utah State University USA. Weblink: (http://genome.jpipsf.org/lacde/lacde.ho,e.html.)

Lactobacillus delbrueckii subsp. *bulgaricus* is *homofermentive* and produces lactic acid as a major end product through fermentation of carbohydrates (Khalid, 2011, Fernanda Mozzi, 2010). The production of lactic acid is in the form of D (-) lactic acid which takes place at an optimal temperature of 40 °C to 44 °C and requires low pH (5.5 to 4.5) to grow; feeding on lactose (Germond et al., 2003).

The wall structure of gram positives is composed of a cytoplasmic layer, a peptidoglycan layer and many capsule polysaccharides. Like other prokaryotic cells, it is composed of cytoplasm, DNA and RNA, nucleolus and internally metabolises lactic acid as a major end product from glucose (Archer, 2004).

1.9.3 Fermentation pathways of LAB

Due to anaerobic and aerotolerant nature of lactic acid bacteria, two main sugar fermentation pathways are distinguished during growth which are dependent upon the growing conditions provided to the cells (aerobic or anaerobic).

Homolactic fermentation runs under standard conditions where Glycolysis (Embden-Meyerhof-Parnas pathway) results in the formation of lactic acid as an end product. During hetrolactic fermentation, the 6-phosphogluconate/phosphoketolase pathway is activated resulting in the production of significant amounts of numerous end products e.g. acetate, ethanol, CO_2 and lactic acid (Salminen et al., 2004).

To make dairy products using lactic acid starter cultures, their growth and fermentation are generally monitored by pH change. Different methods of monitoring pH have been introduced to monitor pH change in biological samples on an industrial scale. For example, the growth rate of the starter cultures is generally monitored by a Cinac system (Rault et al., 2008, Rault et al., 2009). These systems require larger sample volumes and large sized, fragile glass pH probes for pH assessment.

1.9.4 Background of LAB cryopreservation

Lactobacillus delbrukeii subsp *bulgaricus* has been used to manufacture fermented dairy products such as yoghurt and cheese. To improve the food texture, flavour and safety, it is essential to improve the acidification activity of LAB starter cultures. For ready access, starter cultures in dairy or food industries use fresh cells that have been freeze dried or cryopreserved using suitable cryoprotectants. In order to prevent food fermentation and obtain higher and consistent yield, there is a need to improve starter culture production of LAB (Daly et al., 1998, Grattepanche et al., 2008).

Important parameters for starter culture production are pH control, harvesting time and the method of storage/preservation. Starter cultures have been preserved in the past by methods such as freeze drying (Fonseca et al., 2001, Schoug et al., 2006), spray drying (Peighambardoust et al., 2011), microencapsulation (Heidebach et al., 2010), drying over silica gel and freezing by slow cooling and vitrification (Fonseca et al., 2000).

pH control value influences biomass concentration, fermentation time, growth rate and sugar consumption. Harvesting time and mode of preservation influences the cell viability and stress tolerance e.g. cryotolerance during cryopreservation (Adamberg et al., 2003, Beal and Corrieu, 1991) of the culture.

pH-controlled cultures provided higher yields as compared to uncontrolled cultures (causing acidic fermentation) (Cachon et al., 1998). Controlling extracellular pH of the cells would regulate their intracellular pH level. Controlling intracellular pH level would result in decreasing the cytoplasmic acidification (due to non-dissociated weak organic acids) thereby preventing the collapse of the proton motive force. Excessive cytoplasmic acidification inhibits nutrient transport and enzymatic

reactions resulting in biomass inactivation and DNA mutation (Even et al., 2002, Gonçalves et al., 1997).

1.9.5 Optimal growing range for LAB

Currently LAB is grown under a controlled pH environment where concentration of H^+ and OH^- ions is regulated by adding ammonium hydroxide (NH_4OH) or ammonia (NH_3) (Savoie et al., 2007, Béal et al., 2008). The optimal pH range is (pH 5.5 to 6) (Beal et al., 1989, Rhee and Pack, 1980).

1.9.6 Importance of LAB cryopreservation

Cryopreservation of lactic acid bacteria (LAB) is an important consideration for long term preservation of its viability and properties such as acidification activity, production of aroma compounds and contribution to product texture (Smittle et al., 1972, Fonseca et al., 2003 , Fonseca et al., 2006). Although the preservation of Lactobacillus has been studied extensively, the effect of ice and glass formation under different cooling and warming regimes on metabolic activity of starter cultures is not yet fully understood (Carvalho et al., 2003, Fonseca et al., 2006). An understanding of the impact of cryoprotectant, freezing and storage times on the metabolic activity of bacteria is essential for optimising the process of cooling and warming (Fonseca et al., 2006a, Archer, 2004). In bacterial species it is thought that damage at rapid cooling rates is due to osmotic imbalance encountered during thawing, not by the formation of intracellular ice (Morris, 2006).

1.10 Use of disposable screen-printed electrodes in biotechnology

Screen-printed electrodes are printed with a layer of carbon, gold, silver or platinum inks over a substrate e.g. polyester films. A screen-printed electrode comprised a working area where the sample is tested, a reference area and connection points. By means of thick and thin-film technology large and very small sized electrodes can be manufactured. Screen-printing allows the manufacture of low cost and disposable devices which can be currently used in various branches of biotechnology e.g. biosensors, biomedical sensors or immuno-sensors. Electrodes could also be used to monitor electrochemical responses in small volumes of biological samples e.g. glucose level in a drop of a blood or hormonal secretion in µl volume of a sample.

Screen-printing technology has played a vital role in the field of sensor technology to fabricate a wide range of electrochemical or biological sensors. It is an approach to fabricating electrodes that does not require prolonged pre-treatment of electrodes or polishing methods (Kadara et al., 2009). Advantages of screen-printing electrodes include a) a simple preparation process, b) disposable nature, c) low-cost, easy production and d) flexible design (Chang and Zen, 2006, Wang, 2002).

Electrodes for monitoring transition events in cryotubes and straws

Interdigitated electrodes are commonly used in wide range of sensor designs (Langereis et al., 1997, Jacobs et al., 1995). They have a comb like structure, detecting signalling response over small areas. The space between the interdigitated areas is kept narrow to observe the phase change in smaller volume samples.

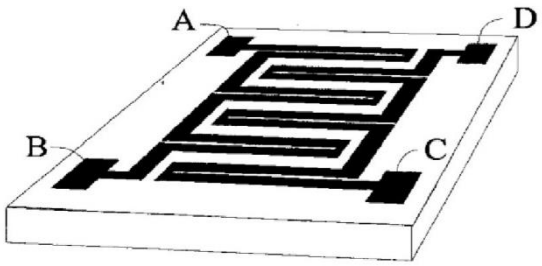

Figure 1.5: Shape of the multi-purpose interdigitated structure of screen-printed electrode measuring temperature between A and B and conductivity between C and D. (Image from Langereis et al., 1997). Weblink: http://ieeexplore.ieee.org/xpl/articleDetails.jsp?arnumber=613707.

Screen-printed electrodes consist of working area, reference area and dielectric layer. The working area is the point where electrochemical signals from the outer environment are sensed by an electrode. The reference electrode is generally used for sensors e.g. pH electrodes or CellSense electrodes which require a reference element (silver-silver chloride) screen-printed along with the working electrode. The dielectric layer is a non-conductive layer preventing the carbon layer from mechanical or electrochemical damage (Nascimento and Angnes, 1998).

Screen-printed electrodes can be used to monitor phase change events and pH change in cryotubes as they allow real-time monitoring of the samples, are affordable, disposable, reusable and do not require calibration before use.

1.11 Introduction to measurement of pH

pH is defined as the negative logarithm (-log) of hydrogen (H^+) ion activity.

$$pH = -\log_{10} a_{H^+}$$

H^+ activity is the molar concentration of hydrogen ions multiplied by an activity coefficient i.e. any other ions interacting with H+ ions in the solution.

$$pH = -\log_{10} [H^+]$$

At 25 ˚C neutral solutions will have pH of 7.00 while solutions pH > 7 are basic and pH <7 are acidic.

pH can be measured by means of a pH sensitive or ion-selective electrode (usually glass) and a reference electrode (usually Ag/AgCl) (Halász, 2009, Mattock et al., 1963).

Theory of pH sensor

By means of potentiometric pH sensor, pH of a solution can be monitored between two electrodes i.e. pH sensitive electrode and a reference electrode. While in contact to the solution, a pH electrode creates a potential difference dependent on the pH of the solution. Reference electrode is essential part of the pH probe because it regulates the probe's potential at certain temperature by providing a known, stable and constant reference potential for pH electrode. The ion selective

or working electrode responds to the change in hydrogen ion (H^+) concentration in the solution. The difference in potential of working and reference electrodes give rise to a potential mV signal which is proportional to the pH.

pH sensors are mostly designed to produce 0 mV at pH 7.00 with a sensitivity of -59.16 mV /pH units at 25 ˚C (theoretically ideal Nernst slope).

The general Nernst equation is:

$$E = E^{\circ} - \frac{RT}{nF} \log_e \frac{a_{ox}}{a_{red}} \dots\dots\dots (equation\ 1a)$$

The Nernst equation at 25 ˚C is:

$$E = E^{\circ} - \frac{0.0592}{n} \log_{10} \dots\dots\dots (equation\ 1b)$$

Where E˚ is the electrode's standard potential (V), R is molar gas constant (8.31 J K^{-1} mol^{-1}), T is the absolute temperature (K), n is the number of electrons taking part in the reaction, F is the Faraday constant (96,485 C mol^{-1}) and Q is the reaction quotient i.e. the function of concentration or activities of chemical species participating in a chemical reaction.

The reference combination electrodes display an "isopotential point" where the potential mV and pH is constant with the change in temperature (0 mV at pH 7.00 (Glanc-Gostkiewicz et al., 2013).

pH meter

pH probes are connected to a pH meter to measure and display the pH readings . For precise measurements the pH meter is calibrated before any experimental work. Normally it is calibrated at the start of each day by means of at least two or ideally three standard pH buffers that are in the range of pH values to be measured. The pH meter has two controls, one control is used to set or calibrate the reading equal to the first standard buffer and second control is used to set pH reading of the probe with the second pH buffer. Normally pH 4.00, pH 7.00 and pH 10.00 pH buffers are used for the calibration. The pH probe is immersed in a standard buffer and calibration is performed by first rinsing the glass bulb of the probe with deionised water (D.O), dab dried and immersed into the standard pH buffers one by one. Ideally a three point calibration is preferred for precise measurements where pH 7.00 buffer works as a “zero point” calibration and make the pH closest to the point of interest e.g. pH 4.00 or pH 10.00. Third point enables more linear accuracy to the work. After each measurement the probe is rinsed with deionised water (D.O.) to remove the solution traces from the working area of the probe and blotted with wipe to absorb remaining water to reduce the chances of its dilution with other samples (Buck et al., 2002, Lawn and Prichard, 2003).

Storage of glass probes

The tip of glass electrode is soaked in a standard pH buffer solution at all times when not in use to avoid the dehydration of pH sensing membrane.

A combined pH electrode is immersed in bridge electrolyte (3 M KCl) to avoid the diffusion of the fill solution. A glass electrode without combined reference is stored in an acidic solution of pH 3.00 (Lindner, 2014, Buck et al., 2002).

Electrode aging

As electrodes are used, their slope response decreases. Higher temperatures and frequent use with strong acids or alkalis affect the electrode due to mechanical and chemical degeneration of the gel layer of the membrane glass, change in chemical composition of the glass bulb and contamination of the fill solution present in the glass electrodes cause electrode aging (Qingwen et al., 2000).

Advantages of thick-film electrodes

Although glass electrodes are commercially used due to their performance, long-term stability, sensitivity, slope and accuracy they have certain drawbacks such as their fragile nature, reproducibility, large size and internal liquid reference system (Glanc-Gostkiewicz et al., 2013). Thick-film technology resolves this issue by constructing metal-oxide pH electrodes and thick-film Ag-AgCl reference element (Glanc-Gostkiewicz et al., 2013, Glanc et al., 2013).

Purpose of salt bridge

Salt bridge is a common structure found in glass electrodes. In the present study salt bridge was constructed to prevent diffusional mixing of outer and inner solutions. While keeping the contents separate there is no possible interaction between ionic species (Kakiuchi, 2014).

Salt bridge can be constructed with filter paper soaked in an electrolyte, constructing a narrow capillary filled with stable salt solution or a gel.

1.12 Present study

The work sets out to develop a low cost and easy to use methodology for monitoring phase change of CPAs and developing optimum cryopreservation protocols to monitor post-thaw metabolic activity of LAB by means of exploiting sensor and cryobiology technologies.

Ultimately, it is envisaged that successful development of impedance and pH monitoring electrode systems, and the combination of the two onto a single device, would enable the monitoring of key events during the cryopreservation process (cooling and warming) and the post thaw metabolic activity of cryopreserved cells.

1.13 Aims and Objectives

Aims

The aim of the work described was to develop sensor systems to inform the process of cryopreservation of *Lactobacillus sp.* cultures and their post-thaw recovery.

Objectives

a) To design, develop and evaluate instrumentation to allow monitoring of phase transitions during cooling and warming of cryoprotectant mixtures in cryotubes and cryostraws;

b) to explore the use of screen-printed impedance and temperature sensors to monitor phase changes and temperature profiles during cooling and warming of cryoprotectant mixtures;

c) to investigate the potential of screen-printed pH sensors to monitor post-thaw activity of cryopreserved *Lactobacillus*; and

d) to demonstrate how the sensor systems could be used to optimise the cryopreservation of *Lactobacillus.*

If the aims and objectives were achieved, the devices and probes designed or screen-printed in this study would be disposable, non-fragile, portable, lighter in weight, smaller in size and would allow measuring post-thaw metabolic activity of starter cultures with relatively smaller volume samples.

Chapter 2

Materials and Methods

2 Introduction

The main areas of research covered in the present study were, a) validation of sensor systems to monitor transition temperatures of cryoprotectant mixtures in micro-volume samples during cooling and warming phases; b) development and validation of a pH sensor system to monitor metabolic activity of lactic acid bacterium after cryopreservation; c) investigation of the effect of cryopreservation protocols glass transition temperatures of CPA mixtures and post thaw cell viability; and d) design and application of screen-printed temperature probes for temperature measurements in cryo-samples.

The experimental work was performed in the University of Bedfordshire Institute of Biomedicine and Environmental Science and Technology (iBEST), UK.

2.1 Materials

2.1.1 Materials

Ammonium hydroxide solution (320145), antimony metal powder (266329), chitosan of medium molecular weight (448877), citric acid (251275), dimethyl sulfoxide (Me_2SO) (472301), ethyl acetate (270989), ethylene glycol (85978), glycerol (G7893), MRS (De Man, Rogosa and Sharpe) broth (69966), nitric acid (438073), pH buffer standard solutions (colour-coded) of pH 4.00 (82598), pH 7.00 (33666) and pH 10.00 (33668), potassium chloride (P9541), ruthenium(IV) oxide (238058), sodium chloride (S7653), sodium citrate tribasic dihydrate (C3434), sodium phosphate dibasic (S3264), sucrose (55016) Triton™X-100 (X100) and Tween® 80 (P8074) were purchased from Sigma-Aldrich (Poole, UK). Carbon paste (C2000802P2) and dielectric blue paste (D2071120D1) were purchased from Gwent Electronic Materials Ltd (Pontypool, UK). All the solutions were prepared using laboratory grade R.O. water from Progard®Pack (Milli-Q® and Elix®) with a Vent filter of E-POD™ Millipore UK.

For ice-initiation in cryosamples, Asymptote nucleating beads and Snowmax beads were obtained from Asymptote Ltd, Cambridge UK.

Freeze dried cultures of *Lactobacillus delbruekii* subsp. *bulgaricus* CFL1, were obtained from the French National Institute for Agricultural Research (INRA, Thiverval-Grignon, France).

2.1.2 Culture medium for Lactobacillus bulgaricus cryopreservation

The culture medium was composed of 56.6 g L^{-1} of de Man, Rogosa and Sharpe medium (MRS) autoclaved for 10 min at 110 ℃. The medium was centrifuged (Denley BS400) at 17000 rpm with a rotor radius of 11.1 cm. The machine delivered a centrifugal force of 358 *x g* using a conversion equation:

$$g = (1.118 \times 10^{-5}) R\, S^2$$

where,

g = relative centrifugal force (RCF)

R = radius of the rotor in centimetres, and

S = speed of the centrifuge (revolutions per minute RPM) (Gleason, 2012)

After centrifugation, filtered the supernatant using 0.45 µm syringe filter (Whatman® GD/XP, Z33840) and added 1 ml of Tween® 80 to 1 L volume of MRS nutrient broth.

2.2 Electrodes

2.2.1 Screen-printed electrodes

Screen-printed sensors were fabricated using a semi-automatic printer (1760RS, DEK International Ltd, UK). Electrodes were designed by Dr Roberto Andres in AutoCad and sent to Philips Digital Print Letchworth, to make laser photoplots. The screens were made from the photoplots by MCI Precision Screens (Melbourne, UK). The electrodes were screen-printed and tested by me.

The electrodes were printed on polyester flexible films. Initially electrical connectors, conductive tracks and 'base' electrodes were printed using carbon-paste (no of strokes 1 and pressure 2 Pa) and then dried in a fan-assisted oven (30 min, 70 ℃; Gallenkamp Oven300).

A second screen was used to print the dielectric paste over the area that needed to be electrically insulated from contact with test materials. Similar printing and drying settings were used for dielectric layers.

Where necessary, an additional screen was used to overprint the working electrode area for preparing pH sensitive electrodes (section 2.2.1.2).

2.2.1.1 Interdigitated electrodes for impedance measurements

Three types of interdigitated electrodes were screen-printed for impedance measurements in cryotubes and cryostraws by means of TMS 1 and TMS 2. They had a similar interdigitated working area but were of different sizes and lengths depending upon the size of the straws and tubes to be used.

Type A electrodes were used for transition measurements in cryotubes. They had the width of 0.6 cm and working length of 1 cm, Figure 2.1a.

Type B electrodes were designed for straws, having working length of 0.5 cm and width of 0.2 cm, Figure 2.1b.

Type C electrodes could easily be incorporated into cryotubes or cryostraws. They had a working length of 0.5 cm and width of 0.2 cm, Figure 2.1c.

a)

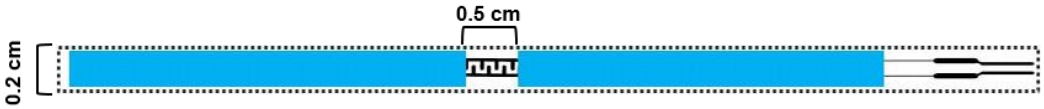

b)

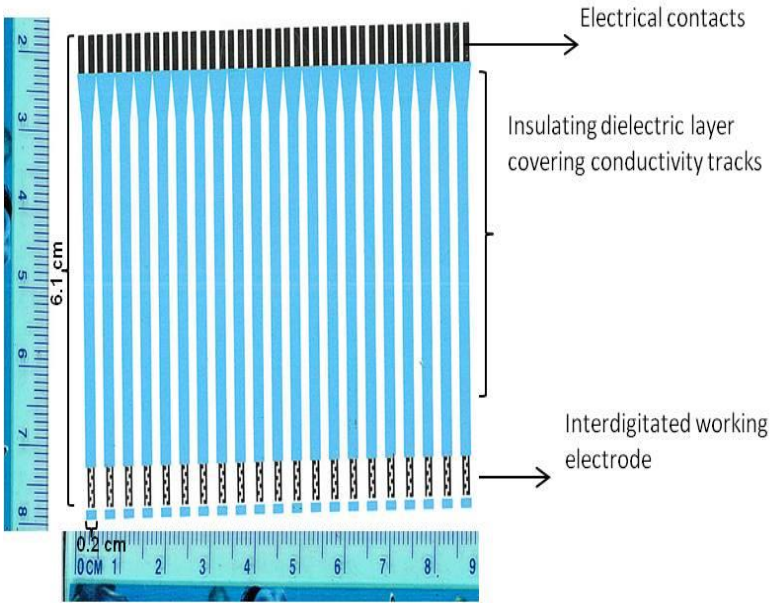

c)

Figure 2.1: Arrangement of interdigitated screen-printed electrodes for cryotubes and straws used to monitor transition events during cooling and warming phase.

(a) Schematic of 'Type A' electrodes.

(b) Schematic of 'Type B' electrodes.

(c) Scanned image of 'Type C' electrodes.

2.2.1.2 Screen-printed pH electrodes

Two types of carbon-metal pH electrodes were screen-printed: (1) carbon with ruthenium (IV) oxide; and (2) carbon with antimony. Ruthemium (Ru) and antimony (Sb) are metal elements used to fabricate conductive tracks in screen- printed electrodes (Renedo et al., 2007, Vonau and Guth, 2006, Domínguez Renedo and Arcos Martínez, 2007). Mixtures at different % concentrations of carbon + ruthenium or carbon + antimony were prepared using ethylene glycol as a solvent. Mixtures were blended using an asymmetric centrifuge (Speed Mixer, DAC 150.1 FV2). A container of cup holder type (PP5, Fisher Scientific UK) was used for mixing the inks. The carbon-metal layer was screen-printed (using an additional screen) over the base working electrodes. The size of the overprinted material was 0.25 cm in diameter, Figure 2.2. The layer was heated for 30 min at 70˚C for ink binding.

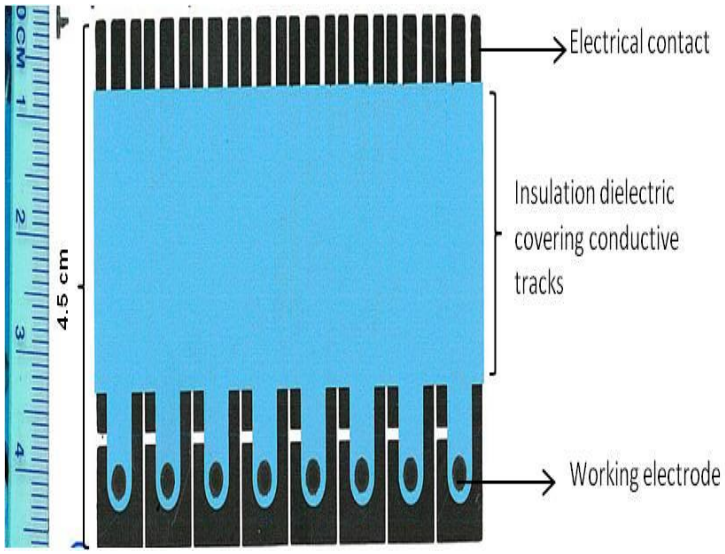

Figure 2.2: Scanned image of arrays of carbon-metal screen-printed electrode used as working electrodes for pH measurements.

2.2.2 Conventional pH combination electrodes

Conventional glass pH combination electrodes (Accumet, Cat No: 13-620-221, Fisher Scientific UK) was used for routine pH measurements (Figure 2.3).

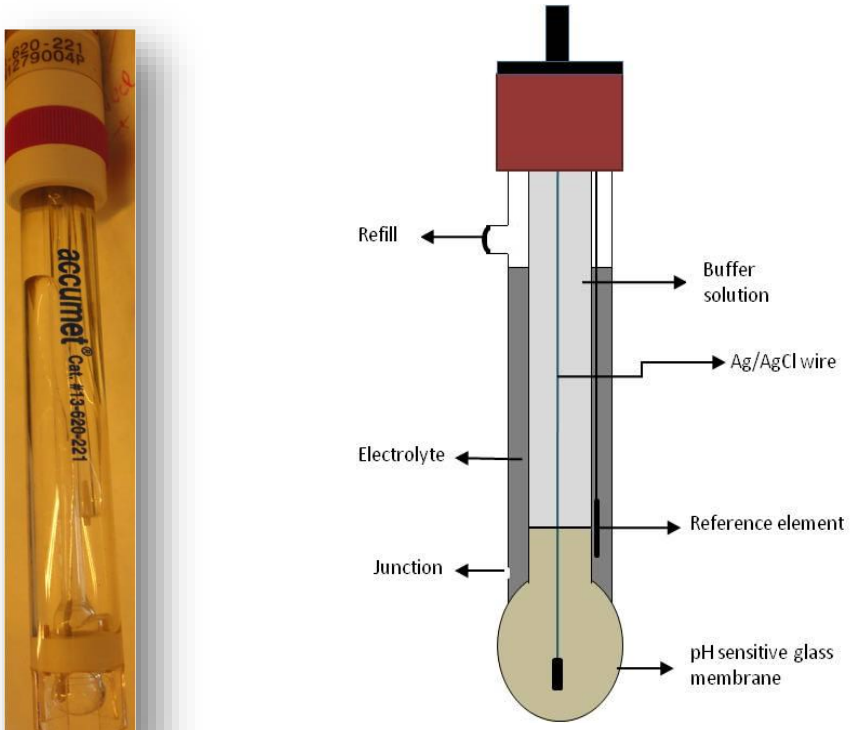

Figure 2.3: Conventional glass pH combination electrode.

(Left) Photographic image

(Right) Schematic arrangement of parts of conventional combination electrode.

2.2.3 Reference electrodes

Potentiometric sensors require stable reference electrodes in order to make measurements. Two types of reference electrodes were used in the work reported here: (1) the reference electrode element from a conventional glass pH combination electrode; and (2) a planar screen-printed Ag/AgCl electrode by Danielson Products (Aylesbury, England).

2.2.3.1 Reference element of conventional glass pH combination electrode

When necessary, the reference element (Figure 2.3 right) from a conventional glass pH electrode was used as the reference part of external pH indicator electrodes. This was achieved by connecting only the shielded part of the BNC (Bayonet Neill–Concelman) cable attached to the combination electrode. The central pin in the BNC connector (connected to the pH sensitive glass bulb) was not used in these cases. For example see Figure 2.4.

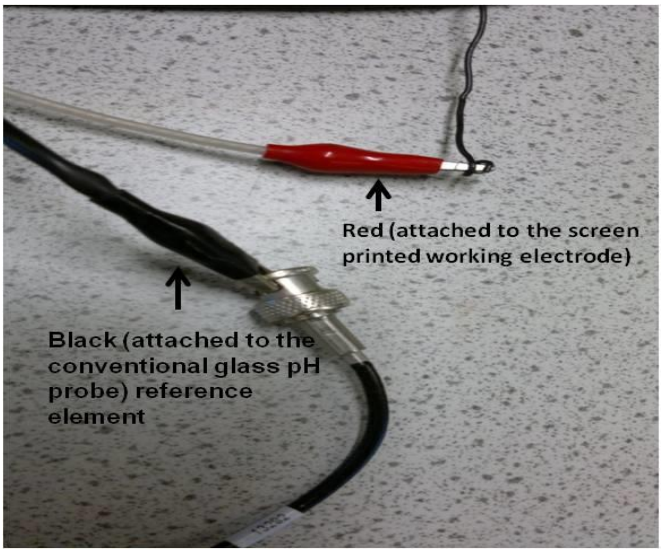

Figure 2.4: Assimilation of a BNC connector with reference element of glass pH and screen-printed working electrode for pH measurements.

2.2.3.2 Planar reference electrode

A planar Ag/AgCl reference electrode having a length of 3.5 cm was also used along with the screen-printed working electrode for pH assessment (Figure 2.5). Comparative study of the response of conventional glass reference element and planar reference electrode enabled the evaluation of the functionality of the probes. For an indirect exposure of the external medium to the screen-printed Ag/AgCl reference electrode, two methodologies were adopted:

A) Coating the planar Ag/AgCl with chitosan solution;

B) Creating a salt-bridge over the screen-printed Ag/AgCl reference electrode.

A) Method of preparing chitosan solution

Chitosan (0.1 g) was mixed with 2 ml of citric acid (8.6 mol/dm^3) for 5 minutes and then 5 ml of distilled water was added with continuous agitation overnight (for hydration). Adjustment of the pH of the final solution to 4.00 was made by adding 8.4 M NH_4OH (drop wise).

Addition of 0.5 ml of the chitosan solution was added (dropwise) on to the Ag/AgCl surface of the screen-printed electrodes and spread evenly. These were then dried in an oven (at 70 ℃).

B) Salt-bridging of screen-printed Ag-AgCl reference electrode

A capillary channel of 2.5 cm in length was made over the screen-printed reference electrode using double-sided tape and transparency film sheets washed with a 0.1% of Triton solution. A salt bridge was then layered over the reference element of screen-printed GEM carbon electrode for indirect exposure of the medium to the Ag/AgCl reference element as illustrated in Figure 2.5 and 2.6.

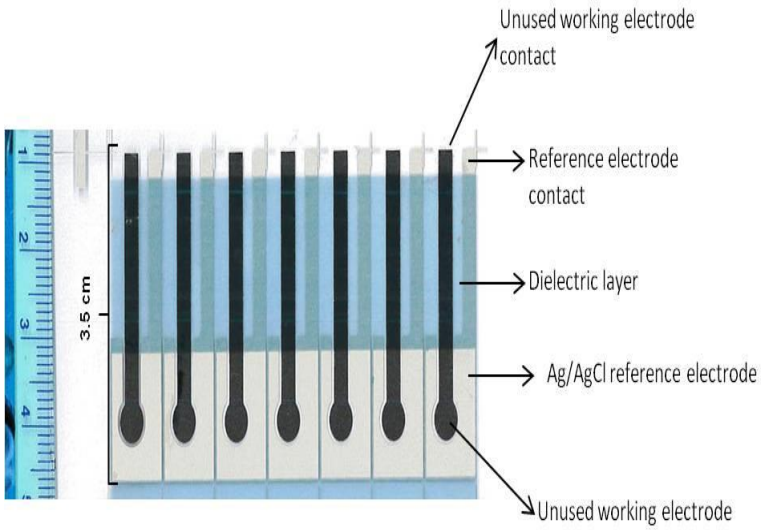

Figure 2.5: Scanned image of the array of electrodes (Danielson Ltd) used as the basis for preparing Ag/AgCl reference elements.

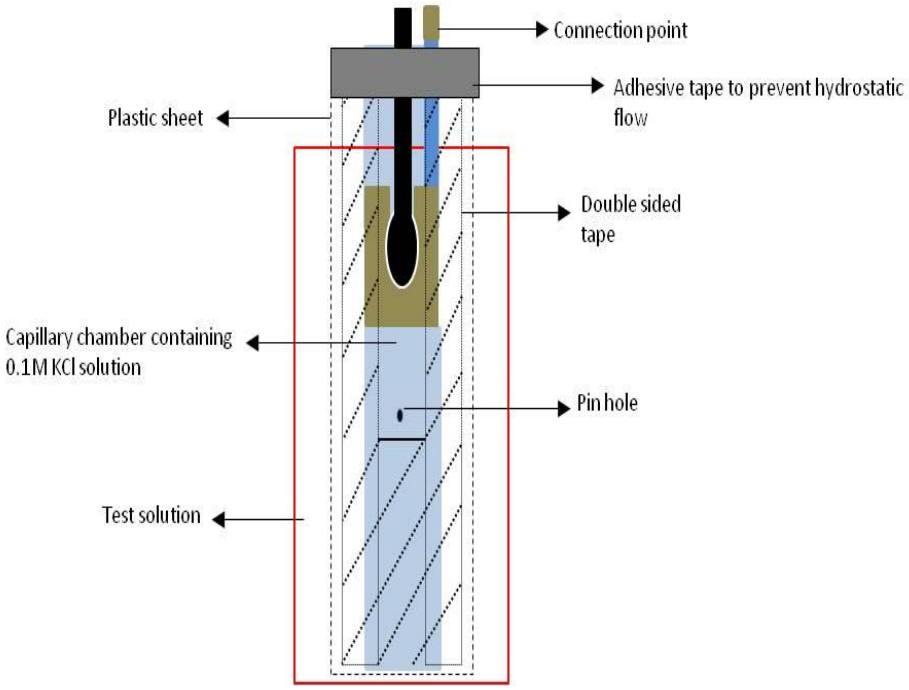

Figure 2.6: Layering of salt-bridge over screen-printed Ag-AgCl reference electrode (see Fig 2.5). The (__) indicated the test solution. The electrode is covered with comb-shaped double-sided tape, covered with plastic sheet (---) providing a capillary chamber. The capillary was filled with 0.1 M KCl via a pin hole giving diffusion distance of 2.5 cm.

2.2.3.3 Calibration of planar electrodes

Calibration was performed to evaluate the signalling response of chitosan-coated and salt-bridge Ag-AgCl planar reference electrodes (see Chapter 3).

2.3 Instrumentation

Two systems were designed in collaboration with Dr. Andres to monitor phase changes in cryoprotectant mixtures: 1) a single-channel transition monitoring system (TMS 1); and 2) a multi-channel transition monitoring system (TMS 2).

The impedance change in both devices was assessed by interdigitated screen-printed sensors and the temperature change was monitored using a platinum resistance temperature detector (Pt-RTD). Transition measurements were studied during cooling and warming phases.

2.3.1 Single-channel transition monitoring system (TMS 1)

The circuit of TMS 1 was developed on a bread board. The circuit included: a) function generator; b) precision rectifier circuit attached to the screen-printed interdigitated probes; and c) root-mean-square to direct current (DC) circuit (Figure 2.7).

The function generator is a simple circuit designed to generate square wave oscillation using solitary operational amplifier. The square wave generated at the output was fed to the precision rectifier circuit, followed by a low-pass filter converting AC signal to DC. The precision rectifier circuit used an operational amplifier (op-amp) providing rectification of opposite polarity signals coming from the input. The low-pass filter circuit is a root-mean-square to DC converter filtering

the signal coming from precision rectifier circuit to an average value (root- mean-square) of the wave.

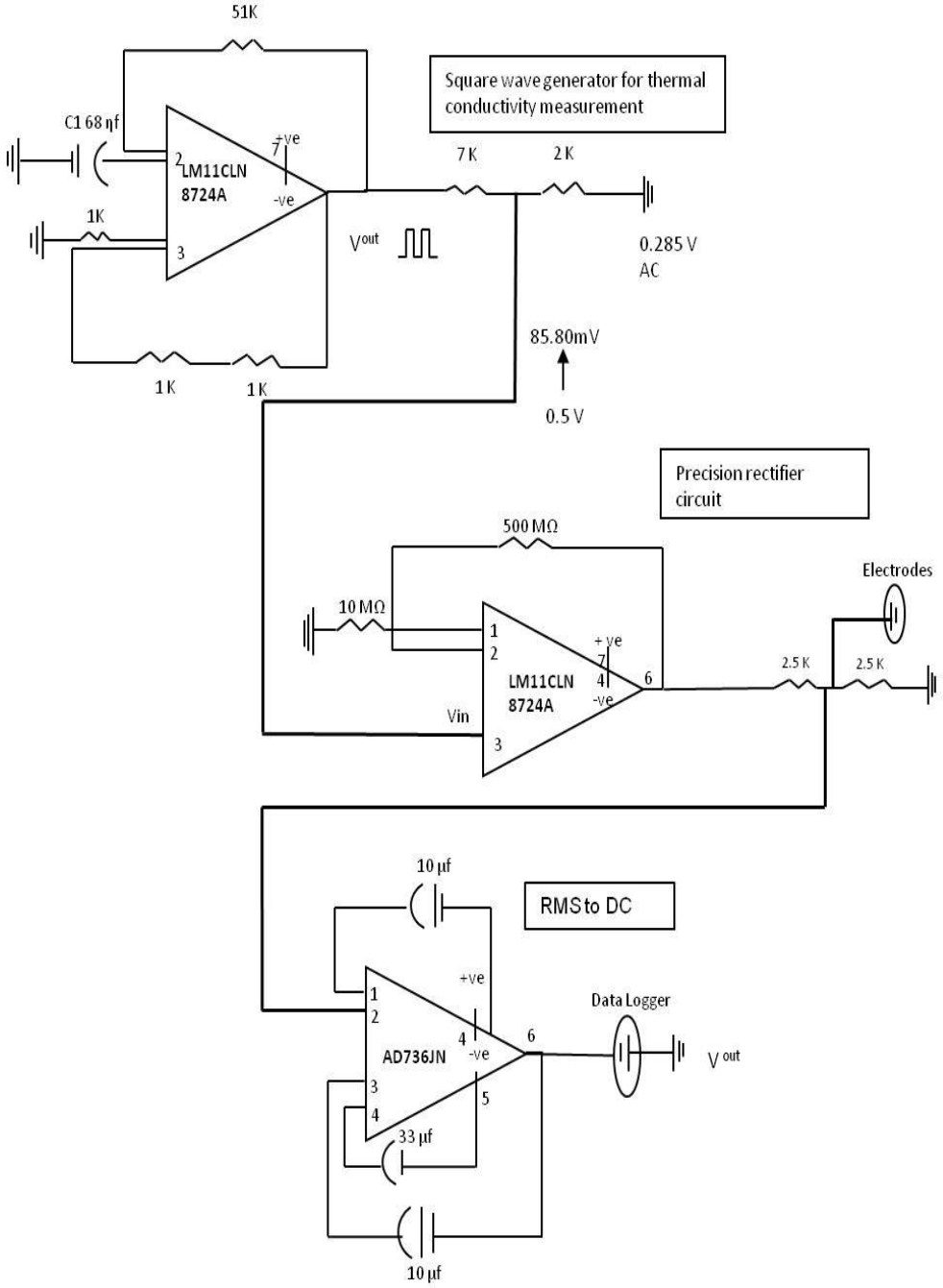

Figure 2.7: Circuit design of transition monitoring system (TMS 1) comprising function generator (FG), precision rectifier circuit (PRC) and RMS-DC (root- mean-square to direct current) circuit.

2.3.2 Multi-channel transition monitoring system (TMS 2)

TMS 2 was constructed in the form of a printed circuit board (PCB) connected to the data logger.

The TMS 2 is comprised of seven output channels. Six were used to connect interdigitated electrodes (for impedance measurements), the seventh output channel was connected with a temperature probe Platinum-Resistance Temperature Detector (Pt-RTD) (Figure 2.8).

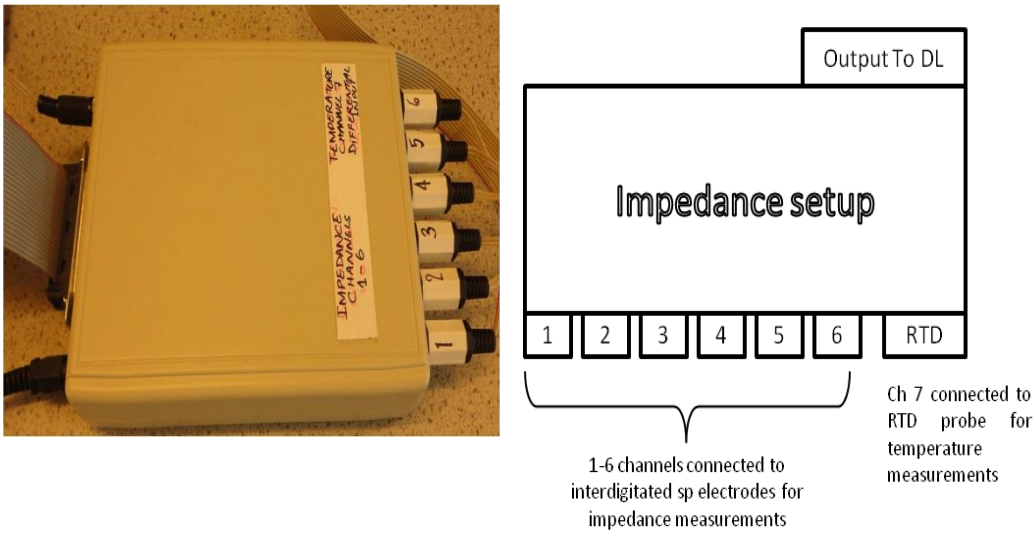

Figure 2.8: Setup of transition monitoring system 2 (TMS 2). Six channels are separately connected to interdigitated probe while the channel 7 was dedicated to RTD temperature probe. The output of the device was connected to the data logger saving the raw data.

2.3.3 Calibration of TMS 1 and TMS 2 systems

The calibration of two systems was performed with (resistors in series) to study the performance of sensor systems. Calibration equations were derived after performing series of calibration to convert the instrument output to impedance values (see Chapter 3).

2.3.3 Data logging

An electronic data logger (Picolog ADC-20, 1076338 Farnell UK) was used to record the data over time. This multichannel, high-resolution USB data logging device was interfaced to a personal computer (PC) via a USB link and was controlled with Pico Technology Software (version 2.1). Collected data were monitored using the Picolog software and analysed in Microsoft Excel.

The outputs of the sensor systems used in the project i.e. transition monitoring system 1 (TMS 1), transition monitoring system 2 (TMS 2), temperature probe (RTD), screen-printed interdigitated (impedance monitoring) probes, pH working, pH reference probes and conventional glass probes, were connected to the Picolog data logging system. Temperature and pH probes were connected as a differential input. Interdigitated probes were linked as single ended inputs, which allowed for monitoring of the signalling response of different samples. Figure 2.9 illustrates the schematic presentation of phase transition and pH monitoring setups connected to the logger.

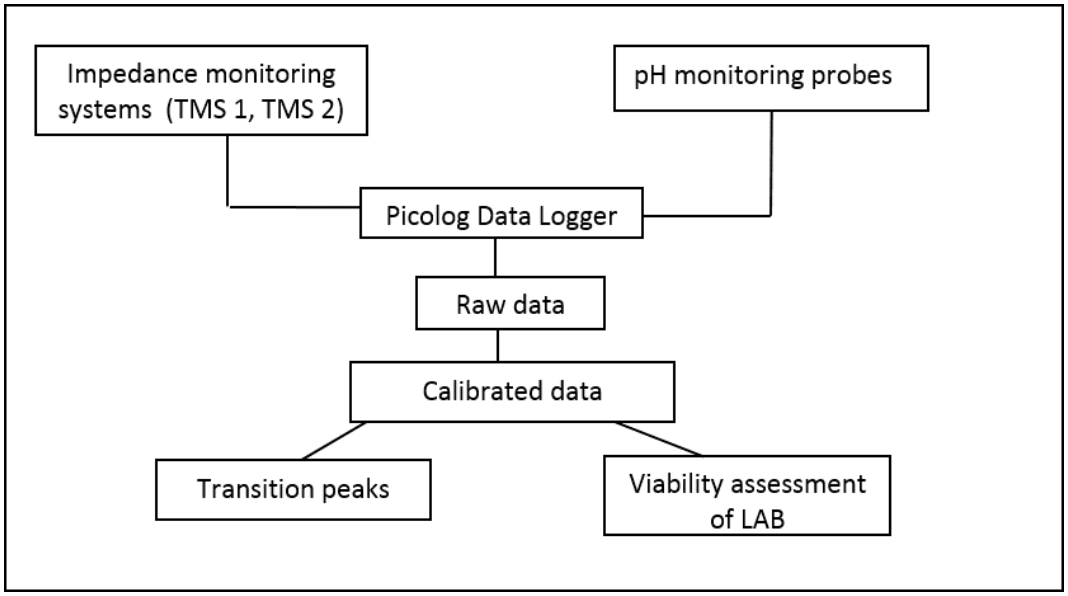

Figure 2.9: Connectivity of sensor systems and probes with the data logger and processing of raw data to compute the transition peaks of cryoprotectants in addition to assessing the post-thaw viability assessment of LAB after cryopreservation.

2.3.4 Grant-Asymptote EF600

The EF600 is a pre-programmed controlled rate slow cooling device (Grant Asymptote Centre Cambridge, UK). It was specifically designed for cryopreserving cryosamples in cryotubes or cryostraws. It was the world's first nitrogen or cryogen-free controlled rate freezer. It consists of a sample plate accommodating upto twelve cryotubes and ten cryostraws at one time. The device can cool down to -100 ˚C and hold that temperature until the machine is switched off. It was programmed to log and run slow cooling rates of 0.1 to 15 ˚C min^{-1}. The temperature ranges of the device were from + 20 to -100 ˚C (Faszer et al., 2006).

EF600 was chosen to observe the post-thaw recovery of the cells, in addition to ice initiation and glass transition temperatures of cryoprotectant mixtures at different cooling rates.

Cryosample (0.5 ml) was introduced to cryotubes and straws. The seeding and final temperatures were set manually on the EF600 software. For transition temperature measurements of cryoprotectants during the cooling and warming phase, temperature and screen-printed probes were inserted into the cryotubes or straws (containing cryosample) which were then placed on the metal plate of the EF600, and the device switched ON to run the temperature cycle. Warming was achieved either by resetting the slow cooler without removing the cryostraws and cryotubes which returned the plate temperature to 20 ℃, or by removing the cryotubes from the EF600 and warming them in air at room temperature.

2.3.5 Temperature sensor

Temperature changes during cooling and warming phase were monitored using a Honeywell S4a HEL-705-T-0-1200 platinum resistance temperature detector (Pt RTD) (Farnell Prod no: 1608185). Its temperature measurement range was (-200 to + 200 ℃) Fig. 2.10. A Pt-RTD was chosen because it has previously been shown to provide the most stable and linear response (Baker, 1998).

The temperature probe had a dedicated circuit connected to the data logger for logging the temperature profiles during transition events. To monitor impedance change with respect to temperature, the interdigitated and RTD probes were positioned in parallel (in tubes) or ‘end on’ (in straws) to each other.

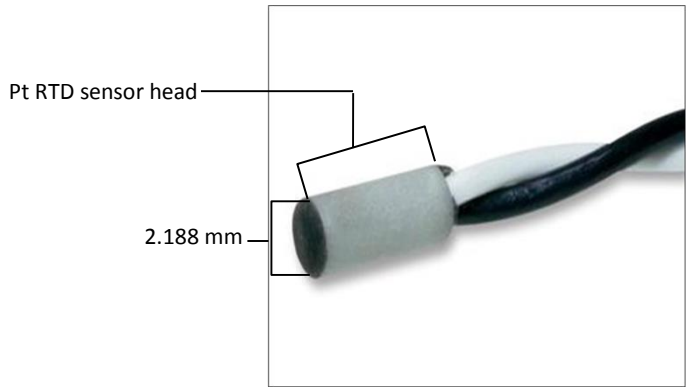

Figure 2.10: Platinum resistance temperature detector (Pt-RTD) probe used for temperature measurements. (Image from: http://uk.farnell.com)

The RTD probe was calibrated every six months using freezing point standards of dry-ice, liquid nitrogen, ethyl acetate and melting points of ice R.O water and saturated solution of NaCl. Calibration of temperature probe allowed monitoring its performance.

2.4 Cryoprotectant mixtures

10% Glycerol+0.15 M NaCl, 10% Me_2SO+0.85% NaCl and 5% sucrose+0.1 M NaCl concentrations were used to monitor transition events via the transition monitoring systems i.e. TMS 1 and TMS 2. Glycerol, sucrose and Me_2SO were selected due to their extensive use in the measurement of Tg and in *L. bulgaricus* preservation in the literature, enabling the comparison of experimental data with literature values for these mixtures (Panoff et al., 2000, Morris et al., 2006 , Oldenhof et al., 2005, Nesarikar and Nassar, 2007, Fonseca et al., 2006).

The reason for selecting 10% glycerol+0.15M NaCl for LAB cryopreservation was its better cryoprotective properties during cryopreservation (Fonseca et al., 2006).

Different percentage mixtures of glycerol and sucrose (5% glycerol+ 5% sucrose +0.15 M NaCl) and (7.5% glycerol+2.5% sucrose+0.15 M NaCl) were prepared for LAB cryopreservation as well. The aim was to evaluate the post-thaw viability after cryopreservation in non-penetrating and penetrating cryoprotectant mixtures.

2.4.1 Ice nucleators

Transition events of cryoprotectants and cryopreservation of LAB in glycerol suspension were performed with and without nucleators. Ice nucleation was performed by adding 0.1 g ml^{-1} of Asymptote nucleator, or 0.0025 % w/v of Snowmax beads, to the cryoprotectant mixtures. Ice nucleation, glass transition temperatures and post-thaw viability were all investigated and compared with the results obtained without nucleators.

2.5 Instrumentation to monitor glass transition events

Instrumental setup

The setup for monitoring glass transition (Tg) of cryoprotectants consisted of the Asymptote EF600 slow cooling device, screen-printed interdigitated electrodes, Pt-resistance temperature detector (Pt-RTD), multichannel data logger, and cryotubes or cryostraws as cryoprotectants containers (Figure 2.11). Both the screen-printed electrode and temperature detector were immersed in 0.5 ml of cryoprotectant solution inside a straw or tube and placed in the slow cooling device EF600.

The screen-printed interdigitated electrodes were connected to monitor transition monitoring system 1 or transition monitoring system 2 to monitor impedance change during cooling and warming phase. RTD probe monitored change in temperature by means of its own signal conditioning circuit.

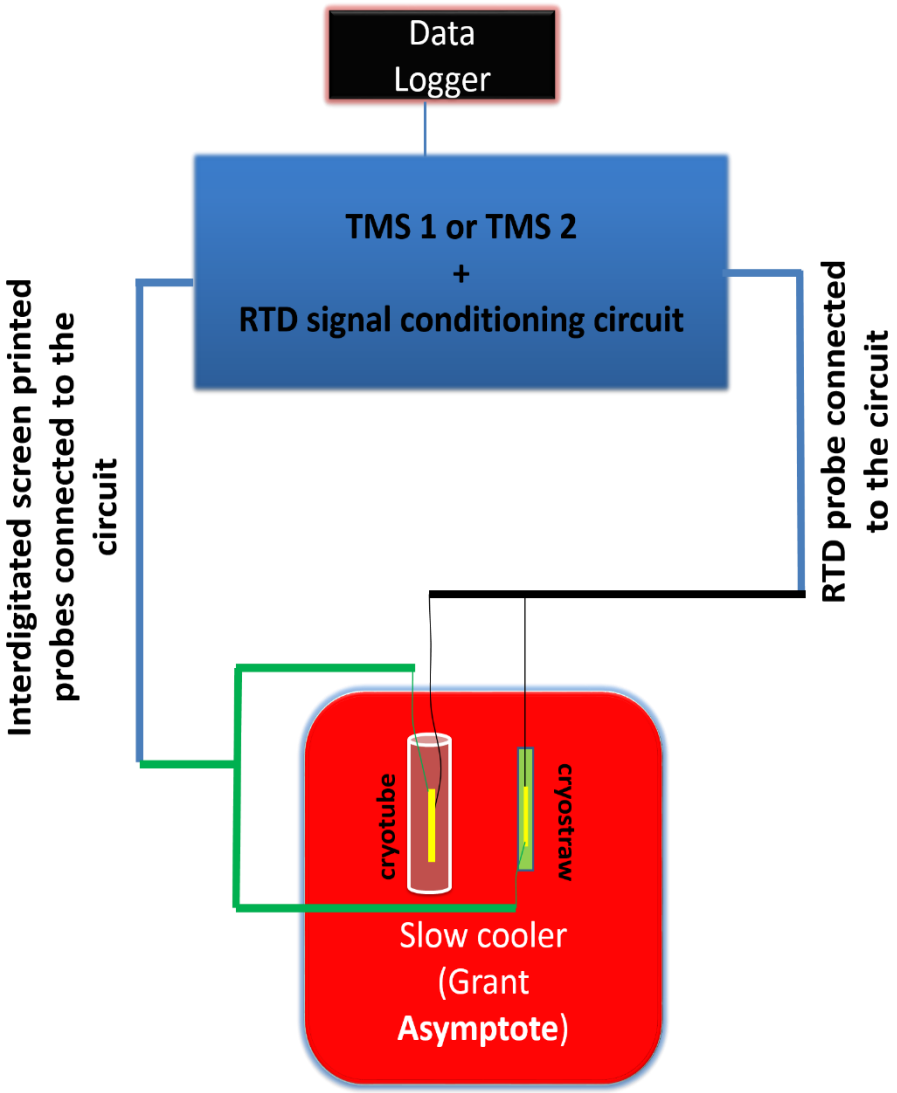

Figure 2.11: Experimental setup for monitoring transition events of cryoprotectants in cryotubes or cryostraws to obtain temperature vs impedance thermograms from Transition Monitoring System 1 (TMS 1) and Transition Monitoring System 2 (TMS 2).

2.6 Method of determining glass transition of cryoprotectants using fabricated sensor and sensor systems

Interdigitated screen-printed and RTD temperature probes were used to monitor glass transition events of cryoprotectants mixtures in cryotubes and straws. A sample volume of 0.5 ml was used to monitor phase change events during the cooling and warming cycle. Thermodynamics of cryoprotectant mixtures were monitored with and without nucleators. To investigate the effect of ice nucleation on post-thaw cell viability, the starter culture was prepared. Freeze dried sample of cells was resuscitated in saline, cells were incubated at 42 ℃ overnight in MRS broth. The pH of the culture medium was adjusted to 5.5 after two hours, and the cells centrifuged twice, harvested and the cell pellet mixed with CPAs. The cells+CPA mixture was slowly cooled in the presence of the probes that monitored the change in impedance with respect to the change in temperature over time.

2.6.1 Derivatisation process and determination of Tg points during cooling and warming phase

To obtain glass transition temperatures in cryotubes or cryostraws using impedance monitoring systems (TMS 1 and TMS 2), a mathematical approach was applied to the raw data obtained after cooling and warming phase of cryoprotectant mixtures. Firstly, the raw data was calibrated by means of calibration equations (see Chapter 3: section 3.1.2 and 3.1.3) and ice-initiation (θ^i) and ice melting (θ^m) temperatures of the cryoprotectants during cooling and warming cycle were observed (Fig.2.12).

Calibrated impedance and temperature values were mathematically derivatised to identify the transition temperatures of cryoprotectant mixtures. This approach

allowed the rate of change in impedance (*Z*) with respect to temperature alterations (θ) over time to be determined. First and second order derivatives were used to identify the slope and interception points accordingly.

The first order derivative (dy/dx) identified the slope of the line whereas 2nd order derivative (d^2y/dx^2) calculated the inflection point along x-axis. The inflection point is a point at which the curvature of the curve changes its sign (-ve or +ve) along the x-axis.

2.6.2 Derivatisation steps

Step 1): The data of temperature and impedance data were tabulated and plotted to observe the relationship of temperature, time and impedance with each other.

Step 2): The first order derivative of the data obtained from Pt-RTD and interdigitated screen-printed transition detecting probes were taken (dy/dx) and abbreviated as ($dZ/d\theta$)

Where;

dZ = derivative of impedance and;

$d\theta$ = derivative of the temperature.

Step 3): Second order derivative was calculated by polynomial equation (order 5) giving best fit to the slope acquired during cooling and warming phase of 1st order derivative.

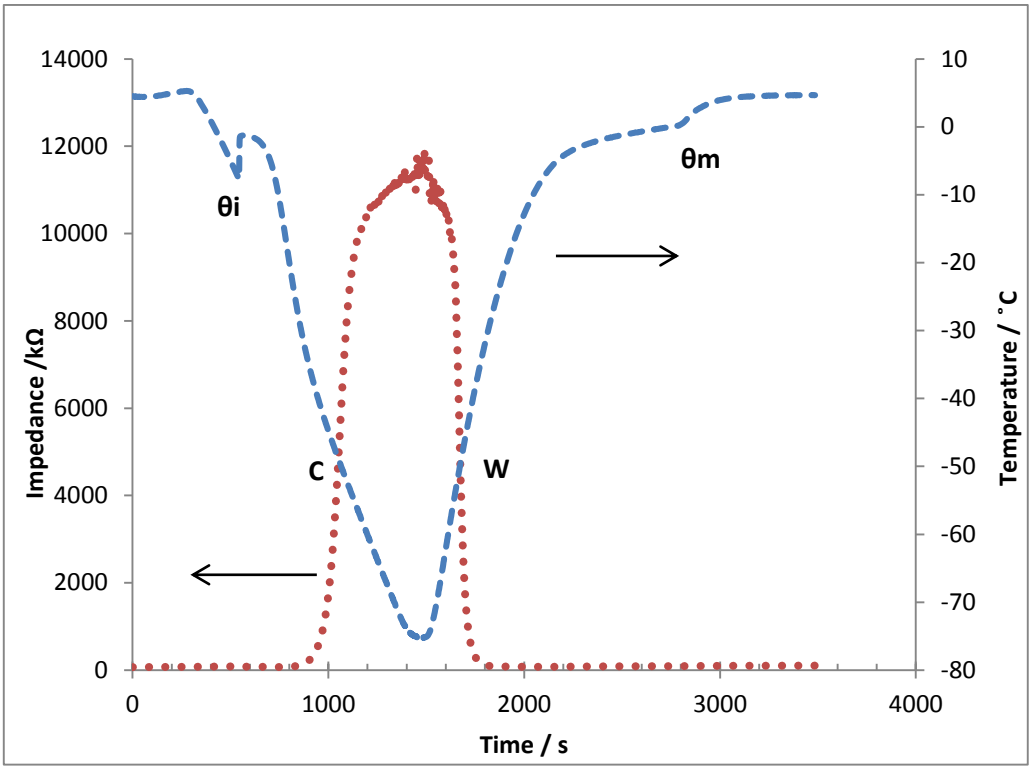

Figure 2.12: Example profiles of cooling (C) and warming (W) phase of a cryoprotectants solution monitored using temperature and impedance sensors. The graph is showing the exothermic θi (ice-initiation) and endothermic θm (ice melting) events during cooling and warming. Arrows indicate the appropriate axis. (• • •) Impedance. (- - -) Temperature.

2.6.2.1 First order derivatisation

The common equation of first order derivative is

$$\frac{\boldsymbol{dy}}{\boldsymbol{dx}} = 1st\ order\ derivative$$

Where;

$$\boldsymbol{dy} = derivative\ of\ dependant\ axis$$

and

$$\boldsymbol{dx} = derivative\ of\ an\ independant\ axis$$

By taking impedance and temperature values as an example to explain derivatisation, equation for 1st order derivative is explained as;

$$1st\ order = \frac{d\mathrm{Z}}{d\theta} \qquad (1)$$

The derivatisation of equation 1 was performed in Microsoft Excel as equations:

$$(\frac{dZ}{d\theta})_1 = (Z_4 - Z_1) \div (\theta_4 - \theta_1) \ldots derivative\ at\ Z_1$$

$$(\frac{dZ}{d\theta})_2 = (Z_5 - Z_2) \div (\theta_5 - \theta_2) \ldots derivative\ at\ z_2$$

$$\left(\frac{dZ}{d\theta}\right) n = Zn + 2 - Zn - 2/\theta n + 2 - Zn - 2 \qquad (2)$$

Where dn indicates the nth measured data points of the parameter. The transition function in Microsoft Excel was used to fit the curve via polynomial and applied equation 2 to the measured data in the region of events (i.e. cooling or warming phase transition event). An example of the result is shown in Fig 2.13.

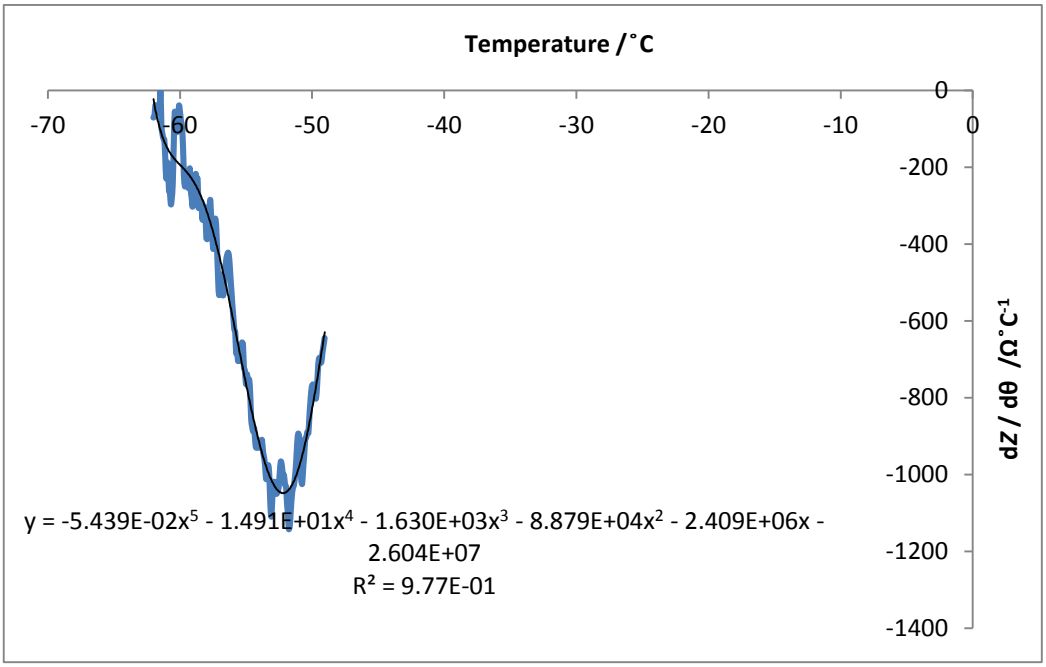

Figure 2.13: Example of first order derivative of impedance versus temperature data during cooling event. The polynomial equation was obtained by using the trendline function in Excel to fit a first order polynomial to the measured data points.

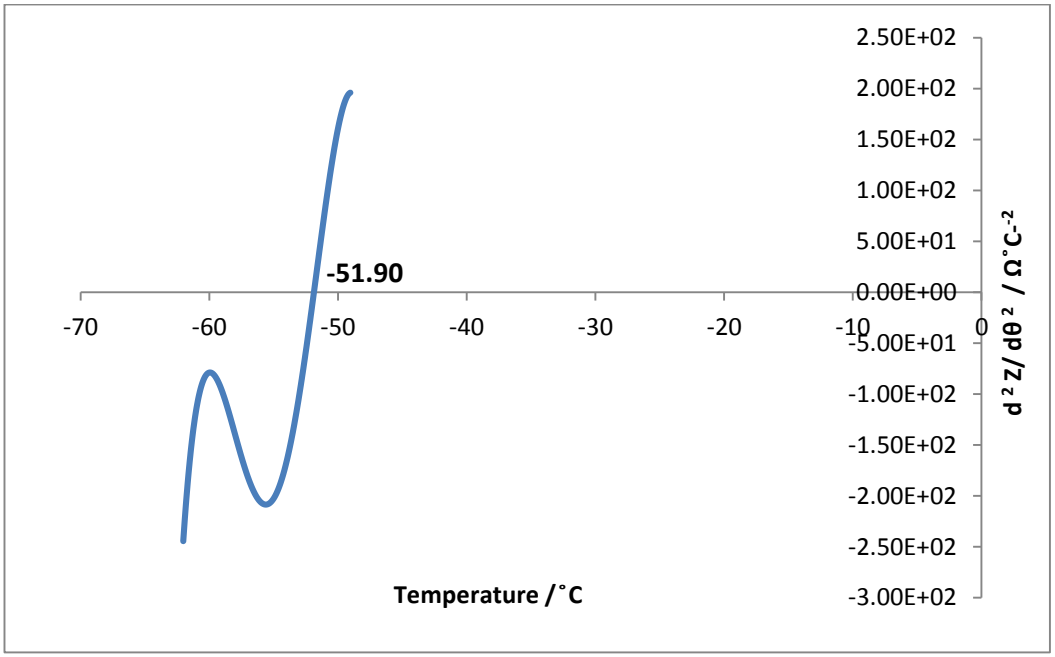

Figure 2.14: Second order derivative of temperature vs impedance during cooling event obtained by analytical differentiation of polynomial in Fig. 2.13 and numerical evaluation of result between -62 °C and -48 °C. The point of intercept on the temperature axis is the transition point of a cryoprotectants solution.

2.6.2.2 Second order derivatisation

Second order derivatives were obtained in Microsoft excel using the coefficients of the polynomial deriving the first-order derivative (Section 2.6.2.1, above).

For example,

$$dZ/d\theta \approx \theta^s + b\theta^4 + c\theta^3 + d\theta^2 + e^\theta \qquad (3)$$

then

$$\frac{d^2Z}{d\theta^2} \approx 5a\theta^4 + 4b\theta^3 + 3c\theta^2 + 2d\theta + e \quad (4)$$

An example of the result is shown in Fig 2.14.The intercept of the second order derivative with the x-axis was used as the point where the phase transition occurred.

2.6.3 Approaches used for derivatisation

Four different approaches were tested to explore the most reliable parameters used for derivatisation of the data, obtained using impedance and temperature probes. The approaches were:

a) Temperature vs Time;
b) Impedance vs Time;
c) Temperature vs Impedance; and
d) Impedance vs Temperature

(Figure 2.13 and 2.14).

2.7 Method to assess viability of lactic acid bacteria

Metabolic activity of fresh and post-thaw cultures of *L. bulgaricus* was monitored by determining the pH change in the growth medium using a digital pH meter (WPA CD330) connected to a glass pH electrode (Accumet 13-620-221, Fisher Scientific UK). Conventional measurements obtained from glass pH electrode were compared with the pH results obtained using carbon-metal screen-printed electrodes. Different kinds of reference electrodes (mentioned in section 2.2.3) were tested with the carbon-metal screen-printed sensors.

2.7.1 pH monitoring of LAB using screen-printed pH and conventional glass pH electrodes

pH monitoring of LAB was performed with a screen-printed working C-antimony + salt bridged Ag/AgCl reference electrode. The carbon-antimony working electrode, having a working surface of 0.2 cm and width of 0.5 cm, was joined with the screen-printed and salt bridged Ag/AgCl electrode. Back to back testing of the metabolic activity of the cells was monitored using conventional glass pH electrodes to compare the signalling response and results obtained from the two different kinds of probes.

A C-antimony working electrode with screen-printed salt-bridged Ag/AgCl reference, was connected to the data logger and immersed in 15 ml of the cell suspension (fresh/post-thawed) to monitor metabolic activity of LAB after cryopreservation. Both working and reference electrodes were calibrated before use, to ensure their sensitivity to pH change in the range from 8 to 2.

Conventional measurements were taken using a glass pH sensor to compare the results (obtained from screen-printed reference + C-antimony working electrode). The Ag/AgCl reference element of a conventional glass pH electrode as well as screen-printed Ag-AgCl electrode were used as a reference with the C-antimony working electrode to acquire post-thaw viability results of LAB.

The conventional glass probe was connected to the digital pH meter for monitoring the pH change of culture medium in mV units. The output of the pH meter was connected to the data logger for responses from screen-printed C-antimony + screen-printed salt-bridged Ag/AgCl electrodes and screen-printed C-antimony + reference element of conventional glass pH electrodes to compare sensitivity and accuracy in signalling response.

2.7.2 Cell culturing and cryopreservation

2.7.2.1 Media preparation and batch culturing of *Lactobacillus delbrueckii* subsp. *bulgaricus*

Freeze dried *Lactobacillus delbrueckii* subsp. *bulgaricus* CFL1 was used in this study as a cold-sensitive strain. For starter culture production, the culturing broth was prepared. 30 ml of the MRS broth was added into 100 ml conical flasks and sterilised for 20 min at 110 ℃.

Freeze dried cells were rehydrated by 1 ml of 0.15% NaCl and suspended in 30 ml of MRS broth, incubated at 42 ˚C (without rotation) for 19 hours and sub-cultured by adding 1 ml of hydrated cell suspension to fresh medium. The pH was adjusted to 5.5 with 8.2 M NH_4OH for optimal growth of cells.

2.7.3 Monitoring culture growth

Optical density analysis

Optical density of the initial inoculum was monitored at 480 nm to follow the growth rate in a culture medium. 100 µl of the cell suspension was diluted with 900 µl of 0.15 M saline in a micro cuvette for optical density measurements via spectrophotometer. An optical density of 1.5 to 1.6 was obtained after 19 h of incubation of the culture medium at 42 °C. Any cultures showing optical density lower than 1.5 (after 19 hr culturing) were not used for experimentation.

pH monitoring

Acidification due to the metabolic activity of the cells in the culture medium (nutrient broth MRS) was investigated every three hours by a conventional glass pH electrode connected to the pH meter. It allowed monitoring the metabolic activity of fresh and post-thawed LAB by determining the pH change before and after cryopreservation.

2.7.4 Sub-Starter culture production

Fresh starter cultures were incubated at 42 ˚C without agitation for 19 h. 2 ml of the starter culture was inoculated into the fresh medium for the sub-starter cultures. 19 h culture was used for cryopreservation and post-thaw culturing as it gave a final pH of 4.00 or an optical density of 1.5. If the culture was not metabolically active and did not show reduction in pH followed by increase in cell density, it was not used for sub-culturing or cryopreservation.

2.7.5 Cryoprotocols for cryopreservation

Three different cooling regimes with subsequent liquid nitrogen vapour storage for three days, were chosen to observe the effect of cryoprotocols and cold-storage on post-thaw viability of LAB. Thawing was performed at room temperature. Very slow (0.1 ˚ C min^{-1}), slow (5 ˚ C min^{-1}) and very rapid (liquid nitrogen plunge) cooling regimes were used for LAB cryopreservation. Very slow and slow cooling regimes were programmed into Grant Asymptote EF600 (from 0 to -90 ˚C) and held for 10 min to -90 ˚C, followed by liquid nitrogen plunge and storage of 0.5 ml cell suspensions for three days in liquid nitrogen vapours.

2.7.6 Post-thaw viability setup

Three sets of sub-starter cultures were prepared in MRS broth from a freeze-dried sample (provided by INRA France) of LAB CFL1 species. The cells were incubated (for 19 h) in 30 ml of MRS broth overnight at 42 °C without agitation, pH was adjusted to 5.5 by using 8.2 M NH_4OH (Sigma Aldrich) dropwise (after 3 h of incubation). The pH change was monitored by conventional glass electrode. The optical density and pH of 19 h old culture was approximately ±1.5 at 490 nm range and ± 4.25 range respectively. The cells were centrifuged twice with 0.15 M NaCl. The centrifuge (Denley BS400) was run at the speed of 3000 rpm for 10 minutes, providing a centrifugal force of 1116.8 x *g*. The pellet was mixed with 10% glycerol + 0.15 M NaCl with or without nucleator and 0.5 ml of cell suspension was added to each of 36 cryotubes. Twelve cryotubes were directly plunged into liquid nitrogen and stored in liquid nitrogen vapours for three days. Twelve cryotubes were slow cooled at 5 °C min^{-1} and twelve were cooled at 0.1 °C min^{-1} from 0 °C to -90 °C. Once -90 ˚C was reached, the tubes were plunged into liquid nitrogen and stored in liquid nitrogen vapours for 3 days. After storage and thawing at room

temperature, the contents of two cryotubes were incubated in 100 ml flasks containing 30 ml of the MRS broth. Three sets of six flasks were used for cell culturing:

a) set 1 (very slow cooling), i.e. 0.1 ˚C min^{-1};

b) set 2 (slow cooling), i.e. 5 ˚C min^{-1} and;

c) set 3 (direct liquid N_2 plunge).

After 19 h of culturing, the cells were stored in the fridge (to reduce their metabolic activity). pH of flasks were monitored one by one using six screen-printed antimony working electrodes each attached to an Ag/AgCl reference electrodes. Screen-printed probes were calibrated before experimentation by using MRS broth of pH 7, 4 and 5.5. Conventional measurements were also taken using glass pH probe. Figure 2.15 shows the schematic diagram of experimentation.

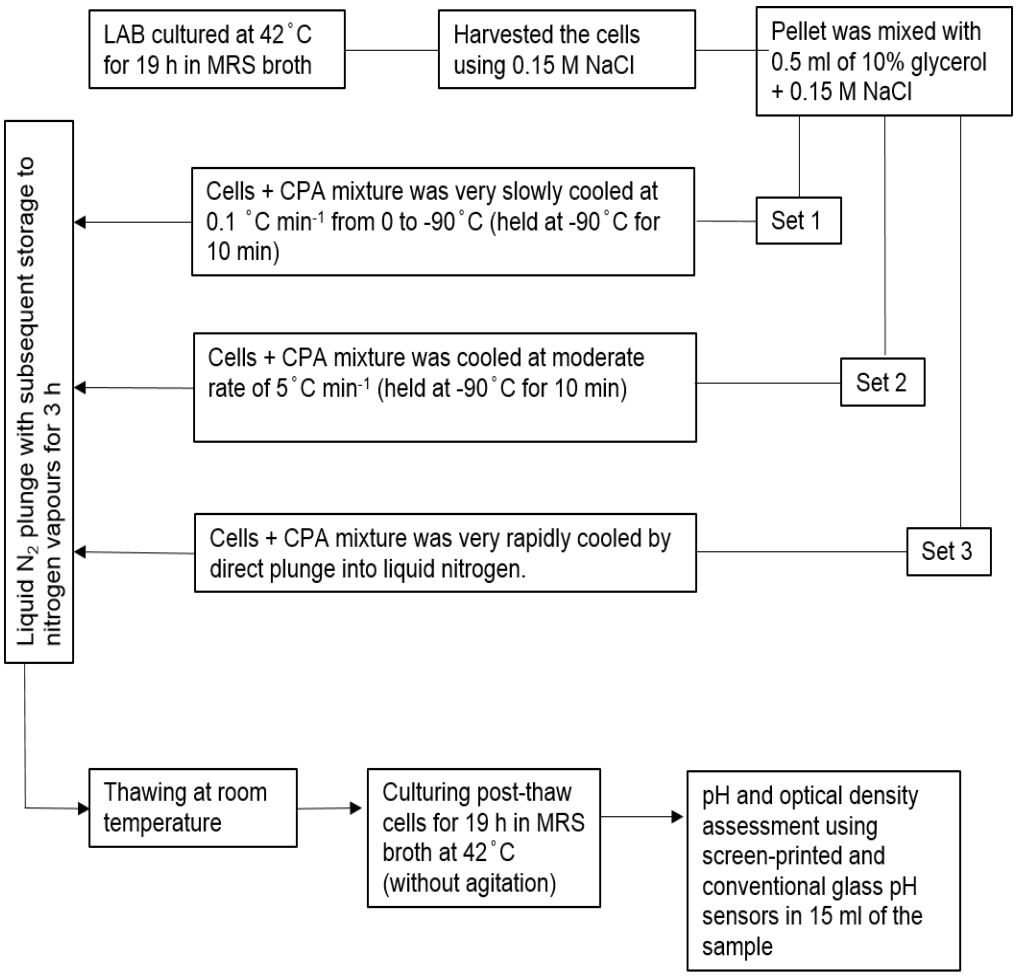

Figure 2.15: Schematic presentation of cryopreservation protocols used to assess post-thaw viability of LAB after storage for three days in liquid nitrogen vapours. The cells were cryopreserved with and without nucleators.

Chapter 3

Validation of the Instruments and Sensor Systems

3.1 Instrument Validation

Calibrations were performed to obtain acceptable impedance values from TMS1 and TMS 2 systems. The reasons for calibration were:

a) To study the functionality of systems by monitoring the relationship of the observed output with resistance of certain resistors and;

b) Omitting the offset (if present) and obtain the calculated values giving the linear response and converting the output mV to impedance MΩ.

Derived equations were used with the test data to obtain the values in MΩ. Transformations helped to minimise the circuit interference and obtain the data in impedance because impedance gives the information in direction

3.1.1 Transition monitoring system 1

The calibration of the transition monitoring system (TMS 1) was performed using resistors connected in series from 10 MΩ to 300 MΩ in place of the impedance sensors. The resistors were attached to the output channel of the TMS 1. The output signals were plotted against the corresponding resistance values and the regression analysis showed a linear relationship (Fig. 3.1).

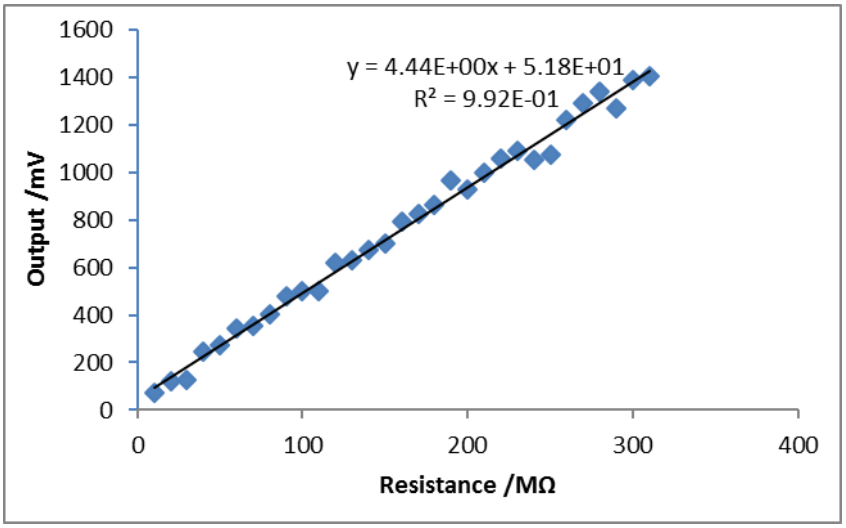

Figure 3.1: Calibration of transition monitoring system (TMS 1) using resistances in the range of 10 MΩ to 300 MΩ. (◆) Measured data. (——) Regression line with regression equation and coefficient of determination reported alongside

The calibrated impedance values were obtained using the following transformation:

$$Calibrated\ impedance\ /\ M\Omega = ((measured\ output - intercept)\ /\ mV) \div slope$$

Where the intercept and slope were the calibration values obtained by regression analysis (Fig 3.1).

3.1.2 Transition monitoring system 2

The six channels of transition monitoring system 2 were calibrated using resistances from (10,000-100,000) MΩ and (10-813.24) kΩ in series. The relationship was curved instead of linear (Fig. 3.2). The curved relationship was due to the difference in the circuit design making the output non-linear to the resistance. TMS2 was a printed circuit board (PCB). Similar calibration method was applied in this system yet a mathematical model was used to omit the offset and obtain linear relationship in MΩ.

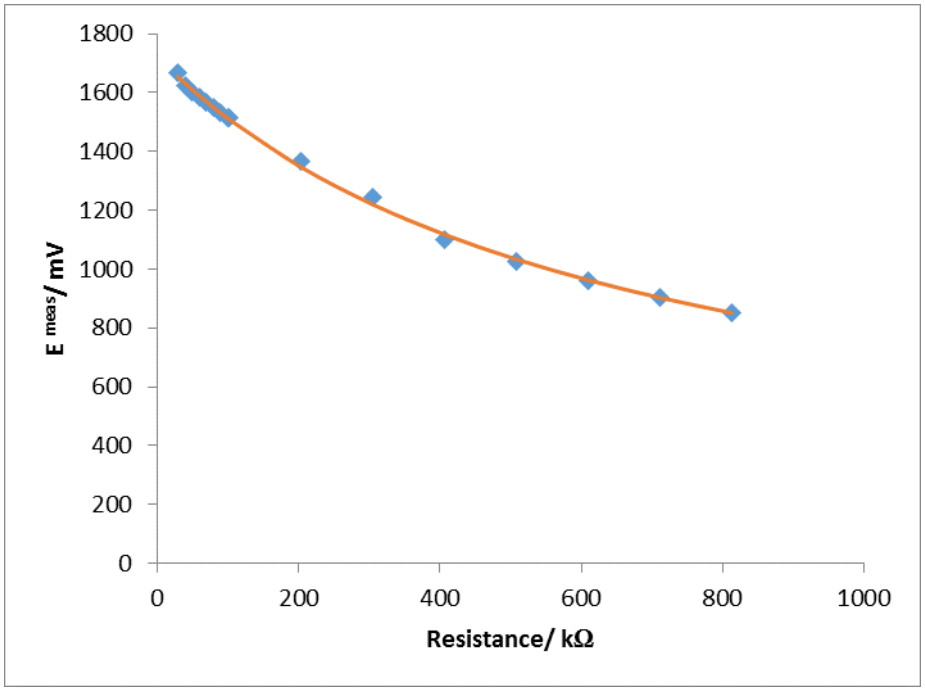

Figure 3.2: Calibration curve of channel 1 of the impedance circuit using resistors of (10 to 813.24) kΩ**.** (◆) Measured data. (——) Regression curve calculated using Microsoft Excel solver tool.

The SOLVER tool in Microsoft Excel was used to optimise the parameters R_{offset}, slope and intercept in the equation 3.1:

$$Output\ /\ mV = slope\ /\ mV\ k\Omega \div (R\_actual + R\_offset)/k\Omega\ + intercept\ /\ mV$$

…… (3.1)

Equation 3.1 was used for calibration by using an additional parameter (R_{offset}). The optimised parameters for each of the six channels are collected in Table 3.1.

Table 3.1: Values derived from equation 1 for each channel of impedance monitoring system with their offset points.

Channel	Slope mV / kΩ	Intercept /mV	R_{offset}/kΩ
1	1042781	164.9	680.4
2	968678	198.21	637.9
3	1075959	138.65	688.9
4	967003	205.6	638.5
5	164771	1054.7	242.7
6	996611	164.94	638.9

Calibrated impedance values were obtained using the following transformation (equation 3.2):

$$\mathrm{Z}\ calc\ /\ k\Omega = slope/mV\ k\Omega \div ((Emeas - intercept)/mV) - R_{offset}/\ k\Omega \ldots (3.2)$$

Where the values for slope, intercept and R_{offset} were taken from Table 3.1. Equation 3.2 was used for real measurements.

3.2 Sensor validation

3.2.1 Commercial RTD sensor

Pt-RTD temperature probe was calibrated to monitor the performance of the probe. Freezing points of dry-ice, liquid nitrogen, ethyl acetate and melting points of ice, R.O. water and saturated NaCl solution were used for calibration. Table 3.1 indicates the expected (from the literature) and measured values of melting points used for probe calibration.

The calibrated values indicate the temperatures obtained from the probe after applying the following transformation (equation 3.3):

$$\boldsymbol{Calibrated\ temperature\ /\ °C} = ((\boldsymbol{measured\ temperature} - \boldsymbol{intercept})\ /\ °\boldsymbol{C}) \div \boldsymbol{slope} \ldots . (\boldsymbol{3.3})$$

Where the values for slope and intercept were taken from the trendline through the calibration data, Fig 3.3. In Table 3.2, the error values indicate the difference between accepted and calibrated values obtained after applying equation 3.3.

Table 3.2: Calibration of Pt-RTD temperature probe using melting points of dry ice, Liquid nitrogen, ethyl acetate, ice, R.O. water and saturated NaCl solution.

	Accepted values /°C	Measured values /°C	Calculated values /°C	Error /°C
Dry ice	-78.5	-76.33	-79.37	0.87
Liq N_2	-195.78	-192.53	-195.57	-0.20
Ethyl acetate	-83.6	-78.45	-81.50	-2.09
Mp of ice	0	2.21	-0.83	0.83
Dist water	0	4.20	1.162	-1.16
NaCl saturated	-21.1	-18.89	-21.94	0.84

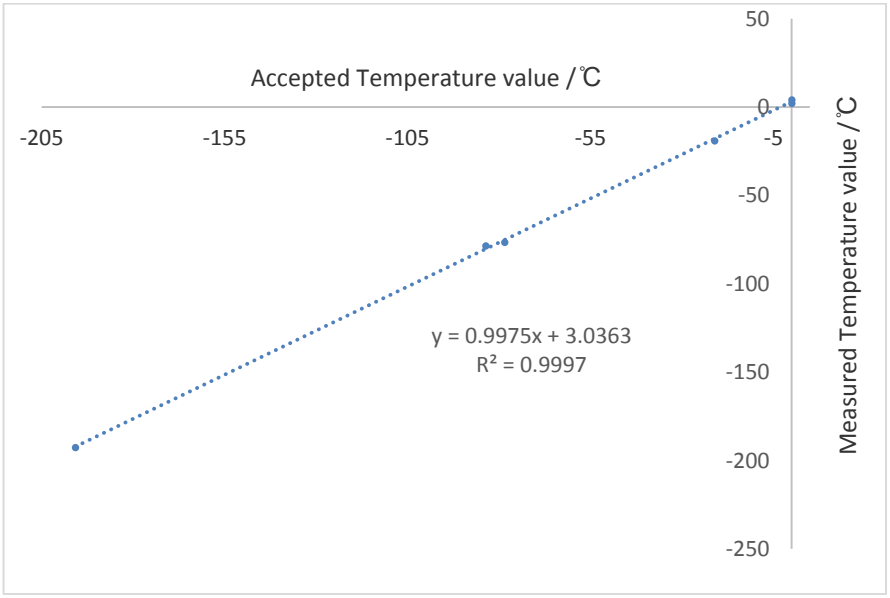

Figure 3.3: Calibration of Pt-RTD temperature probe. (•) Measured data. (·····) Regression line with regression equation and coefficient of determination reported alongside.

3.2.2 Screen-printed temperature sensor

Screen-printed temperature probes could be an alternative to omit the limitation of the sensor system. Initial experiments were carried out to design the probe. The carbon layer was painted over the polyester flexible films, dried in an oven for 30 min at 70 °C and observed their resistance using data logger (Fig 3.4) at a variety of temperatures.

The electrode was cooled from 20 °C to -100 °C and warmed back to 20 °C to determine the influence of temperature change on the working surface of electrode. The potential values at 20 °C before and after cooling cycle were ± 1.7 mV different. The results indicated that electrodes were responding at cooling and warming temperatures and giving consistent potential change before and after the cooling cycle (Fig 3.4) (Appendix I, Table IA).

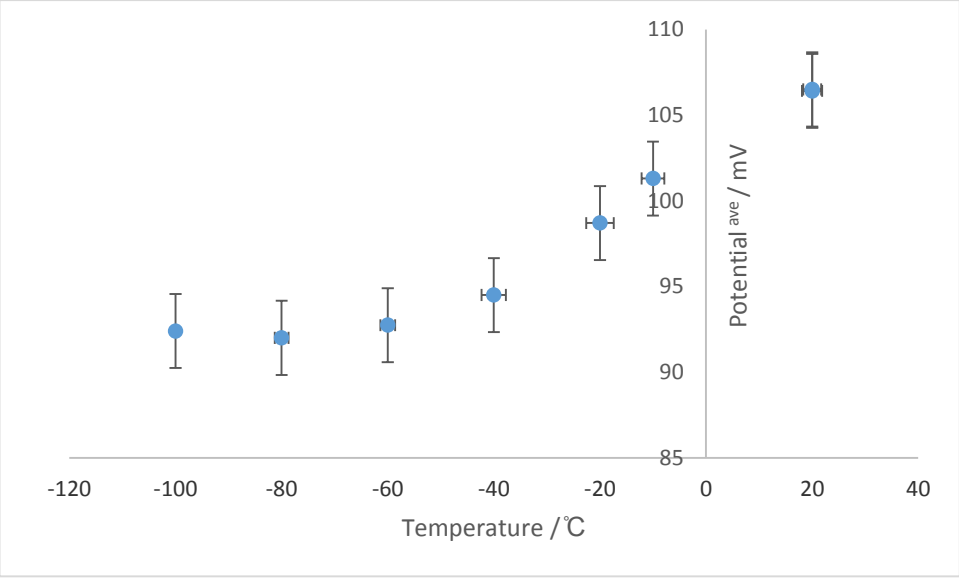

Figure 3.4: Response of screen-printed temperature probe in temperature range of +20 to -20 °C.

The results indicated that there is a possibility of using screen-printed temperature probes to observe temperature transitions of multiple CPA samples. Screen-printed temperature probes need further assessments and improvements in their design to make them more suitable for future use.

3.2.3 Screen-printed pH probes validation

3.2.3.1 Ruthenium pH electrodes

Titration was performed with 0.1 M of citrate and phosphate buffer solution and the pH of the buffer was adjusted to pH 9.00 before titration. Added 3 M nitric acid dropwise to reduce the buffer pH from pH 9.00 to approximately 1.00. (The ideal range of pH for LAB growth is from the range of pH 6.00 to 3.00).

Ruthenium (IV) oxide electrodes gave long response times towards calibration (from pH 8 to 2). This might be due to a drift of electrode potential, high electrical resistance or presence of highly oxidised metal causing ligand formation or metal complex. Although 37.5% of metal-oxide mixture was reduced with 0.5 M NaOH by cyclic voltammetry (CV) to obtain pure metal, but sensitivity towards pH change (from 8 to 2) was very poor. The response was neither linear (before and after CV) nor showing similar standard potential values at specific pH before and after CV confirming it not suitable for pH assessment Fig. 3.5 (Appendix I, Table IB).

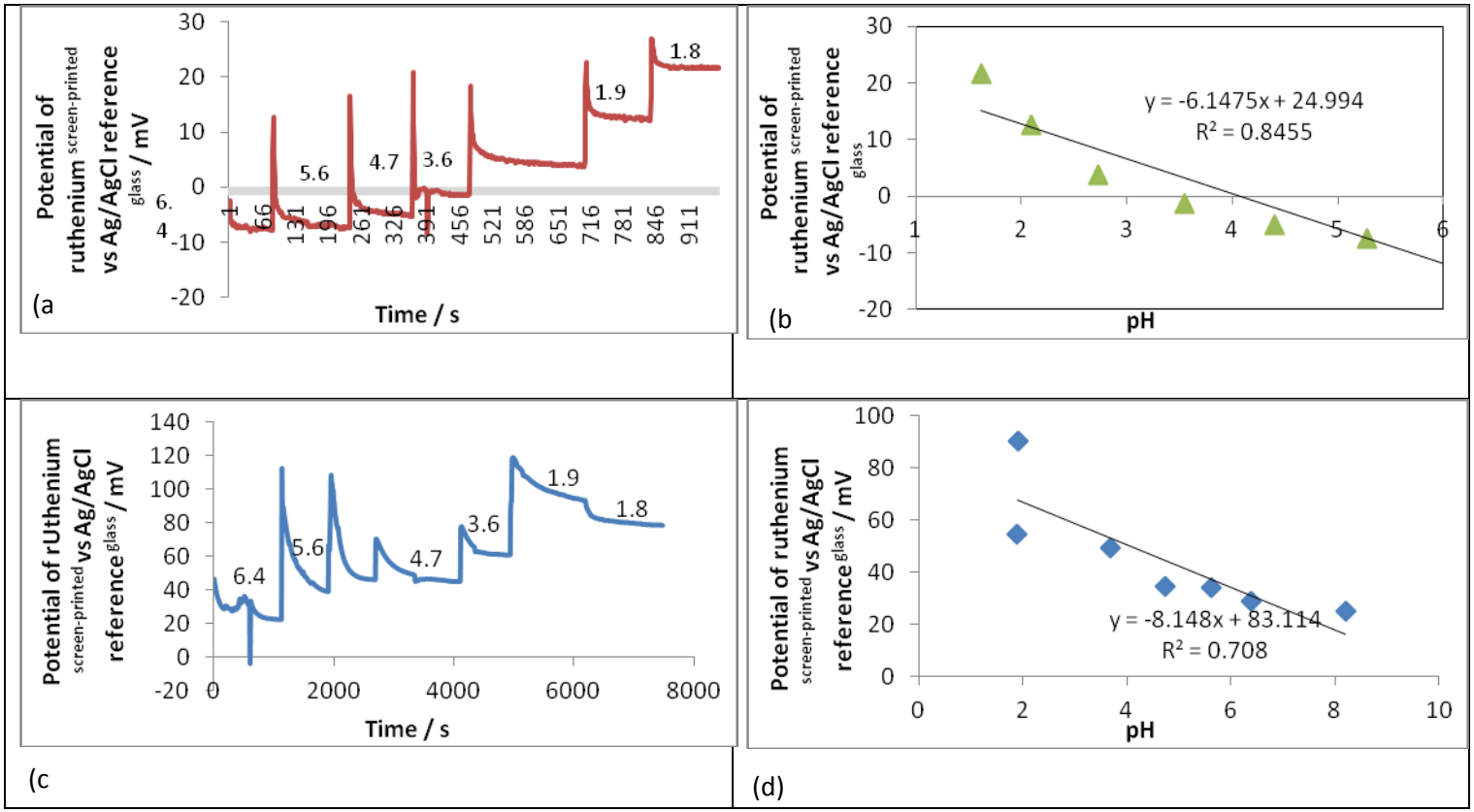

Figure 3.5: Calibration of a single screen-printed ruthenium(IV) oxide pH sensor before (a-b) and after (c-d) cyclic voltametery. (a,c) Measured potential of ruthenium electrode during titration of citrate-phosphate buffer with nitric acid. The numbers alongside the curves indicate the solution pH measured using a conventional glass electrode. (b,d) Corresponding 'steady-state' potentials as a function measured solution pH. '(▲, ◆) Measured data. (-------) Regression lines with regression equations and coefficients of determination reported alongside.

3.2.3.2 Response of antimony electrodes

An experiment was performed to compare the responses of a conventional glass Ag-AgCl reference electrode and a screen-printed antimony electrode. Potential measurements were performed in a water bath where temperature was controlled to 28 ˚C using a Ag/AgCl glass reference electrodes. Pre and post exposure to nutrient broth (NB) was investigated to check the linearity. Response to pH change was linear for 54.5% as compared to the other % of antimony electrodes. Figure 3.6 represented the results of calibration for 54.5% antimony electrodes in phosphate or citrate buffer (pre and post-exposure to NB).

The reason for immersion in nutrient broth (NB) for three hours was to investigate its effect on working electrode surface. Standard potentials of electrodes before and after immersion in NB were investigated to explore the linearity change. A pH range from 4 to 6 (before immersion in NB) showed linear change in standard potential. After immersion in NB, interference was observed in the linearity which might be due to interaction of ionic species with the metal to form metal oxides. Further confirmation was obtained by titrating the electrodes in NB (via suitable reference electrode) to investigate their response towards pH change in a culture medium.

Potentials were not greatly different after immersion in NB for 3 hours. The response of antimony electrodes towards pH change was linear as compared to ruthenium electrodes. 54.5% antimony electrodes were chosen to assess the metabolic activity of *L. bulgaricus*.

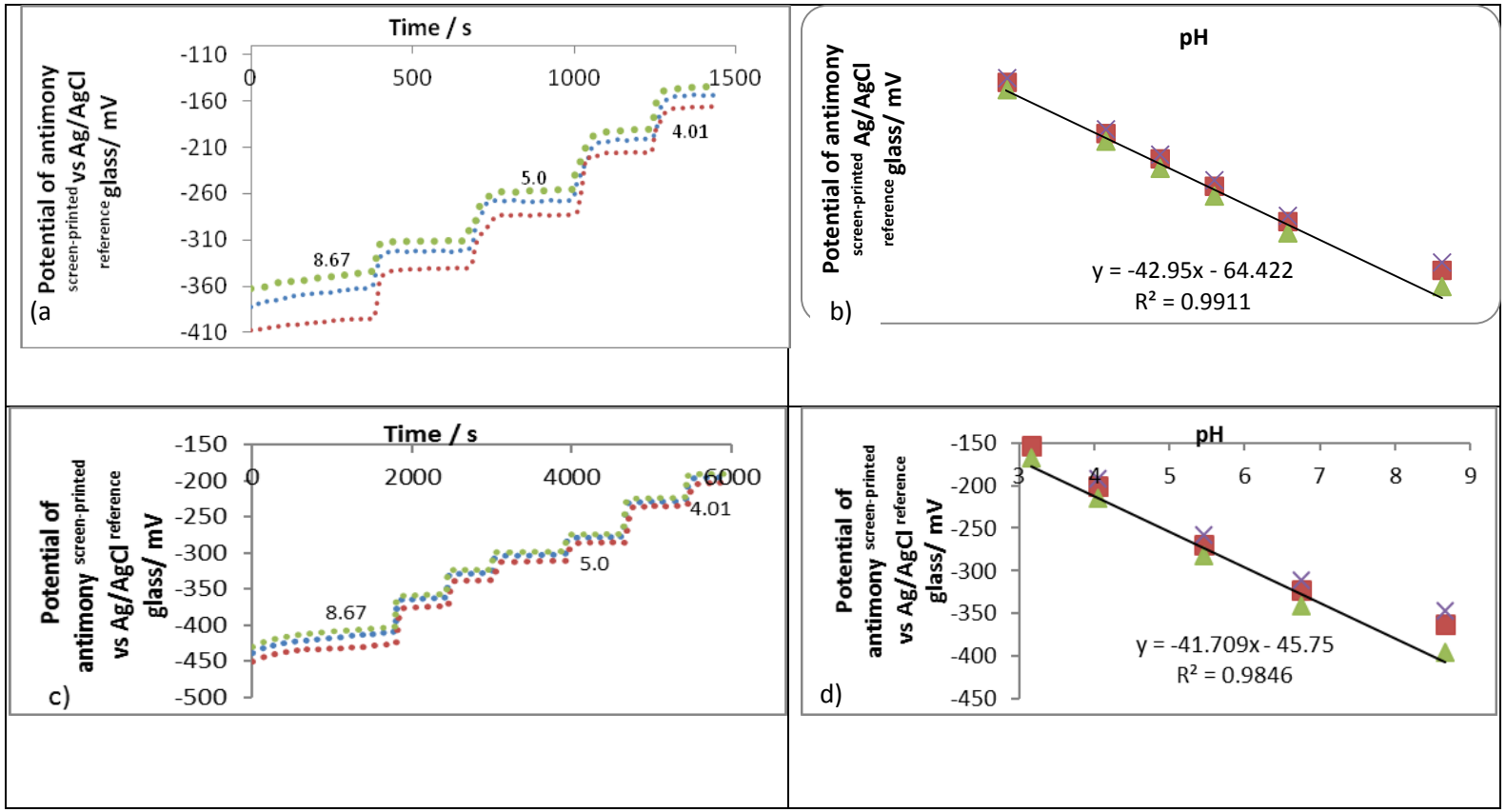

Figure 3.6: Calibration of antimony electrodes in citrate and phosphate buffers before (a.b) and after (c.d) exposure to nutrient broth. (a,c) Measured potentials before and after immersion in nutrient broth. Dotted lines indicated measurements of three antimony electrodes. (b,d) Corresponding 'steady state' potentials as a function of measured solution pH. '(▲, ■, ×) Measured data. (-------) Regression line through the combined data set with regression equation and coefficient of determination reported alongside.

3.2.3.2.1 Calibration of screen-printed antimony and glass pH electrodes with standard buffer solutions and MRS broth

Glass and screen-printed antimony electrodes were calibrated with standard pH buffers, MRS broth of pH 5.7 and 3 M HNO_3 before and after immersion in nutrient broth of pH 5.5 (Table 3.3). The reason for monitoring response of both probes in neutral, acidic and basic pH range was to determine their functionality as a working and reference electrode in different pH environments. When LAB grows in a culture medium, it decrease the pH of the broth from 5.5 to 3 (due to the production of lactic acid). Different pH ranges used in the experiments would conclude the functionality of the probes in certain pH levels.

Table 3.3: Calibration of antimony and glass electrodes with standard buffer solutions before/after titration with nutrient broth (NB).

St buffer solutions	Potential of glass pH electrode / mV		Potential of Antimony sp vs glass Ag-AgCl electrode / mV	
	Before	After	Before	After
pH 4.00	206.1	202.2	-180.9	-168.8
MRS broth (pH 5.74)	82.5	86	-304.3	-304.9
pH 7.00	14.4	11.4	-356.2	-338.8
pH 10.00	-159.3	-155.6	-432.54	-450.3
3M HNO_3 (pH 0.90)	369.4	362.1	-33.01	-38.3

Table 3.3 describe the difference in potential response before and after immersion in nutrient broth for 5 hours. The responses of the probes before and after immersion were not very different, indicating that the broth was not interfering with the working surface of the probes.

Titration of probes was also performed by addition of 3 M HNO_3 dropwise to the culture medium to reduce the pH. A glass Ag/AgCl reference electrode was used with the screen-printed antimony electrodes to investigate the pH responses. The response of glass electrode was monitored separately and the difference in potential response before and after immersion compared. Checking the responses before and after immersion in nutrient broth enabled interference due to ions or proteins present in the culturing medium to be detected. Responses at different pH levels were studied and linearity was investigated by regression analysis (Fig. 3.7 and Table 3.4).

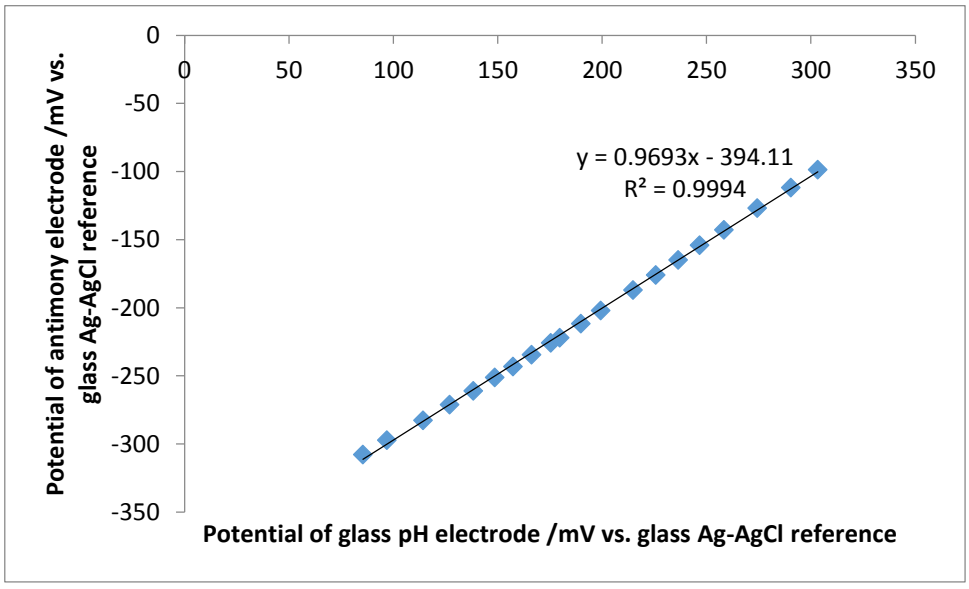

Figure 3.7: Comparison of antimony and conventional glass pH electrodes in nutrient broth titrated with nitric acid (3 M) to change the pH from 4 to 10. (◆) Measured data. (——) Regression line with regression equation and coefficient of determination reported alongside.

Table 3.4: Regression equations obtained from each channel connected to the screen-printed antimony and Ag/AgCl reference electrode with the comparison to the conventional glass pH electrode connected to the pH meter.

ch 1 /mV = (0.973±0.006)*(glass /mV)-(393.6±1.2)	$\mathbf{R_2}$ = 0.9993
ch 2 /mV = (0.966±0.006)*(glass /mV)-(394.2±1.2)	$\mathbf{R_2}$ = 0.9993
ch 3 /mV = (0.969±0.007)*(glass /mV)-(394.6±1.5)	$\mathbf{R_2}$ = 0.9990

The potential differences of the three antimony electrodes during titration in NB were not significantly different, concluding that electrodes gave reproducible responses and were sensitive to pH change (Table 3.4).

3.2.3.2.2 Long term responses of antimony

A) Response in MRS broth+ cells for three days

An experiment was performed to compare the responses of the glass Ag/AgCl and screen-printed antimony electrodes. The glass Ag/AgCl was used as 'working 1' and the screen-printed antimony as 'working 2'. The reference element of a conventional pH combination electrodes was used as the reference for both working 1 and 2 electrodes. Working electrodes were tested individually using MRS broth containing cells, to test the performance of electrodes in the presence of biological material. MRS buffer + cells at pH 7.00, 5.5 and 4.00 (adjusted using 8.2 M NH_4OH or 3 M HNO_3) were incubated at 42 °C, and used to calibrate the electrodes on each of three consecutive days (Appendix I Table IC) Fig. 3.8.

The responses of screen-printed antimony was near to expected Nernst response (i.e. -59 mV decade^{-1}) while there was the desired negligible response of conventional glass Ag/AgCl electrode. Consequently, it was concluded that the antimony (54.5%) screen-printed electrodes were suitable for pH determination in

nutrient broth when used in combination with conventional glass reference element.

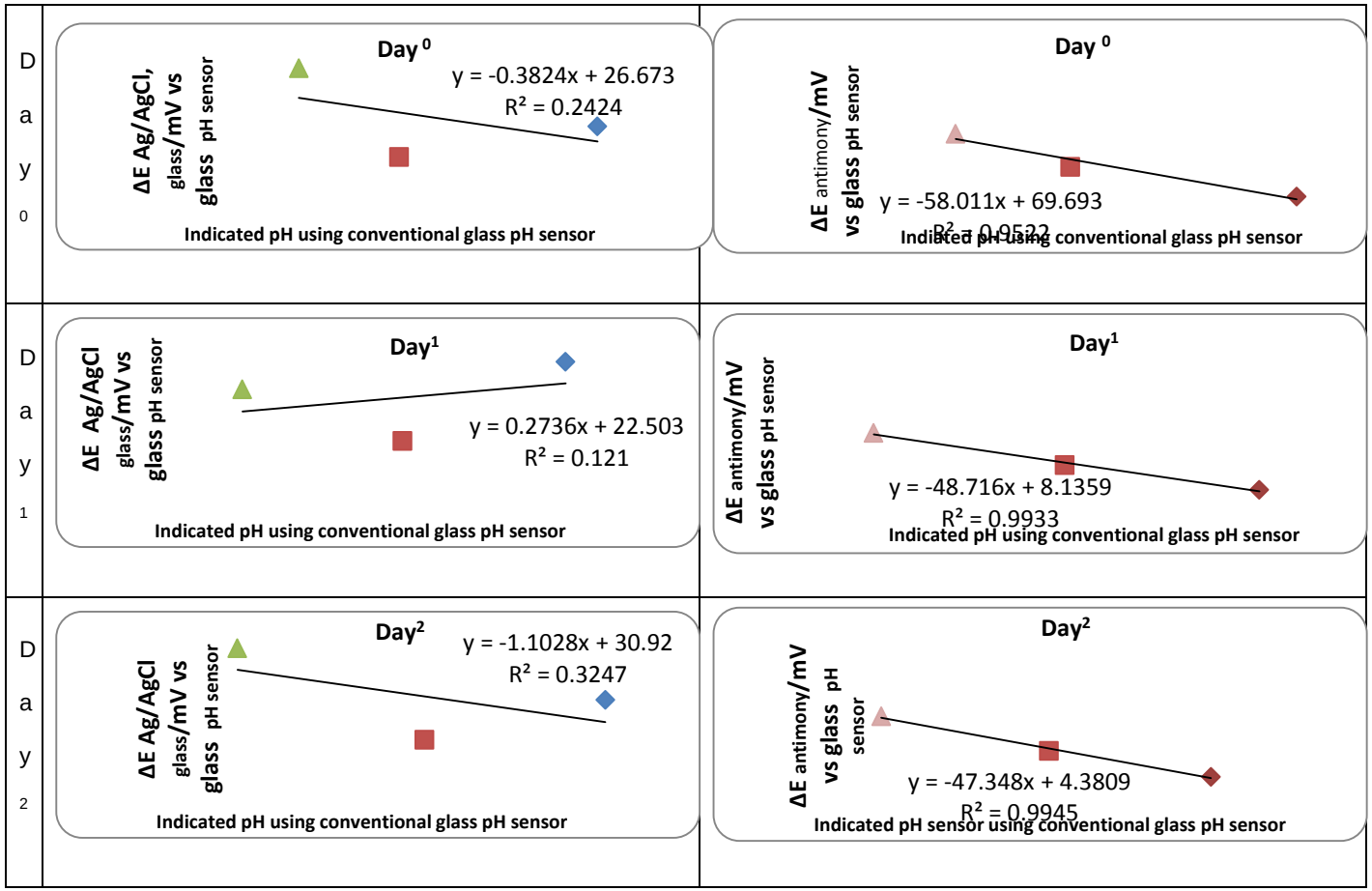

Figure 3.8: Nernst plots response of conventional glass Ag/AgCl reference electrode and screen-printed antimony electrodes intermittently calibrated during bathing in MRS broth and cells using combination glass pH sensor as a reference element. (Left)' after 'Ag/AgCl reference electrode. (Right) after 'antimony electrodes'

B) Response of screen-printed antimony for 5 days in MRS broth+ cells

Screen-printed antimony electrodes were intermittently calibrated using MRS broth at pH 7.00, 5.5 and 4.00 in the presence of cells incubated at 42 °C. The resultant calibration information is shown in Fig. 3.9. Regression of the calibration data over the five days of the exposure shows that the pH sensitivity of the antimony electrodes was maintained at 54 mV decade^{-1} with, if anything, a small increase in response over time.

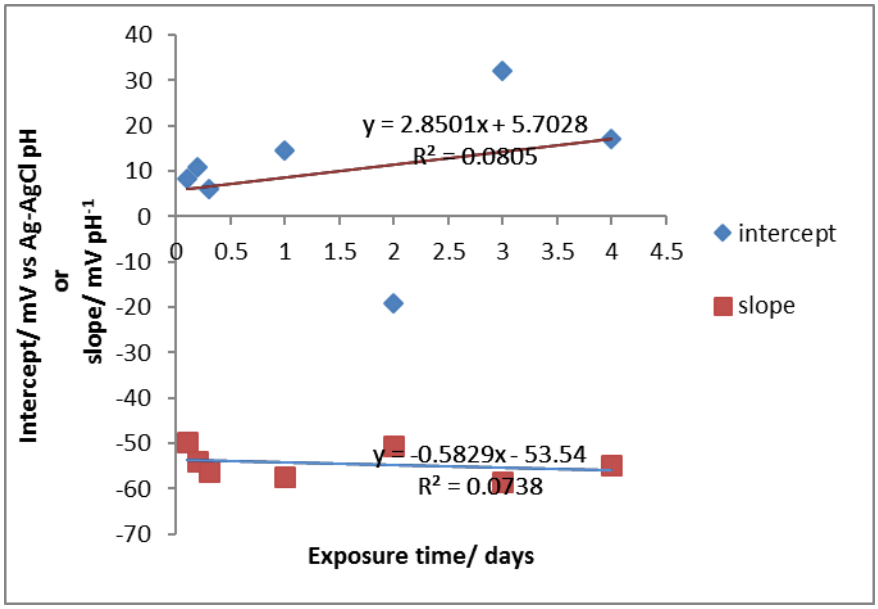

Figure 3.9: Intermittent pH calibration of pH calibration in MRS broth. Intermittent calibration results: (■) slope; and (◆) intercept. (—) Regression lines through intermittent calibration data. The corresponding regression equations and coefficients of determination are reported in the figure.

It was concluded that the screen-printed antimony electrode was robust and capable of monitoring post-thaw pH measurements in MRS broth.

3.2.4 Reference electrode selection and calibration

Different reference electrodes were tested with working electrodes to select the most suitable reference for LAB post-thaw viability assessment:

a) conventional glass silver/silver chloride electrode;

b) silver/silver chloride reference element of conventional glass electrode (pH sensor old);

c) silver/silver chloride reference element of conventional glass electrode (pH sensor new);

d) reference element of GEM carbon screen-printed Ag/AgCl electrode and;

e) screen-printed and salt-bridged Ag/AgCl reference electrode.

Conventional, glass encapsulated Ag/AgCl reference electrodes was used as 'gold standards' in the work described here, but the aim was to use a reference element that could be easily incorporated into small volumes of post-thawed cell cultured samples (MRS broth +cells) i.e. 1 to 0.5 ml. Much of the initial work was carried out using a single glass pH combination electrode but, a second combination was purchased. The two devices are distinguished as 'old' and 'new'.

Although the responses of reference elements of conventional glass electrodes were appropriate when used for research studies, the devices are inappropriate for future commercial use due to: a) their large size; b) the requirement for large volumes of samples for measurements; c) their inability to be integrated with screen-printed working electrodes, and d) their fragile nature.

3.2.4.1 Bare screen-printed silver/silver chloride reference electrode

The bare screen-printed silver-silver chloride reference electrode was tested against reference element of conventional glass pH combination electrode. Electrodes were tested with standard buffers (pH 4, 7 and 10.00) and non-standard solutions of MRS broth+ cells of pH (4, 7 and 5.5).

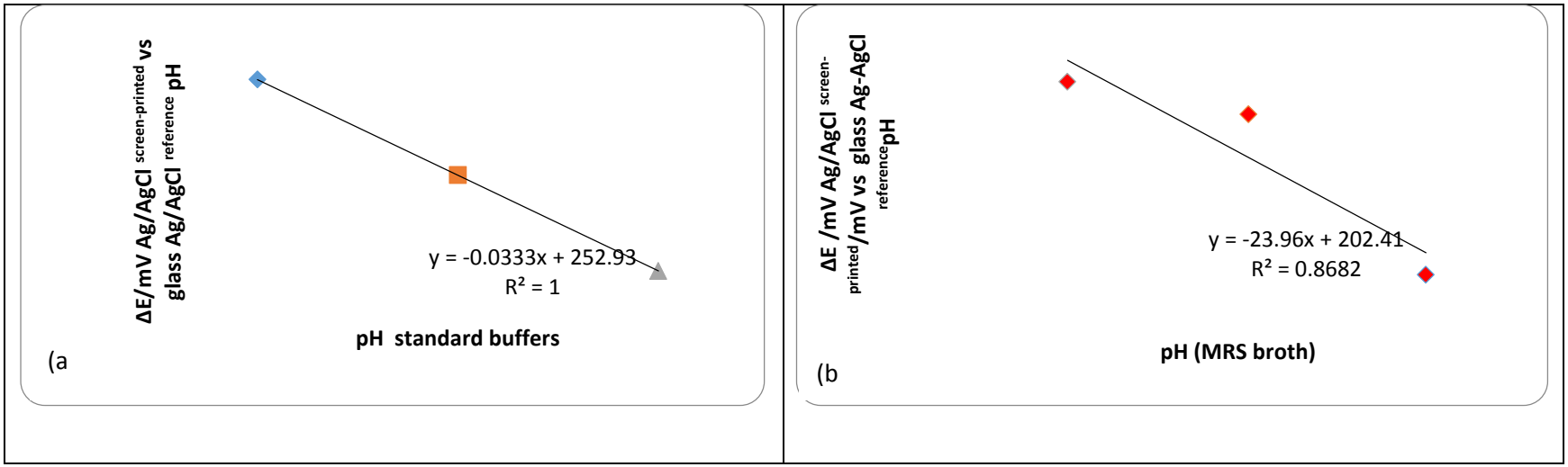

Figure 3.10: Calculated Nernst-type response of screen-printed Ag/AgCl reference electrode as a function of pH.

(a) Standard buffers, (b) MRS broth with adjusted pH. pH measurements were made by using a conventional glass pH combination electrode. Potential measurements were made with respect to the reference element of the same pH combination electrode. (♦,■,▲) Measured data; (—) Regression lines through measured data. The corresponding regression equations and coefficient are reported in the figures.

An ideal reference electrode must have a negligible Nernst-type response with the test solutions. The aim was to calculate the potentiometric response of Ag/AgCl screen-printed reference electrode in standard and non-standard buffers and determine the interference of test solutions with Ag/AgCl reference area of screen-printed electrodes. The graphs indicated satisfactory and unsatisfactory responses in Figure 3.10 (a and b respectively). Response of bare screen-printed electrode in standard buffers (pH 4, 7 and 10) indicated it as a good reference as potentiometric response is negligible i.e. 33µV pH units^{-1} (Fig. 3.10 a), however non-standard buffers of MRS broth+cells (pH 4, 7 and 5.5) indicated it as a bad reference due to Nernst-type response of -23 mV pH units^{-1}(Fig 3.10 b). The cells and protein components of the non-standard MRS buffer solutions were interfering with the bare screen-printed electrode and showing abnormal potentiometric response.

It was then decided to layer a salt-bridge barrier over the bare screen-printed Ag/AgCl electrode to expose the test solution indirectly. The salt bridge is a common structure present in conventional glass reference electrodes and could improve the Nernst-type response in non-standard test solutions.

3.2.4.2 Screen-printed Ag/AgCl reference electrode with salt bridge

A salt bridge was adopted to separate the test solution from the screen-printed Ag/AgCl reference, allowing minimal exposure of the reference element to the test solution. The hole in the film covering the layer of electrolyte permitted ionic contact between the outer test solution and the internal filling solution (0.1 M KCl).

The pH sensitivity and stability of their constructs was determined by measuring their potentials when transferred from potassium chloride (0.1 mol L^{-1}) into standard buffers (pH 4, 7 and 10). Measurements were repeated using the reference elements of either the old or new pH combination electrodes (Fig 3.11 and 3.12).

Performance of the screen-printed electrodes was acceptable but comparison of data in the two figures suggested that the reference element in the old pH combination electrode was less stable than in the new pH combination electrode. Consequently, the reference element in the new pH combination electrode was used for all subsequent measurements.

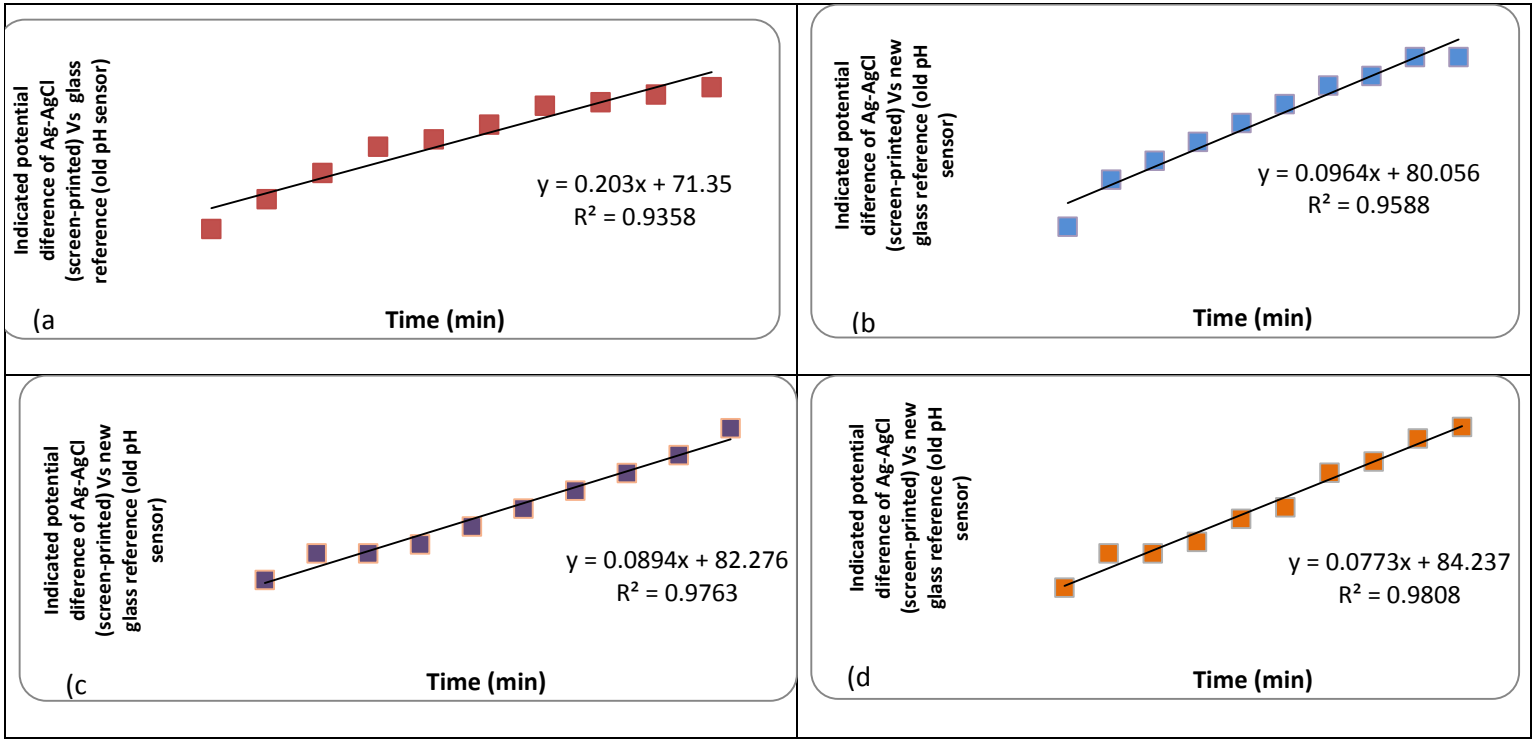

Figure 3.11: Responses of screen-printed Ag/AgCl salt-bridge constructs when moved from potassium chloride (0.1 mol/L; immersed overnight) to test solutions.
Test solutions: (a) Potassium chloride (0.1 mol/L): b) pH 4.00 standard buffer; c) pH 7.00 standard buffer; and c) pH 10.00 standard buffer. (■, ■) Measured data; (—) Regression lines through measured data. The corresponding regression equations and coefficient are reported in the figures.

Note: Reference element from old pH combination electrode was used for the comparison

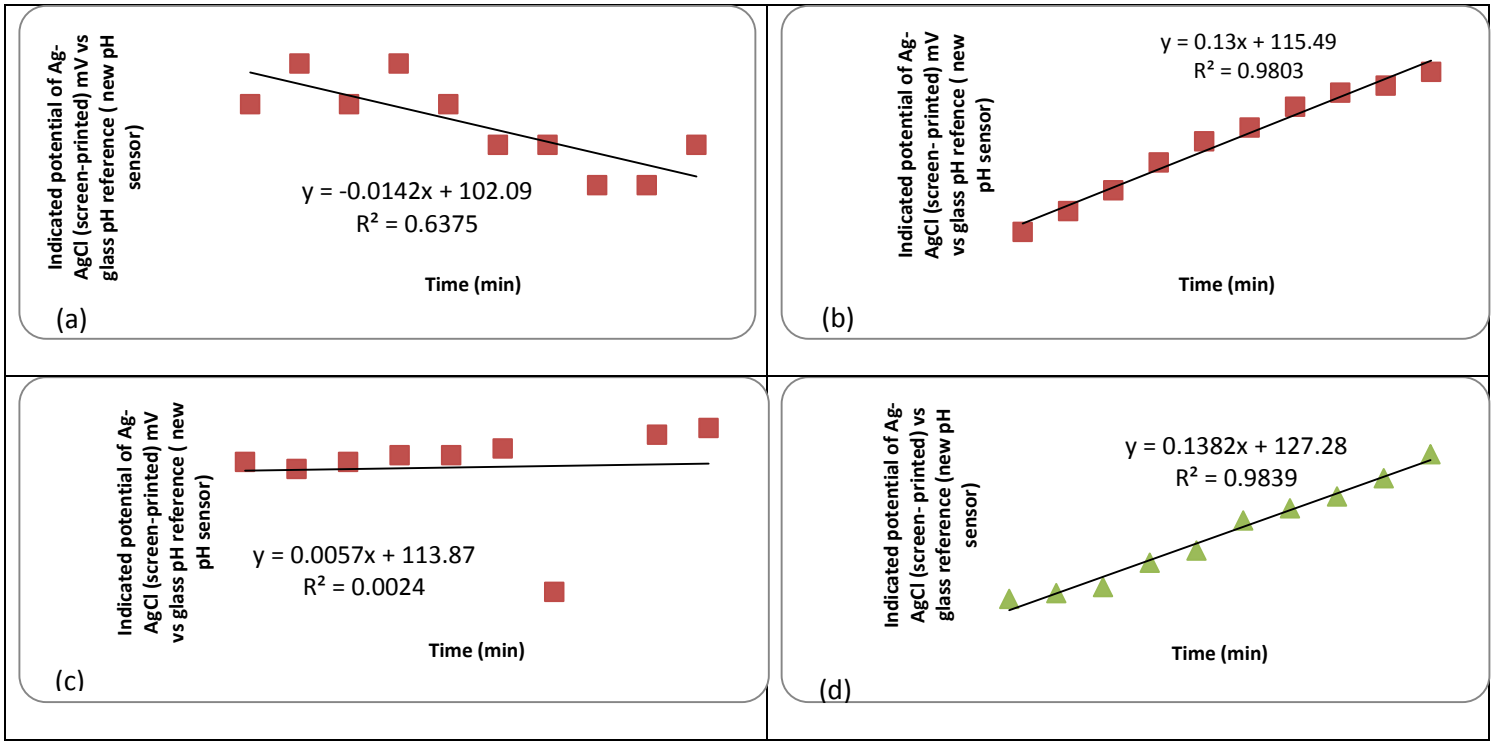

Figure 3.12: Responses of screen-printed Ag/AgCl salt-bridge constructs when moved from potassium chloride (0.1 mol/L; immersed overnight) to test solutions.
Test solutions: (a) Potassium chloride (0.1 mol/L): b) pH 4.00 standard buffer; c) pH 7.00 standard buffer; and c) pH 10.00 standard buffer. (■, ▲) Measured data; (—) Regression lines through measured data. The corresponding regression equations and coefficient are reported in the figures.

Note: Reference element from new pH combination electrode was used for the comparison

3.2.4.3 Stability evaluation of old and new conventional glass pH sensors

The stability of old and new conventional glass pH electrodes was studied in standard buffers of pH 4, 7 and 10 to examine the stability in potential response over time. The measurements were taken for 20 minutes. After 20 minutes electrodes were rinsed with distilled water, dried and re-immersed in the next standard buffer solution (Fig. 3.13).

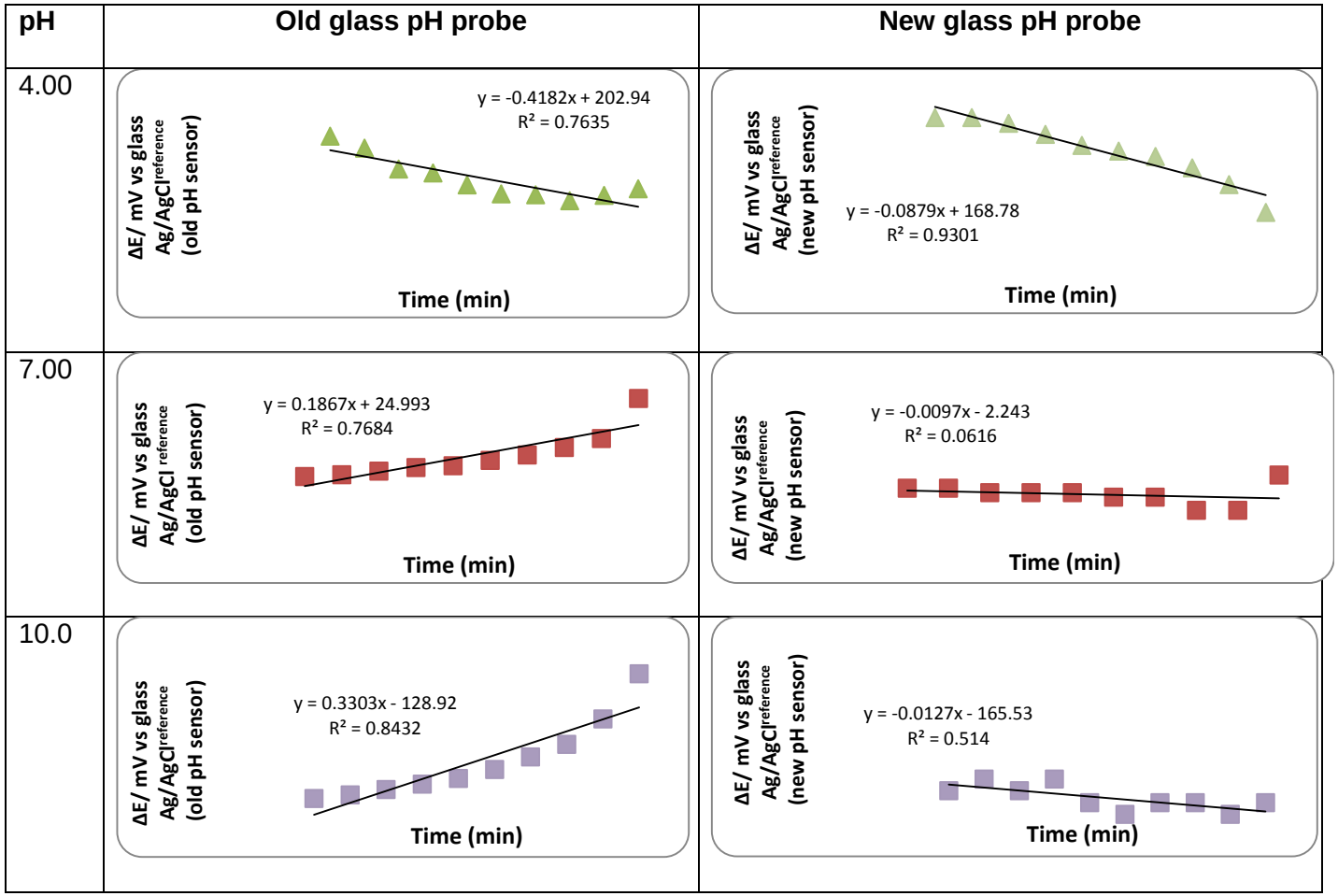

Figure 3.13: Stability of old and new conventional glass pH combination electrodes. Probes were immersed in standard pH buffers of pH 4.00, 7.00 and 10.00 for twenty minutes and measured their electrochemical response using pH meter.

The trend line of the new glass pH probe was 10 times more significant than the older glass reference element. As might be expected the new glass pH reference element was more suitable than that in the old pH combination electrode.

3.3 Conclusion

Transition monitoring systems (TMS1) and (TMS2) were calibrated to give acceptable impedance values across the calibrated ranges. One channel (channel 5) of TMS 2 was misbehaving during validation and was not used for future assessments. However, channels 1, 2, 3, 4 and 6 were responding over an acceptable range of impedance. Equations derived after calibrations were used to omit the offset of the systems. The equations were used to calibrate the raw data of the future experiments.

Screen-printed temperature probes would be ideal to monitor temperature in multiple samples at the same. Initial experiments showed the electrode gave an appropriate response towards temperature change. However further study is required to improve the responses of such devices.

54.5% of antimony screen-printed electrode was found to be most stable and sensitive carbon-metal electrode to monitor pH change in standard buffers and MRS broth as compared to ruthenium electrodes.

An appropriate reference electrode is required to work with screen-printed antimony working electrode. Conventional glass pH sensors and their reference elements were evaluated and shown to give expected responses both in standard buffers and MRS broth. Bare GEM carbon screen-printed Ag/AgCl reference electrodes showed interference in signalling response. A salt bridge was layered

over the Ag/AgCl screen-printed electrode and tested with reference elements of conventional pH sensors and screen-printed antimony electrode. The screen-printed salt bridged Ag/AgCl constructs gave acceptable performance as compared to the bare Ag/AgCl screen-printed electrodes.

The screen-printed antimony pH sensor was acceptable in performance with screen-printed salt-bridged Ag/AgCl reference and Ag/AgCl reference element of conventional glass pH electrodes. Additionally, the reference element of new glass pH sensor was more stable towards pH change as compared to the old glass pH reference element.

Chapter 4

Transition Events of Cryoprotectant mixtures During Cooling and Warming Events

4 Introductory information

The research was performed to develop a low cost transition monitoring sensor system to measure phase-change events during cooling and warming of cryoprotectant mixtures, in the presence or absence of electrolytes and ice nucleating beads. Binary and ternary mixtures of CPAs were used in cryotubes and cryostraws to study phase transition events using TMS 1 and TMS 2. Results were compared with the literature values by means of t-test analysis to explore the significant difference of the observed and the literature values.

Rationale

The base of the study was: 1) to explore the influence of cooling rate and ice initiation temperature on the glass transition temperature of cryoprotectant solutions; 2) to compare experimental values with the literature values obtained using conventional methods; 3) to select a suitable cryoprotectant or mixture of cryoprotectants for LAB cryopreservation.

Experimental design

Transition monitoring systems designed in this project monitored phase change events in 0.5 ml of single and multiple cryosamples. A Pt-RTD probe was used to monitor the temperature and interdigitated screen-printed probes were used to monitor impedance change in 0.5 ml of the CPA samples in cryotubes or cryostraws.

Cooling rates of (a) 5 °C min^{-1}, (b) 0.1 °C min^{-1} were set using a Grant Asymptote (EF600) controlled rate freezer and (c) direct plunge into liquid nitrogen. Protocols (a) and (b) were run from 0 °C to −90 °C followed by rapid plunge into liquid nitrogen. The warming event of the three protocols was monitored during slow warming of the samples in air at room temperature (for TMS 2) or switching the controlled rate freezer to return the plate temperature to 20 ˚C (for TMS 1).

General Introduction

The monitoring of ice initiation (θ^i), glass formation Tg^c, glass melting Tg^w and ice melting (during cooling and warming cycles) are described in this chapter. Table 4.1 shows the cryoprotectant mixtures used in this study.

Table 4.1: Cryoprotectant mixtures and electrolyte used in this study to monitor phase change events via sensors and sensor systems.
(+) indicates the presence of nucleator and/ or electrolyte to the CPA mixture;
(-) indicates the absence of nucleator and/ or electrolyte in CPA mixture.

CPA	Electrolyte (NaCl)	Nucleator
	+(0.15M)	-
10% Glycerol	-	-
10% Glycerol	+(0.15 M)	-
10% Glycerol	+(0.15 M)	+
20% Sucrose	-	-
20% Sucrose	+(0.1 M)	-
5% Sucrose	+(0.1 M)	-
5% Sucrose	+(0.1 M)	+
10% Me_2SO	-	-
10% Me_2SO	+ (0.85%)	-
5% Glycerol + 5% Sucrose	+(0.15 M)	+
5% Glycerol + 5% Sucrose	+(0.15 M)	-
7.5% Glycerol + 2.5% Sucrose	+(0.15 M)	+
7.5% Glycerol + 2.5% Sucrose	+(0.15 M)	-

In preliminary experiments phase change events of CPAs investigated in cryotubes and cryostraws were performed with the transition monitoring system 1 (TMS 1). The influence of electrolytes, rapid and slow cooling cycles was examined by monitoring change in ice-initiation temperature and glass transition temperature of the cryoprotectant mixtures.

The experiments provided the opportunity to determine the most appropriate electrodes, containers (cryotubes or cryostraws) for probes insertion, and the value of electrolytes in transition measurements of cryoprotectant mixtures.

Likewise, the influence of slow and rapid cooling cycles was examined to observe the influence of cooling regimes on transition temperatures of CPAs.

4.1 Principal of Transition Monitoring Systems TMS 1 and TMS 2

TMS 1 and TMS 2 had different circuitry but their mode of signalling response was in form of impedance (*Z*). Phase change events of different CPA mixtures were determined in different cooling regimes in the presence or absence of additive or nucleators. The systems determined ice initiation (θ^i), ice melting (θ^m) and glass transition (Tg) events during cooling and warming of the samples.

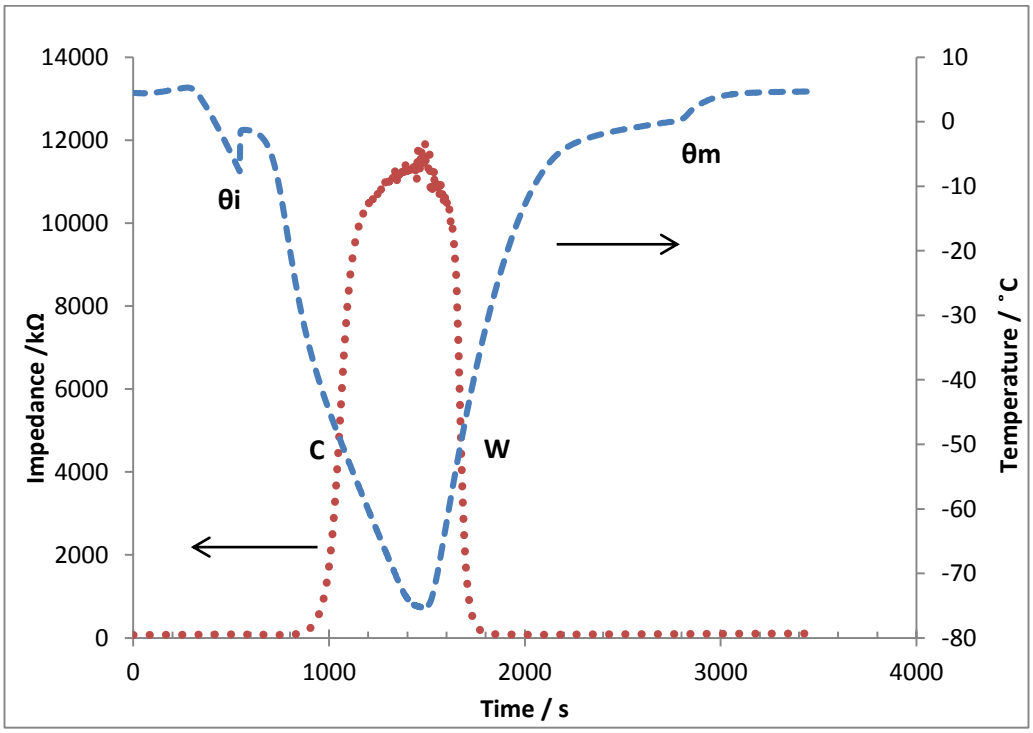

Figure 4.1: Example profiles of cooling (C) and warming (W) phase of a cryoprotectant solution monitored using temperature and impedance sensors. The graph is showing the exothermic θi (ice-initiation) and endothermic θm (ice melting) events during cooling and warming. Arrows indicate the appropriate axis. (⋯) Impedance. (- - -) Temperature.

The change in impedance (during cooling and warming) was monitored with respect to the change in the temperature (Fig 4.1). The aim was to study the effect of different cooling rates and ice initiation temperatures on Tg temperatures of CPA samples. Figure 4.1 explains the phase change events observed in a 0.5 ml of a CPA sample during cooling and warming events. As the temperature falls, a sudden peak is generated in the graph (Fig 4.1) indicating the point of ice initiation and ice melting of the sample. Further temperature drop resulted in freezing of the sample resulted in increasing the viscosity of CPA. The point at which water is maximally frozen, highly viscous CPA mixture present between the frozen channels is turned into glass. The point at which this change takes place is known as the glass transition temperature (Tg). In this study Tg was determined by a mathematical approach (derivatisation) mentioned in Chapter 2 determining the glass transition temperatures during cooling and warming events of cryosamples. During warming, the energy was released by the system resulted in ice and glass melting. The point at which glass melts is known as Tg temperature during warming.

4.2 Determination of eutectic point of electrolytes

The point at which a solution solidifies (during cooling) or melts (during warming) is termed as eutectic freezing or melting point of a solution (Rey, 1960). Electrolytes are generally used to depress the freezing point of ice. Additionally; they provide conductivity to the non-conductive solutions. Cryoprotectant solutions are organic and non-conductive in nature. In order to observe their transition events, an electrolyte provides the cationic and anionic movements in the solution. Moreover, to attain osmotic equilibrium in the biological systems, selection of the concentration of the electrolyte is essential during cryopreservation. 0.15 M NaCl

and 0.85% NaCl have been described as favourable concentrations of NaCl to preserve bacterial cells in the literature (Cocks et al., 1975).

The difference between ice initiation and ice-melting temperatures identifies the supercooling temperature of a liquid. It is a state of a liquid when the mobility of molecules slows (below its freezing temperature) while maintaining its liquid state. This phenomenon occurs at controlled slow cooling rates. At very rapid rates of cooling e.g. liquid nitrogen plunge, it could not be identified as the temperature fall is very rapid. Temperatures described in this study refer to the point of ice-initiation in the presence and absence of ice-nucleating beads.

4.3 Study of ice initiation event in cryosamples

The impedance data were converted from mV (millivolts) to nV (nanovolts) to determine if the change in temperature during ice-initiation influenced the impedance or not. Converting the scale values or magnifying the points of inflection would be helpful to observe the phase change event during cooling regime.

10% Glycerol + 0.15M NaCl was cooled at the rate of 1 ˚C min^{-1} until ice-initiation then plunged into liquid nitrogen. The warming was performed in air at room temperature. Figure 4.2.a and 4.2.b describes the ice-initiation phenomenon in detail.

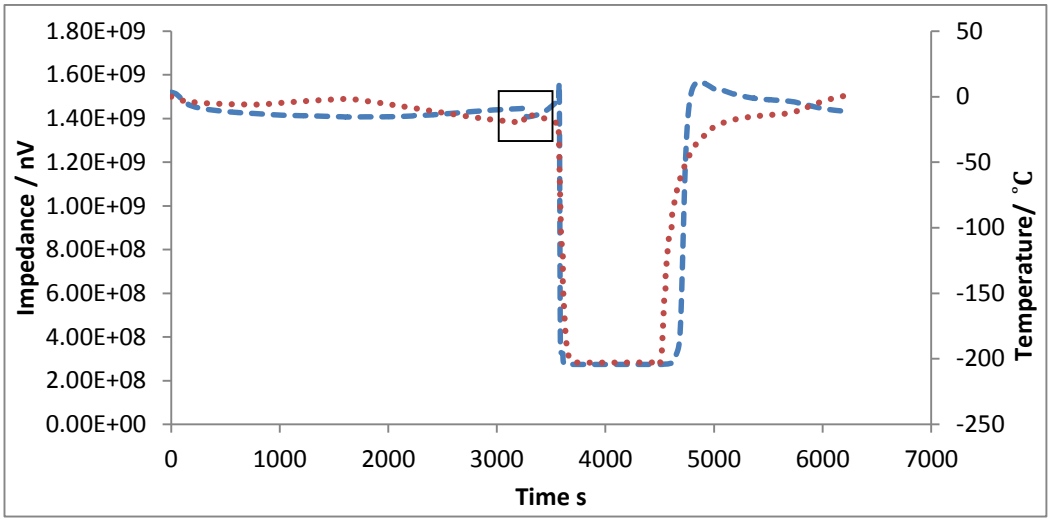

(a)

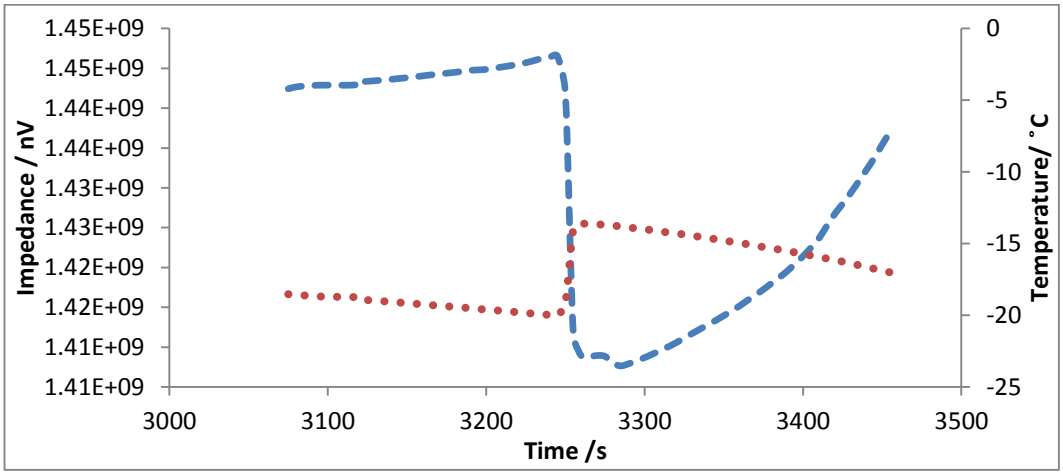

(b)

Figure 4.2: (a) Whole data set of 10% Glycerol+ 0.15M NaCl + LAB during cooling and warming events. Temperature (…) was observed in Celsius (˚C) and Impedance (---) was calculated in nanovolts (nV). The box indicated the point of ice-initiation magnified in graph (b).
(b) Magnified data of graph (a) where ice-initiation event took place, showing the rise in the temperature (due to exothermic reaction) causing loss in impedance.

Evidence of fall in the impedance was observed during ice-initiation. The rise in temperature due to exothermic event altered the impedance as the heat energy was released by the system. After ice-initiation the temperature started decreasing as the system was absorbing heat due to continuous ice formation. A rise in the impedance was observed (Fig. 4.1b) before liquid nitrogen plunge indicating that

changes in heat energy is taking place in the system. A rapid fall in the temperature and impedance was observed when the system was plunged into liquid nitrogen. When the system was in equilibrium phase (no heat gain or heat loss), the temperature and impedance levelled off (Fig. 1a). During warming, energy was absorbed by the system (endothermic event) resulted in initiation of ice-melting. A gradual rise in the impedance and temperature was observed until the entire system was converted from solid (ice) to the liquid phase.

This chapter is divided into three sections. In section 1, the eutectic temperatures of electrolytes and phase change events of binary and ternary systems of glycerol, sucrose and Me_2SO were monitored by transition monitoring system 1 (TMS 1). Impedance monitoring screen-printed electrodes of Type a and Type b (see Chapter 2 Figure 2.1) were used for transition monitoring in cryotubes and cryostraws. Transition temperatures were compared with those given in the literature to study the effect of electrolytes and nucleators presence and absence on transition shifts.

Section 2, covers the phase change events monitored by transition monitoring system 2 (TMS 2). Glycerol and sucrose mixtures with and without nucleators and *L.bulgaricus* were tested in cryotubes using Type c electrodes (see Chapter 2 Figure 2.1). The effect of transition temperature shifts due to the presence and absence of nucleators on post-thaw cell metabolic activity was the main aim of investigation in this section.

Section 3, defines the transition temperatures of quaternary CPA systems i.e. two different concentrations of penetrating and non-penetrating cryoprotectants at different cooling rates, in the presence or absence of nucleators. Tests were performed using TMS 2 and Type c impedance monitoring electrodes.

Section 1

4.4 Transition temperatures monitored by Transition Monitoring System 1

The cryoprotectants used in this study are most widely used agents in the field of cryobiology. By understanding the transition temperatures of CPA mixtures, the mechanism of freezing and thawing damage to cells could be reduced.

Transition temperatures of glycerol, Me_2SO and sucrose were monitored by TMS 1. Cryotubes and cryostraws were used for phase determination. Cryotubes and cryostraws were chosen as the most reliable containers to hold 0.5 ml of the CPA sample (without leakage) whilst allowing the incorporation of both screen-printed and RTD probes.

0.5 ml of the cryoprotectant mixture was added in cryotubes or straws. The Pt-RTD was immersed in the close proximity to the impedance electrodes. The probes were connected to the external monitoring setup. Cooling and warming rates were kept constant.

Temperature profile

Temperature measurements were taken at 5 second intervals, during slow cooling and warming of the cryotubes and cryostraws in the EF600 controlled slow cooler. A slow cooling protocol was used to cool the cryoprotectant down to -100˚C at the rate of 5˚C min^{-1} from 20 °C to -100 °C. The warming rate was 20 °C min^{-1} provided by switching the EF600 to return to the start temperature of 20 ˚C.

Initially, eutectic freezing point of saline mixtures was determined in cryotubes and straws. Experiments were then performed with different concentrations of CPAs in the presence or absence of electrolyte and nucleator.

4.4.1 Determination of transition temperatures of binary and ternary systems

Transition temperatures of binary e.g. H_2O-glycerol and ternary H_2O-NaCl-glycerol systems have been studied to determine its influence on salt segregation in the CPA solutions. It was reported by (Cocks et al., 1975, Hubalek, 2003) that the addition of CPA to salt-water mixture causes further reduction in eutectic melting point of ice.

CPAs are hydrophilic in nature and have a tendency to make H-bond in the solution. The bond resulted in reducing the salt separation from the solution and it delimits the effect of osmotic shock to the cells during ice formation (Lovelock, 1954, Lovelock, 1953b). The reduction in salt separation was due to trapping of salts in a highly viscous (glass) phase (Jochem and Körber, 1987).

Glycerol and Me_2SO are most commonly used penetrating CPAs reflected in the literature to preserve microorganisms. They have a strong tendency of decreasing the freezing-point of biological solutions by binding with intracellular water resulting in prevention of cell dehydration, formation of larger ice-crystals and making cytoplasmic membrane more plastic. They also prevent eutectic crystallisation and stimulate the formation of fine glass phase below eutectic point. The formation of glass prevents hyperosmotic (solution effect) injury to biological samples (Hubalek, 2003). Another protection theory for penetrating CPAs is that they reduce the intracellular vapour pressure during ice formation which results in an increased extracellular vapour pressure. The change in vapour pressure causes the reduction in migration of water across the cells (Mazur, 1960).

Conversely, non-permeable CPAs (sucrose, glucose) are absorbed on the microbial surface without interacting with cell wall or cell membrane of a biological

sample (Meryman, 1974). They form a viscous layer causing partial water efflux and preventing growth of ice crystals in intracellular matrix by increasing the viscosity of the solution as temperatures falls.

Low concentrations of salts dissolved in the CPA solutions help minimise the osmotic shock and are essential to provide osmotic equilibrium to the cells during cryopreservation (Harrison Jr, 1956). Very high concentration of salts in CPA mixtures cause osmotic shock and the denaturation of cell structure during freezing and thawing (Meryman et al., 1977).

In the present study TMS 1, Pt-RTD temperature probe and screen-printed impedance monitoring electrodes were used to examine the ice-initiation temperature and glass transition temperature of binary (CPA-H_2O) and ternary (CPA-NaCl-H_2O) systems, and the influence of electrolytes on ice initiation and glass transition temperatures of the solutions.

The reason for choosing different CPAs systems of glycerol, sucrose and Me_2SO was their extensive application in cryopreservation of cells. By determining their transition events during cooling and warming via sensors and sensor systems developed in this project, and choosing suitable cryoprotocols and CPA systems for LAB cryopreservation would allow the development of cheap, less complicated and real-time preservation technique for LAB cryopreservation. It would also help minimising cryo-damage to the cells during cooling, warming and long term storage of samples, enabling improved longevity of LAB cultures after cryo storage.

4.4.2 Determination of transition temperatures in the presence of ice-nucleators

Effect of ice-nucleators was studied for glycerol-NaCl-H_2O system to determine its effect on ice-initiation temperature and glass transition temperatures during cooling and warming cycles.

4.4.3 Transition temperatures in literature

Table 4.2 and 4.3 show transition temperatures of additives and cryoprotectant mixtures given in the literature. The concentrations described in the tables have informed the literature values of the electrolyte and CPA concentrations used for the experimentation in this study.

Table 4.2: Eutectic melting point of 0.154 M NaCl in literature.

Salt	Volume	Eutectic melting point of ice θ^m (endothermic peak) ˚C	References
NaCl.$H_2$0/ ice	0.154 M	-22	(Rey, 1960, Fujiwara and Nishimoto, 1998, Chen et al., 2005)
	0.85%	-21.8	(Magnusson and Edebo, 1976)

Table 4.3: Glass transition temperatures of different cryoprotectants (CPAs) in literature.

CPAs	Concentration	Additive	Concentration	Glass transition (Tg˚C)	Technique	Reference
Glycerol	10%	NaCl	0.15M	-62.7 (on warming)	DSC	(Fonseca et al., 2006a, Morris et al., 2006a)
Glycerol	10%			-40 to -42	DSC	(Morris et al., 2006)
Sucrose	5%	NaCl	0.1M	-39	DSC	(Nesariker et al., 2007)
Sucrose	20%	NaCl	0.1M	-37 to -48	DSC	(Kilmartin et al., 2000)
Me_2SO	20%			-115	DSC	(Wang et al., 2009)
Me_2SO	8.3%	NaCl	11.7% (4.3M)	-92 to -95	DTA	(Cocks et al., 1975)

4.4.4 Experimental values

4.4.4.1 Determination of eutectic points in electrolytes

Electrolyte used in this study was tested in cryotubes and cryostraws to determine its ice-formation temperature and ice-melting temperature during cooling and warming events. Two different concentrations of NaCl were tested. The resulting transition temperatures were compared with those in the literature.

The rationale behind determining the transition temperatures in cryotubes and cryostraws was to choose a convenient apparatus providing most constant transition temperatures in replicates that were easy to handle, allow probe adjustment and would not permit solution leakage.

Table 4.4: Determination of eutectic point of ice-formation (θ^i) and ice-melting (θ^m) in cryostraws during cooling and warming of 0.15 M and 0.85% NaCl solutions. Three replicates were tested for each concentration of NaCl. The average of the values were obtained and compared to the literature.

Additive(straw)	Concentration	θ^i	θ^m	Literature value (θ^m)
NaCl	0.15 M	-19±4.6	-17.7±4	-22 (Rey, 1960, Fujiwara and Nishimoto, 1998, Chen et al., 2005)
	0.85%	-13.3±6.2	-24±4.5	-21.8 (Magnusson and Edebo, 1976)

Difference in eutectic temperature values during cooling and warming cycles was observed in cryostraws. T-test was performed on the calculated eutectic temperatures and the literature values (Tables 4.4 and 4.5). The results for 0.15 M NaCl (straw) (see Table 4.4) have shown that since the t-calculated was less than t-critical, the difference between measured eutectic points and the literature value is not significantly different (p=0.199) (see Appendix II Table II A).

For 0.85% NaCl (straw) (Table 4.4) solution, the t-calculated was less than t-critical, the measured eutectic points and the literature were not significantly different (p= 0.794) (see Appendix II Table IIB). In both NaCl concentrations, standard deviation for ice-melting exceeded from the value of 4 σ (0.15 M NaCl) to 4.5 σ (0.85% NaCl) (Table 4.4).

Transition results were significantly different from the literature using cryostraws because, during experimentation there was a problem of solution leakage from one side of the straw (at some point in probe insertion). Moreover previous studies have shown that the ice formation phenomenon is directional in straws, which is why the transition temperatures have been different in each replicate of the saline solutions.

Table 4.5: Determination of eutectic point of ice-formation (θ^i) and ice-melting (θ^m) in cryotubes during cooling and warming of 0.15 M and 0.85% NaCl solutions. Three replicates were tested for each concentration of NaCl. The average of the values obtained was compared to the literature.

Additive(Tube)	Concentration	θ^i	θ^m	Literature value (θ^m)
NaCl	0.15M	-29.1±2.2	-24±0.5	-22 (Rey, 1960, Fujiwara and Nishimoto, 1998, Chen et al., 2005)
	0.85%	-16±1.0	-23±0.9	-21.2, -21.8 (Magnusson and Edebo, 1976)

The θ^m values determined in cryotubes were consistent for each concentration of NaCl as compared to the straws. The experimental value of 0.15 M NaCl during warming (θ^m) was 2 °C lower than the literature value. In addition, the replicates gave constant value of ice-melting temperature. The difference of nearly 2 °C in experimental and literature values was observed in 0.85% NaCl solution's ice-melting temperature.

For 0.15 M NaCl (tube) (Table 4.5) t-calculated was greater than t-critical, the measured eutectic temperatures and the literature value is significantly different (p=0.017) (see Appendix II Table IIC).

For 0.85% NaCl (tube) (Table 4.5) t-calculated was greater than t-critical, so rejected the null hypothesis i.e. the measured values of θ^s are significantly different from the literature value (-21.5 ˚C) (p= 0.765) (see Appendix II Table IID). The alteration between cooling and warming rates used in the experimental study and

in the literature could be the reason of differentiation in the values of experimental and literature values.

Although the eutectic temperatures obtained using cryotubes were showing significant difference from the literature, yet the values obtained in cryotubes were more consistent as compared to the results obtained using cryostraws. Solution leakage and directional ice-formation had limited the use of cryostraws.

4.4.4.2 Determination of transition temperatures of cryoprotectant mixtures in the presence and absence of additive (NaCl)

Three different cryoprotectants were studied in the presence and absence of electrolyte to observe its effect on transition temperatures of CPA-H_2O mixtures. Experiments were performed in cryotubes and cryostraws and their values were compared with the literature.

Table 4.6: Ice-initiation temperature (θi) and glass transition temperature during cooling (Tg^c) and warming (Tg^w) events of CPA mixture in the absence of additive (NaCl). Measurements were monitored in cryostraws. Three replicates of each CPA mixture were used for monitoring phase change events.

CPA (straw)	Concentration (%)	θ^i	Tg^c	Tg^w
Glycerol	10	-20±0.0	-35±0.5	-30±1.9
Me_2SO	10	-14.3±1.0	-24 ± 0.5	-25 ± 2.1
Sucrose	20	-11.45±0.4	-23.3±0.8	-21±0.3

Table 4.7: Ice-initiation temperature (θi) and glass transition temperature during cooling (Tg^c) and warming (Tg^w) events of CPA mixture in the presence of additive (NaCl). Measurements were monitored in cryostraws. Three replicates of each CPA mixture were used for monitoring phase change events.

CPAs (straw)	Concentration (%)	Additive	Concentration	θ^i	Tg^c	Tg^w
Glycerol	10	NaCl	0.15M	-17 ± 1.5	-54 ± 0.8	-48±1.7
Me_2SO	10	NaCl	0.85%	-12 ± 1.3	-66 ± 5.7	-61±7.6
Sucrose	20	NaCl	0.1M	-15.3 ±1.1	-37.1 ±1.2	-33.3 ±0.7

In straws the transition events of CPA mixtures were tested in the presence and absence of salt solutions (Tables 4.6 and 4.7). By comparing the transition temperatures obtained in both tables, the influence of NaCl on ice-initiation and Tg temperatures was demonstrated. In the absence of electrolyte the glass transition was taking place at higher than the expected temperature values obtained in the presence of additive. Tg at higher temperatures would not form a clear glass as it would be a mixture of ice-glass crystals (Morris et al., 2006). Hence, the glass transition temperatures observed in Table 4.6 were different due to the absence of NaCl.

T-test analysis for Table 4.6 shows following results;

for glycerol the t calculated was less than t-critical the measured Tg temperature of glycerol and the literature are not significantly different (p=0.195) (see Appendix III Table IIIA),

for Me_2SO the t-calculated was greater than t-critical, the measured Tg temperature of Me_2SO and the literature are significantly different (p=0.014) (see Appendix III Table IIIB);

for sucrose the t-calculated was less than t-critical, the measured Tg temperature of sucrose and the literature are not significantly different (p=0.169) (see Appendix III Table IIIC).

In ternary systems (Table 4.7) the glass transition temperatures of glycerol and sucrose were not significantly different those given in the literature showing the presence of electrolytes was interacting with CPA-H_2O mixture and lowers the glass transition temperature of the solution below its eutectic melting point.

T-test analysis were showing following results for Table 4.7;

for glycerol t -calculated was greater than t-critical, the measured Tg temperatures of glycerol and the literature are significantly different (p=0.016) (see Appendix III Table IIID);

for sucrose the t-calculated was less than t-critical, the measured Tg temperatures of sucrose and the literature are not significantly different (p= 0.425) (see Appendix III Table IIIE);

t-calculated for Me_2SO was greater than t-critical, its measured Tg temperature and the literature are significantly different (p= 0.009) (see Appendix III Table IIIF).

In binary and ternary systems of glycerol, sucrose and Me_2SO, the transition temperatures were neither constant nor showing desirable t-test results in cryostraws. Although sucrose t-test results were showing similarity in the calculated and literature Tg values but it was not achieved fully in all of its replicates due to solution leakage problem. It was also observed that Me_2SO was dissolving

the carbon layer of the interdigitated screen-printed impedance monitoring electrodes, resulted in obtaining incorrect results.

Table 4.8: Ice-initiation temperature (θ^i) and glass transition temperature during cooling (Tg^c) and warming (Tg^w) events of CPA mixture in the absence of additive (NaCl). Measurements were monitored in cryotubes. Three replicates of each CPA mixture were used for monitoring phase change events.

CPA (tube)	Concentration (%)	θ^i	Tg^c	Tg^w
Glycerol	10	-17 ± 0.5	-33 ± 2.6	-38 ± 1.4
Me_2SO	10	-19 ± 0.3	-50 ± 1.9	-47 ± 2.7
Sucrose	20	-11.74±0.2	-20.73±0.7	-18.85±1

Tables 4.8 and 4.9 show the transition temperatures of binary (CPA-H_2O) and ternary (CPA-H_2O-NaCl) solutions in cryotubes in the absence and presence of electrolyte.

In binary systems (Table 4.8) the glass transition temperatures obtained with glycerol-H_2O and sucrose-H_2O systems were not significantly different from the literature values described by (Morris et al., 2006). He has suggested to observe the Tg temperatures during warming events of CPA mixtures. During warming the solution undergoes thermodynamic equilibrium phase due to continuous ice-melting with the minimal chances of ice-recrystallisation to take place close to its Tg temperatures. In binary systems, t-calculated was less than t-critical for glycerol and sucrose (Table 4.8), their measured Tg temperatures were not significantly different from the literature showing values of (p=0.289) for glycerol and (p=0.148) for sucrose respectively (see Appendix III Table IIIG and IIIH). Due to interference of Me_2SO with impedance monitoring electrodes its Tg temperatures were

significantly different from the literature as t-calculated was greater than t-critical (p=0.002) (see Appendix III Table III I).

Table 4.9: Ice-initiation temperature (θi) and glass transition temperature during cooling (Tg^c) and warming (Tg^w) events of CPA mixture in the presence of additive (NaCl). Measurements were monitored in cryotubes. Three replicates of each CPA mixture were used for monitoring phase change events.

CPAs (tube)	Concentration (%)	Additive	Concentration	θ^i	Tg^c	Tg^w
Glycerol	10	NaCl	0.15M	-13 ±1.4	-54 ± 5.5	-59 ±1.6
Me_2SO	10	NaCl	0.85%	-14 ±2.6	-79 ±2.5	-74 ±4.0
Sucrose	20	NaCl	0.1M	-14.2 ±2	-37.2 ±3.4	-33.7 ±2

In ternary systems (water-NaCl-CPA), the glass transition temperatures were much lower from their eutectic point of ice-formation. Additionally the Tg values obtained were close to the literature values (see Table 4.3 and Table 4.9).

Whilst transition temperatures of glycerol and sucrose in ternary systems (Table 4.9) were not significantly different from the literature (p=0.244) for glycerol and (p=0.436) for sucrose (see Appendix III Table IIIJ and IIIK), Me_2SO interfered with screen-printed impedance monitoring sensor because it was dissolving the screen-printed carbon layer of the interdigitated electrodes. Measured Tg temperatures of Me_2SO are significantly different from the literature because its t-calculated was greater than t-critical (p=0.028) (see Appendix III Table IIIL).

4.4.4.3 Determination of transition events in 10% Glycerol solutions in the presence and absence of nucleating beads

Effect of seeding on ice-initiation temperature and glass transition temperatures was determined using Asymptote nucleating beads. Binary and ternary systems of 10% glycerol were assessed to determine the influence of ice-nucleating beads. The tests were performed in 3 set of replicates in cryotubes.

Table 4.10: Ice-initiation (θi) and glass transition (Tg) temperatures of 10% Glycerol (binary and ternary systems) in the absence (-n) and presence (+n) of nucleator during cooling(c) and warming (w) regimes. Experiments were performed in cryotubes. Transition measurements are mean ± standard deviation (n=3).

CPA	Additive	Concentration of additive	$\theta i^{(-n)}$ / ˚ C	$\theta i^{(+n)}$ / ˚ C	$Tg^{c\ (-n)}$	$Tg^{w\ (-n)}$	$Tg^{c\ (+n)}$	$Tg^{w\ (+n)}$
Glycerol			-17 ± 0.5	-10 ±0.4	-23 ± 6.6	-32 ± 0.6	-49 ± 0.1	-47 ± 0.1
Glycerol	NaCl	0.15M	-13 ± 1.4	-10 ± 0.3	-54 ± 5.5	-59 ± 1.6	-65 ± 0.4	-61 ± 0.7

Comparison of ice-initiation temperature and glass transition temperature (+ and – nucleator) determined the influence of early and delayed ice-initiation temperature on glass transition temperature of binary and ternary systems of glycerol solution.

The addition of 0.05 g of nucleating beads to 0.5 ml of Glycerol-H_2O and Glycerol-NaCl-H_2O samples resulted in the formation of ice at higher temperatures (Table 4.10). In binary system, there was a difference of 7 °C in ice-initiation temperatures (with and without nucleator). Similarly in ternary system, ice initiation was taking place 3 °C higher than the ice-initiation temperature observed in the absence of nucleator.

Ice-initiation influenced the glass-transition temperature. Binary and ternary mixtures of glycerol were showing lower Tg temperatures compared to the Tg temperatures observed in the absence of nucleator. During cooling event, the difference in Tg temperature between 'with' and 'without' nucleator was 26 °C and 11 °C in binary and ternary systems respectively whereas the difference was reduced to 14 ˚C (in binary) and 2 °C (in ternary) during warming events.

Nucleators cause solution solidification that changes its composition and results in an early ice-initiation event. This phenomenon is termed as "constitutional supercooling" (Morris et al., 2006). Nucleators act as a catalyst that speeded up the ice-initiation process resulted in the formation of maximally freeze concentrated matrix that turned to a glass phase at lower temperatures. Upon warming, the glass melted at equilibrium phase resulting in minimal amount of ice-recrystallization. In the absence of nucleator, rapid warming rates are preferred to omit the occurrence of recrystallization phase. However addition of nucleators would reduce the chances of ice-recrystallization at slower warming rates as well.

4.5 Key findings with TMS 1

The presence and absence of additives in the CPA mixture influence the glass transition temperature of the solutions. In binary systems (CPA-H_2O) glass transition temperatures were determined at much higher temperatures as compared to ternary system (CPA-H_2O-NaCl). Glass transition temperatures of binary mixtures were close to the system's ice-initiation temperature. However in ternary systems, the glass phase was obtained at much lower temperatures. The results obtained by ternary systems of glycerol and sucrose (in cryotubes and cryostraws) were not significantly different to those reported in the literature. Due to the interference of Me_2SO with screen-printed probe, it was not possible to determine its Tg.

Cryotubes were more convenient to perform experiments compared to cryostraws because, they did not allow solution leakage or give probe adjustment problems. The transition temperature ranges obtained using cryotubes were more constant per set of replicates.

Additionally the presence of nucleators lowered the glass transition temperatures in binary and ternary systems. Early ice-initiation temperature and lower glass transition temperature would be beneficial for LAB cryopreservation due to equilibrium ice formation (during cooling) and the formation of maximum freeze concentrated matrix that prevents the cells from mechanical damage or extensive dehydration during cooling, besides prevention of osmotic shock during warming due to equilibrium ice-melting.

Section 2

4.6 Transition measurements using transition monitoring system 2 (TMS 2)

In this section transition events were measured using transition monitoring system 2 (TMS 2). Experiments were performed in cryotubes. Interdigitated screen-printed electrodes (Type c) were used for impedance measurements (see Chapter 2).

Effect of different cooling rates, ice-nucleating agents and mixture of cryoprotectants were studied to determine the shifts in ice-initiation temperature and glass transition temperature during cooling and warming profiles. Mixtures of glycerol and sucrose CPAs were tested for transition measurements. Experiments were carried out for the following reasons: a) to determine the influence of the presence of cells towards glass transition temperatures of CPAs, and b) to test the effect of different cooling cycles (in the presence and absence of ice-nucleators) on transition temperatures of CPAs. The warming rates were monitored in air at room temperature.

Initially, the phenomenon of ice-initiation was investigated in detail to observe the change in impedance with respect to the change in temperature. Afterwards, the transition temperatures of CPAs were studied at different cooling rates.

The aim was to generate different cooling profiles for use in LAB cryopreservation, determine their influence of certain cooling regimes on post-thaw metabolic activity of *L. bulgaricus* CFL1 and to identify the most suitable cooling profile and CPA concentration for LAB cryopreservation with better post-thaw survival (see Chapter 5).

4.6.1 Rapid cooling of LAB + 10% Glycerol + 0.15 M NaCl (+ and – nucleator) using three different protocols

10% glycerol in the presence of 0.15 M NaCl and lactic acid bacterium (LAB) was rapidly cooled in liquid nitrogen (N_2) to observe glass transition shift (Tg) of CPAs mixtures. The Tg temperatures were observed in the presence and absence of Asymptote nucleator. Influence of LAB on Tg temperatures was studied as well. Experimental values of Tg obtained in the presence of cells were compared with the literature to determine the influence of LAB in the CPA mixture on Tg temperatures.

Experiments were performed in cryotubes, using resistance temperature probe (RTD) for temperature and screen-printed interdigitated electrodes for impedance measurements. Temperature and impedance change was monitored in milliseconds (ms) to determine the point of inflection during rapid cooling.

Three protocols were examined in following experiment

- cells + CPA (rapid plunge in liquid nitrogen) without nucleator;
- cells + CPA (rapid plunge in liquid nitrogen) with nucleator;
- cells + CPA (cooled at the rate of 1˚C min^{-1} until ice nucleation occurred then plunged into liquid nitrogen) without nucleator.

The warming of the samples was performed in air at room temperature. Warming rates were kept constant in order to study the influence of cooling rates and ice-initiation temperatures on glass transition temperatures of CPAs.

Table 4.11: Ice-initiation temperature (θ^s) , glass transition temperature during cooling (Tg^c) and warming (Tg^w) events of three different protocols is compared with the literature value of 10% Glycerol + 0.15M NaCl. In protocols a and b (θi) was not identified (N.I.) besides their measured Tg temperatures during cooling event were significantly different from the literature. During warming the Tg results of protocol a and b were not significantly different to the literature values. Protocol (c) has indicated the (θi) temperature as the rate of cooling was slower until ice-initiation. In addition, the Tg values (during cooling and warming) were not significantly different to the literature in protocol c.

Protocols		θ^i / °C	Tg^c / ˚C	Tg^w/˚C	Literature Value /˚C
a	Cells + CPA (rapid plunge in liq N_2)	N.I.	-78.1	-54.6	-62.7 (Fonseca et al., 2006 , Morris et al., 2006)
b	Cells + CPA + Nucleator (rapid plunge in liq N_2)	N.I.	-73.2	-50.2	
c	Cells + CPA (slow cooling at 1 °C min^{-1} until ice nucleation then rapid plunge in liq N_2)	-9.074	-57.0	-54.3	

Protocol a: t-calculated was less than t-critical the measured Tg temperatures of Protocol a and the literature are not significantly different (p=0.808) (see Appendix IV Table IVA).

Protocol b: t-calculated was less than t-critical the measured Tg temperatures of Protocol b and the literature are not significantly different (p=0.944) (see Appendix IV Table IVB).

Protocol c: t-calculated was less than t-critical the measured Tg temperatures of Protocol c and the literature are not significantly different (p=0.1204) (see Appendix IV Table IVC).

Observations

a) The lower Tg temperature during cooling event of Protocol a and b could be the artefact of rapid cooling causing longer delays in the thermal mass to reach the RTD probe. The size of RTD is different to than of the impedance probe resulted in difference in both of their thermal mass during rapid cooling, resulted in the variation between actual and observed Tg temperatures. In contrast, when the system was controlled slow cooled until ice nucleation (Protocol c), the thermal mass had less effect as the system was gradually cooled and there were no delays in thermal mass to reach the RTD probe.

b) Slow cooling until ice nucleation followed by liquid nitrogen plunge did not shift the Tg temperature to any great extent during cooling and warming events (Protocol c). Conversely, during cooling event of protocol a and b, abrupt solidification of the system (due to rapid plunge into liquid nitrogen) caused water sequestration which resulted in delaying the formation of maximally freeze concentrated matrix.

c) Monitoring glass transition temperature during warming events was preferred to monitor Tg during cooling. The difference between Tg values during cooling and warming was approximately ±15 ˚C, observed during rapid plunge in liquid nitrogen without ice-initiation. However when the system was plunged after ice-initiation, ± 5 ˚C of Tg difference was determined.

d) During cooling (especially very rapid cooling) ice formation is generally very rapid, causing rapid sequestration of supercooled water between the ice channels resulted in lowering the glass transition temperature due to several

recrystallization events taking place in the system causing unequilibrium ice formation.

e) The alteration in Tg temperatures during cooling event in protocols of a and b were probably due to the rate of cooling and presence or absence of ice initiation.

4.6.2 Transition temperatures of glycerol and sucrose in the presence of cells

4.6.2.1 Transition temperatures of glycerol

Experiments were performed with glycerol and sucrose in the presence of cells. Four different cooling rates were tested with CPA mixtures in the presence and absence of nucleating beads. The warming was performed in air at room temperature.

The investigation would help identifying potential cooling rates for LAB preservation and study the effect of differentiation in ice initiation temperature and glass transition temperature on post-thaw cell recovery (see Chapter 5). Cooling rates and nucleating agent's effect on transition temperatures will help to determine the effect of different cooling rates and ice initiation temperatures on glass transition temperatures of CPAs during cooling and warming cycles.

Table 4.12: Ice initiation temperature (θi) and glass transition temperature during cooling (Tg^c) and warming (Tg^w) of 10% Glycerol+0.15M NaCl+LAB in the absence of nucleator. Transition temperatures were monitored in cryotubes using four different cooling rates. The measurements are mean ± standard deviation (n=3).

CPA + cells	Cooling Protocols	θ^i	Tg^c / ˚C	Tg^w / ˚C
10% Glycerol+0.15M NaCl + LAB	**5 ˚C min^{-1}**	-20 ± 0.06	-53 ± 0.82	-53.4 ± 0.67
	1 ˚C min^{-1}	-16 ± 0.47	-53 ± 0.52	-54 ± 0.9
	0.5 ˚C min^{-1}	-18 ± 0.84	-54 ± 0.18	-53 ± 0.34
	0.1 ˚C min^{-1}	-24 ± 0.63	-54 ± 1.3	-53.± 0.8

Table 4.13: Ice initiation temperature (θi) and glass transition temperature during cooling (Tg^c) and warming (Tg^w) of 10% Glycerol+0.15M NaCl+LAB in the presence of nucleator. Transition temperatures were monitored in cryotubes using four different cooling rates. The measurements are mean ± standard deviation (n=3).

CPA + cells + Asymptote nucleator	Cooling Protocols	θ^i	Tg^c /˚C	Tg^w / ˚C
10% Glycerol+0.15M NaCl + LAB	**5 ˚C min^{-1}**	-12 ± 0.61	-50 ± 0.4	-55 ± 0.14
	1 ˚C min^{-1}	-13 ± 0.8	-52 ± 0.3	-53 ± 0.76
	0.5 ˚C min^{-1}	-13 ± 1.4	-51 ± 0.4	-52 ± 0.8
	0.1 ˚C min^{-1}	-15 ± 0.3	-52 ± 1.2	-54 ± 0.9

Table 4.12 and 4.13 shows the transition temperatures of 10% glycerol+0.15M NaCl + cells in the absence and presence of nucleating beads. The difference in ice initiation temperature and its influence on glass transition. The effect of ice-

initiation temperatures (in the presence of nucleating beads) on glass transition temperatures were observed during warming events of certain cooling profiles (table 4.13). At 5 ˚C min^{-1} cooling regime, ice was initiated 8 ˚C warmer in the presence of nucleating beads, which resulted in an observed 2 ˚C fall in Tg temperature during warming event. At 0.1 ˚C min^{-1} in the presence of nucleator, ice formation was initiated 9 ˚C higher (table 4.13) than the ice-initiation temperature observed in the absence of nucleating beads (table 4.12). Ice-initiation at higher temperatures (in the presence of nucleator) resulted in lowering the Tg temperatures by approximately 2 ˚C during warming event. Similarly a difference of 3 ˚C and 4 ˚C in ice initiation temperatures (in the presence of nucleator) was observed during cooling rates of 1 ˚C min^{-1} and 0.5 ˚C min^{-1} respectively. Cooling profiles of 5 ˚C min^{-1} and 0.1 ˚C min^{-1} were chosen for LAB cryopreservation as their response towards presence and absence nucleating agents was different. It was planned to investigate the influence of Tg temperature shifts due to ice nucleators presence, and absence and very slow and moderate cooling rates on post-thaw metabolic activity of LAB.

4.6.2.2 Transition temperatures of sucrose

Influence of nucleating beads on transition temperatures of sucrose is given in Tables 4.14 and 4.15.

Table 4.14: Ice initiation temperature (θi) and glass transition temperature during cooling (Tg^c) and warming (Tg^w) of 5% Sucrose+0.1M NaCl+LAB in the absence of nucleator. Transition temperatures were monitored in cryotubes using four different cooling rates. Transition measurements are mean ± standard deviation (n=3).

CPA + cells	Cooling Protocols	θ^i	Tg^c / ˚C	Tg^w / ˚C	Literature value
5 % sucrose+ 0.1M NaCl	**5 ˚C min^{-1}**	-20 ± 0.16	-33 ± 0.79	-35 ± 0.51	-39 ˚C (Nesariker et al., 2007)
	1 ˚C min^{-1}	-23 ± 1.2	-36 ± 0.78	-36 ± 0.17	
	0.5 ˚C min^{-1}	-18 ± 0.63	-38 ± 0.84	-35 ± 0.82	
	0.1 ˚C min^{-1}	-20 ± 0.57	-35 ± 0.57	-35 ± 0.38	

In cooling profiles of 5 ˚C min^{-1} and 1 ˚C min^{-1} (in the presence of nucleating beads), the ice initiation temperature was 9 ˚C higher as compared to the ice-initiation temperature observed without nucleating beads in the following cooling profiles. Ice-initiation at a higher temperature resulted in lower Tg temperatures by an average of 3 ˚C in 5 ˚C and 1 ˚C cooling regimes.

Conversely during warming, ice initiation was 6 ˚C higher in the cooling regimes of 0.5 and 0.1˚C min^{-1} min. Ice-formation at higher temperatures resulted in lowering the Tg temperatures during warming event at an average of 2 to 3 ˚C in both cooling profiles.

Table 4.15: Ice initiation temperature (θi) and glass transition temperature during cooling (Tg^c) and warming (Tg^w) of 5% Sucrose+0.1M NaCl+LAB in the presence of nucleator. Transition temperatures were monitored in cryotubes using four different cooling rates. The measurements are mean ± standard deviation (n=3).

CPA + cells + nucleator	Cooling Protocols	θ^i	Tg^c / ˚C	Tg^w / ˚C	Literature value
5 % sucrose + 0.1M NaCl+ asymptote nucleator	**5 ˚C min^{-1}**	-10 ± 0.14	-34 ± 0.02	-37 ± 0.98	-39 ˚C (Nesariker et al., 2007)
	1 ˚C min^{-1}	-13 ± 0.53	-34 ± 0.92	-36 ± 0.65	
	0.5 ˚C min^{-1}	-12 ± 0.6	-35 ± 0.85	-37 ± 0.61	
	0.1 ˚C min^{-1}	-14 ± 0.3	-35± 0.84	-38 ± 0.78	

Ice-initiation temperature influenced the glass transition temperatures of glycerol and sucrose CPAs. On the basis of these results it was decided to study the effect of moderate (5 ˚C min^{-1}), very slow (0.1 ˚C min^{-1}) and very fast (liquid N_2 plunge) cooling regimes on post thaw metabolic activity of LAB in the absence and presence of nucleating beads (see Chapter 5).

Section 3

4.7 Glass transition values obtained using two different concentrations of glycerol and sucrose CPAs

In this section the Tg of mixture of glycerol and sucrose CPAs were determined for use in exploring their cryoprotective effect on LAB.

Two different concentrations of glycerol and sucrose were made (Chapters 2) in the absence of cells.

The aim was to determine the transition events of mixture of CPAs and observe the differences in Tg values in the presence and absence of nucleating agents. The cooling rate was kept constant at the rate of 5 ˚C min^{-1} from 0 ˚C to -90 ˚C then plunge into liquid nitrogen. The warming was performed in air at room temperature. Moderate cooling rate (5 ˚C min) was considered as a control cooling regime. It was to be used later for post-thaw metabolic assessment of LAB.

The Tg temperatures of quaternary systems (Water-Glycerol-Sucrose-NaCl) were investigated and compared to the values obtained in the presence of cells described in Chapter 5. Very few quaternary systems are described in the literature however they are indispensable in the field of cryobiology and pharmacology (Gleason, 2012).

Studying the transition events of a mixture of permeating and non-permeating CPAs would enable the effect of Tg temperatures on post-thaw cell viability of LAB to be determine (Chapter 5), and determine the change in transition temperatures due to presence or absence of cells in the CPA suspension to be found.

Transition temperatures of quaternary systems

Ice initiation and glass transition temperatures of the quaternary system were determined in the presence (+n) and absence (-n) of Asymptote nucleating beads. Phase change events were monitored in cryotubes using TMS 2. Experiments were repeated three times to allow standard deviation values to be determined.

Table 4.16: θ^i (ice-initiation temperatures), Tg^c (glass transition during cooling event) and Tg^w (glass transition during warming event) of 5% Glycerol + 5% Sucrose 0.15M NaCl + LAB + and 7.5% Glycerol+2.5% Sucrose +0.15M NaCl + LAB, without nucleator at a cooling rate of 5 ˚C min^{-1} from 0 to-90 ℃ followed by liquid nitrogen plunge. Tg of 3 replicates of following CPA mixtures was monitored during cooling and warming of samples.

CPA $^{-n}$	θ^i	Tg^{c1}	Tg^{c2}	Tg^{c3}	Tg^{w1}	Tg^{w2}	Tg^{w3}
5% Glycerol+5 %Sucrose +0.15M NaCl+H_2O	-2.78± 0.19	-32±0.16	-42± 0.42		-40± 0.8	-53± 0.3	
7.5% Glycerol+ 2.5%Sucro se+0.15M NaCl+H_2O	-3.7± 0.14	-33.7± 0.9	-43.8± 0.41	-52± 0.45	-33.7± 0.07	-44± 0.4	-54± 0.67

In the absence of nucleator (Table 4.16), more than one transition event was observed after derivatizing the calibrated data of temperature and impedance values obtained during cooling and warming events.

Conversely three phase change temperatures were determined during cooling and warming of 7.5% +2.5% glycerol-sucrose mixtures.

Table 4.17: Table 4.16: θ^i (ice-initiation temperatures), Tg^c (glass transition during cooling event) and Tg^w (glass transition during warming event) of 5% Glycerol + 5% Sucrose 0.15M NaCl + LAB + and 7.5% Glycerol+2.5% Sucrose +0.15M NaCl + LAB, in the presence of nucleator at a cooling rate of 5 ˚C min^{-1} from 0 to-90 °C followed by liquid nitrogen plunge. Tg of 3 replicates of following CPA mixtures was monitored during cooling and warming of samples.

CPA $^{+n}$	θ^i	Tg^c	Tg^{w1}	Tg^{w2}	Tg^{w3}
5% Glycerol+ 5%Sucrose+ 0.15M NaCl+H_2O	1.97±0.24	-30 ± 4.5	-32 ± 0.472		
7.5% Glycerol+ 2.5%Sucrose +0.15M NaCl+H_2O	3.9±0.2	-37±0.22	-39.3±0.5	-47±1.0	-52±1.1

Higher ice-initiation temperatures were observed in glycerol-sucrose mixtures in the presence of nucleating beads. Nucleators tend to provide stability in Tg temperatures during cooling and warming of 5% glycerol-sucrose mixture, however; more than one transition temperature was determined during warming (Tg^w) of 7.5% + 2.5% glycerol- sucrose mixtures.

4.8 Key findings of TMS1 and TMS 2 results

The main concern of the project was to study the influence of ice-initiation and rate of cooling on Tg shifts which was examined using both systems i.e. TMS 1 and TMS 2.

The results of binary and ternary CPA systems obtained by TMS 1 are in line with the literature but TMS 2 monitoring system has a need of further improvements to obtain the Tg temperatures that are not significantly different from the literature.

TMS 2 determined the transition temperatures and influence of cooling rates and ice-initiation on Tg shifts of ternary and quaternary systems however, the temperatures obtained were not in line with Tg temperatures described in the literature. The system requires further improvements in its design to evaluate accurate impedance response during different cryo regimes.

Chapter 5

Post-Thaw Metabolic Activity of *L. bulgaricus* CFL1 after Storage in Liquid Nitrogen Vapour

5 Introductory information

The research sought to develop the sensor technology techniques for the development of cheap, disposable and portable sensor systems and to apply to follow phase change events of CPAs during cooling and warming and, to exploit cryobiology techniques to study the effect of phase change events of cryoprotectant mixtures on post-thaw metabolic activity of *L. bulgaricus* CFL1 species.

Rationale

The aim of the study was to utilise sensor technology and cryobiology techniques to inform the process of cryopreservation of LAB species and study their post-thaw metabolic activity after cryo storage.

Experimental Design

Three different cooling rates (a) very fast (liquid N_2 plunge), (b) moderate (5˚C) and (c) very slow (0.1˚C) were chosen for LAB cryopreservation. Glycerol and sucrose were used cryoprotectants. Combined mixtures of glycerol+sucrose were also investigated to study the effect of mixture of penetrating and non-penetrating CPAs on post thaw metabolic activity of LAB. 10%, 5% and 7.5% of glycerol and 5% and 2.5% of sucrose concentrations were used in the presence and absence of ice nucleator for LAB cryopreservation. 0.5 ml of the cell+CPA sample (+ and – nucleator) in cryotubes were used for the study. The cells were stored for three days at -196˚C (liquid N_2) after experiencing the different cryo regimes. Six replicates of each cooling rate and CPA mixtures were used for to study the LAB longevity after cryopreservation and cryo storage for three days. After storage for 3 days in liquid nitrogen, cells were thawed in air at room temperature. The revived cells were cultured for 19 h in MRS broth and pH and O.D. change was monitored by means of spectrophotometer and conventional glass pH electrode

Six control cultures (prepared from a freeze dried starter cultures incubated overnight at 42 ˚C in MRS broth) were also set up to compare the metabolic activity of fresh and post-thawed LAB samples. O.D. and pH of control and experimental samples was investigated to compare the metabolic activity of fresh and post-thawed samples. To monitor metabolic activity screen-printed pH sensors developed in this project (see Chapter 2 Figure 2.2 and 2.6) were used for pH monitoring in fresh and post-thawed samples. Conventional pH measurements were also undertaken using glass pH electrode (see Chapter 2 Figure 2.6) to compare the pH results obtained by screen-printed and conventional glass pH electrodes.

Impedance monitoring was studied using TMS 2 and screen-printed impedance monitoring electrodes (Type c) in cryotubes to discover the effect of ice initiation and glass transition temperatures on post-thaw metabolic activity of LAB. Three replicates of each cryoregime and CPA mixture were exploited for impedance measurements.

General introduction

In this chapter the results from LAB cultures stored for 3 days in liquid nitrogen temperature were assessed after its post-thaw recovery in nutrient broth for 19 h. The chapter has been divided into 2 sections.

In section one, three factors were examined to assess their impact on post-thaw metabolic activity of LAB; 1) cooling rates of very rapid (Liquid nitrogen), moderate ($5^\circ C\ min^{-1}$) and very slow ($0.1^\circ C\ min^{-1}$); 2) ice nucleation temperature in the presence and absence of nucleator and; 3) glass transition temperature. Glycerol of 10% concentration was used as a medium of cell cryopreservation in the presence and absence of nucleator. Screen-printed antimony with a screen-printed salt-bridged Ag-AgCl reference electrode and conventional glass pH electrodes were used to determine LAB metabolic activity in control and post-thawed samples. The cooling rate that gave maximum post-thaw metabolic activity of LAB cultures and electrode type that helped in quick post-thaw metabolic assessment were chosen for the subsequent experiments performed in Section 2 of this chapter.

In section 2 the effects of three factors on post-thaw metabolic activity of LAB was observed: 1) combined effect of penetrating and non-penetrating cryoprotectant mixtures; 2) ice-nucleation temperature and; 3) glass transition temperatures at three different cooling profiles. 10%, 5% and 7.5% mixtures of glycerol and 5% and

2.5% mixtures of sucrose were used as cryoprotectant media in the presence and absence of ice-nucleator. The aim was to study the effect of penetrating and non-penetrating cryoprotectant mixtures on post-thaw cell metabolic activity after undergoing cryopreservation and storage in liquid nitrogen vapour for three days.

Post-thaw results of LAB metabolic activity were obtained from 6 replicates in both sections. The phase transition events were measured in 3 replicates of each cooling rate and CPA mixture. pH and O.D. of 6 control cultures was monitored to compare the metabolic activity of fresh and post-thaw cells.

Section 1

5.1 Metabolic assessment of Lactic Acid Bacterium after cryopreservation using 10% Glycerol+0.15 M NaCl as a cryoprotecting solution

5.1.1 Introduction

The medium used for controlled cooling was 10% Glycerol + 0.15 M NaCl. Ice nucleation and glass transition temperatures of the medium were determined in the presence of LAB. 12 replicates of 0.5 ml of the cell suspension were cooled using three different cooling regimes (see Chapter 2), and transition temperatures determined from 4 of six replicates by means of impedance monitoring system. The samples were then preserved in liquid nitrogen vapour for 3 days.

Post-thaw metabolic activity was monitored batch to batch by conventional glass and screen-printed electrodes. pH change is a key source of studying metabolic activity of LAB because, metabolism of LAB results in the production of lactic-acid which lowers the pH of the culture medium (see Chapter 1). The pH results obtained from conventional glass and screen-printed pH electrodes were examined to study the effect of cooling rate, ice initiation and glass transition temperatures on post-thaw metabolic activity of LAB after cryopreservation and cryo storage for three days. The post-thaw metabolic activity was monitored in pH (by conventional glass) and mV (by screen-printed pH electrodes). The mV readings obtained by screen-printed electrodes were converted to pH units by using Nernst equation. pH results obtained from fresh and post thawed samples using conventional glass and screen-printed pH probes were compared to study the pH response obtained from both probes and discover the ideal LAB cryopreservation profile and pH measurement technique for future experiments.

5.1.2 Post-thaw metabolic activity assessment

Background

Rates of cooling and frozen storage temperatures affect the post-thaw metabolic activity of lactic acid bacterium (Smittle et al., 1972). Most prokaryotic and eukaryotic cell lines were preserved at cooling rate of 10 ˚C min^{-1} (Nakamura, 1996) but in the case of the lactic acid bacterium (LAB) its preservation has been reported to be species-dependant (Champagne, 1991, Sanders et al., 1999).

Results

In this project, the experiments were undertaken to define the relation between cooling rates (mentioned in Section 5) , ice-nucleation, Tg temperatures, and its effect on LAB post-thaw metabolic activity with a view to optimising the formulations of LAB cultures.

Table 5.1: Average pH change (pH^{ave}) via screen-printed (sp), conventional glass (glass) sensors, and optical density $O.D.^{490nm}$ of post-thawed following incubation of LAB. The results show metabolic activity of cells cryopreserved at 3 different cooling rates, followed by three days of storage in liquid N_2 vapour.

Protocols	Parameters	(- nucleator)	(+ nucleator)
0.1 C min^{-1} (0 to -90°C) then liq N_2 plunge (very slow)	**pH^{ave}** /sp	5.64 ± 0.09	3.53 ± 0.04
	pH^{ave} /glass	5.72 ± 0.02	4.14 ± 0.11
	$O.D.^{ave}_{490nm}$	0.73 ± 0.01	2.19 ± 0.14
5 ˚C min^{-1} (0 to -90°C) then liq N_2 plunge (moderate)	**pH^{ave}** /sp	3.81 ± 0.07	3.64 ± 0.02
	pH^{ave} /glass	4.23 ± 0.02	4.21 ± 0.04
	$O.D.^{ave}_{490nm}$	1.83 ± 0.43	2.27 ± 0.11
direct LN_2 plunge (very rapid)	**pH^{ave}** (sp /mV)	3.75 ± 0.05	3.53 ± 0.04
	pH^{ave} /glass	4.26 ± 0.02	4.18 ± 0.02
	$O.D.^{ave}_{490nm}$	1.98 ± 0.43	2.1 ± 0.10
Control	**pH^{ave}** /sp	**3.63 ± 0.18**	
	pH^{ave} /glass	**4.04 ± 0.11**	
	$O.D.^{ave\ 490nm}$	**2.23 ± 0.19**	

Results were acquired from six replicates (for each cooling rate). Six controls were set to compare their metabolic activity with post-thaw cultured cells. The pH of the nutrient broth was adjusted to pH 5.5 (to minimise the chances of cell death due to higher or lower pH of the MRS broth) before culturing the controls and replicates of post-thawed cells. Table 5.1 shows the post-thaw metabolic activity of the cells cooled at three different rates without **(-)** and with **(+)** ice nucleators. Post-thaw metabolic activity was assessed using pH, and O.D. parameters. Change in pH was observed with two different probes to compare their performance.

pH and O.D. results without nucleator demonstrated post-thaw metabolic activity for cells cooled at very rapid (LN_2 plunge) and moderate (5 °C min^{-1}) cooling rates,

however pH reduction or O.D. increase was less evident at a very slow rate of cooling (0.1 °$Cmin^{-1}$).

Alternatively, in all three cooling rates, evidence of post-thaw cell survival was seen in the presence of nucleators. The presence of nucleator provided improved survival of post-thaw LAB in described cooling profiles.

The results obtained in the presence of nucleators were similar to the controls in terms of pH reduction and increase in cell density. Cells cooled in the absence of nucleators using moderate and very rapid cooling profiles were metabolically active but the metabolic activity was lower than controls.

The pH change was monitored by means of both screen-printed and glass pH probes although the pH values were quicker to obtain with the help of glass pH electrode. However, the fragile nature of glass electrodes limits their use in some situations such as monitoring pH in food processing. Screen-printed electrodes are safe and disposable and could be an alternative approach to test the metabolic activity of LAB cultures in dairy food industries. However, its signalling response must be improved to generate the results more quickly from starter or post-thaw cultured cells.

5.1.3 Impedance results

Successful cryopreservation of cells is dependent on cooling rate (Mazur, 1970). To attain osmotic equilibrium, a slow rate of coolings helps the cells to lose sufficient water to avoid intracellular ice formation (IIF). However, in the study with *Lactobacillus delbrueckii* subsp. *bulgaricus* CFL1, IIF would not be observed during cryopreservation at rapid rate of cooling (2,500 ˚C min^{-1}) (Fonseca et al., 2006). Slow and very rapid cooling rates did not appear to be detrimental to the cell survival in the presence or absence of ice-nucleator due to osmotic equilibrium or avoidance of IIF. The experiments carried out in this project explored the effects of three different cooling protocols along with storage in liquid nitrogen vapour for 3 days, on post-thaw metabolic activity of LAB.

Impedance monitoring was performed to determine ice initiation and glass transition temperatures of 10% Glycerol + 0.15 M NaCl + cells in the presence or absence of nucleators at three cooling rates. The influence of cooling rate and ice initiation temperature (with and without nucleators), on glass transition temperatures was determined along with their effect on post-thaw recovery of LAB.

TMS 2 had certain generic faults such as the abnormal response of Channel 5 (see Chapter 3 Table 3.1) and problems in signalling response on some occasions in TMS 2 requires a redesign of its circuitry. Whilst it was able to detect the shifts in transition temperatures following changes to the cryoprotocol, as seen in the use of nucleators and CPA concentrations, TMS 2 did not give Tg values in line with the values obtained by DSC (see Chapter 4 Table 4.3 and Table 5.2). However, experiments were carried out using this system to determine the Tg shifts in CPAs, as the system allowed multiple cryotubes to be monitored concurrently and delivered the effect of presence and absence of a nucleator at described cooling

profiles (see Section 5) on phase transition events followed by post-thaw metabolic activity of LAB.

Table 5.2: θ^n (nucleation temperatures), Tg^c (glass transition during cooling event) and Tg^w (glass transition during warming event) of 10% Glycerol + 0.15 M NaCl + LAB + without (-) and with (+) nucleator at very slow (0.1 °C min^{-1}), slow (5 ˚C min^{-1}) and very rapid (liquid N_2 plunge) cooling rates. Tg^w was observed during warming at room temperature. Transition measurements were recorded three times for each profile. θ^n (+) and (-) nucleator was not identified (N.I.) during very rapid rate of cooling i.e. liquid N_2 plunge.

LAB+CPA (-) and (+)	**θ^{n-} (°C)**	**θ^{n+} (°C)**	**Tg^{c-} (°C)**	**Tg^{c+} (°C)**	**Tg^{w-} (°C)**	**Tg^{w+} (°C)**
0.1 ˚ C min^{-1} (very slow)	-22 ±1.7	-11.8 ±0.7	-50 ±0.2	-52 ±0.2	-56.3 ±1.0	-52.4 ±0.16
5 ˚C min^{-1} (slow)	-13.7 ±0.63	-9.1 ±0.3	-52.17 ±0.05	-53.6 ±0.2	-51 ±0.22	-51.9 ±0.08
Liquid N_2 plunge (very rapid)	N.I.	N.I.	-50 ±0.3	-50.6 ±0.12	-55.6 ±0.06	-54.5 ±0.7

Transition events of LAB + 10% Glycerol + 0.15 M NaCl (without and with nucleator) were observed in 0.5 ml of cell suspension in cryotubes, using Asymptote EF600 slow cooler (Table 5.2). Ice initiation at lower temperatures was observed in the absence of nucleators but unidentified (N.I.) at very rapid cooling rates. At very slow cooling rate (-n) the ice initiation temperature was lowered further. Formation of ice at lower temperatures resulted in cells facing hyperosmotic conditions in the extracellular matrix (Mazur, 1977, Mazur, 1963a).

Experimental values in this work (Table 5.2) were significantly different to the values mentioned in the literature (see Chapter 4 Table 4.3). Transition temperatures of the 10% Glycerol+0.15 M NaCl (in the absence of LAB) have been determined using these protocols (see Chapter 4).

Determination of transition temperatures of the cell suspension allows the effect of changes in cooling rates and transition temperatures on post-thaw metabolic activity of *L. bulgaricus* CFL1 to be identified. Phase findings would be helpful for selecting the optimal cooling profile and cryoprotectant medium to cryopreserve LAB with improved metabolic activity.

The glass transition temperatures appeared to be influenced by ice nucleation temperatures at particular cooling rates (Table 5.4). In the absence of nucleator (-n) ice initiation took place at much lower temperatures and was probably the main cause of cell death due to flash freezing and excessive cell shrinkage during cooling. Ice nucleator initiated the freezing at higher temperatures resulted in the formation of ice and preventing hyperosmotic conditions in CPA + cell media.

Ice nucleating beads could eliminate the harmful effects of very slow rates of cooling by allowing the cells + CPA suspension to produce equilibrium ice formation resulting in the creation of maximum freeze concentrated matrix during cooling regime. The matrix then forms a glass at lower temperatures resulted in obtaining Tg at lower temperatures. On warming, the matrix does not undergo unequilibrium melting phase as entire maximum freeze concentrated matrix has formed a glass (during cooling) which absorbs energy at equilibrium phase (during warming). The detrimental effect of unequilibrium ice-formation (during very slow cooling) and osmotic shock (during slow warming) could be eliminated by adding the nucleators into cells+CPA suspension before cryopreservation.

5.1.4 Conclusions

Ice initiation by means of a nucleator resulted in improved metabolic activity of post-thaw lactic acid bacterium during very slow cooling rate (0.1 ˚C min^{-1}). Cells survived in the absence of a nucleator at moderate (5 ˚C min^{-1}) and very rapid (liquid N_2 plunge) cooling rates but, the metabolic activity was significantly lower than for cells preserved in the presence of nucleators. At very slow rate of cooling (in the absence of nucleator) cells faced extensive dehydration as the ice formation process was slow and resulted in the formation of hypertonic environment outside the cells (Mazur, 1977).

A mechanism has been proposed (Morris et al., 2006) that very slow rate of cooling in the absence of ice initiation close to its melting point, caused non-equilibrium ice formation in extracellular matrix with extensive cell dehydration causing osmotic imbalance upon thawing, leading to cell damage. Cells have faced this stress at 0.1 ˚C min^{-1} cooling rate without the nucleator due to the presence of hypertonic environment in extracellular matrix. The addition of a nucleator has prevented extensive cell dehydration or post-thaw osmotic stress at the very slow cooling rates due to ice initiation at higher temperature that resulted in the conversion of most of the solution into ice and prevention of unequilibrium melting of ice during warming. Cells cooled at 5 ˚C min^{-1} have survived due to osmotic equilibrium, ice initiation close to its melting point and osmotic balance upon thawing. On the other hand absence of intracellular ice formation in LAB during very rapid rate of cooling has elevated the post-thaw cell survival.

Nucleator addition to the cryoprotectants mixture significantly raised the ice-nucleation temperatures Table 5.2. As a result cells were prevented from extensive dehydration (during cooling rate of 0.1 ˚C min^{-1}) and were metabolically active after

post-thaw incubation. Intracellular ice formation has not been evident in LAB in literature. Most of the cell damage in LAB is caused by factors such as cooling rate, concentration of cryoprotectants, culturing time and storage temperatures.

Storage period of 3 days was not detrimental to the cells post-thaw metabolic activity in the following studies (except 0.1 °C min^{-1} without nucleator). Ice-initiation at higher temperatures facilitates the formation of maximum freeze concentrated matrix which is beneficial for cryopreservation and post-thaw survival of LAB.

Section 2

5.2 Metabolic assessment of LAB after cryopreservation in the presence of a mixture of cryoprotectants

5.2.1 Introduction

Pre-treatment of lactic acid bacteria with mixture of penetrating and non-penetrating cryoprotectants helps to prevent cells from osmotic imbalance intra and extracellularly during freezing and thawing mechanism. Sucrose and glycerol have proven to be the most suitable cryoprotectants individually for *L. delbrueckii* subsp. *bulgaricus* preservation as they cause phenotypic adaptation towards freezing and thawing resulted in improvements in survival rates at lower temperatures (Oldenhof et al., 2005, Fonseca et al., 2000, Tymczyszyn et al., 2007, Ferreira et al., 2005) .

Based on the evidence of sucrose and glycerol performance as a cryoprotectant in literature, it is of interest to study the combined effect of both of the cryoprotectants on LAB cryotolerance and study their influence on post-thaw survival after cryopreservation and cold storage. Glass transition temperatures of sucrose and glycerol have been reported in Chapter 4. The combined effect of the mixture of glycerol and sucrose in the presence of cells is reported here.

Importance of CPA osmolality for cryopreservation

Freezing increases the chance of osmotic stress due to high concentration of cryoprotectants, leading to osmotic imbalance at thawing and excessive cell dehydration. The osmolality of 10% Glycerol+0.15 M NaCl is 1.27 Osm kg^{-1} H_2O and has been reported as a suitable concentration for LAB cryopreservation in literature (Morris et al., 2006). The solutions were prepared by taking the reported osmolality in consideration. Mixtures were prepared with osmolality in the range of 0.9 – 1.27 Osm kg^{-1} H_2O as the CPA mixtures used in the literature had osmolality in the described range (Le Marrec et al., 2007) .

The osmolality of 5% Glycerol+5% Sucrose + 0.15 M NaCl was 0.9 Osm kg^{-1} H_2O and the osmolality of 7.5% Glycerol+2.5% Sucrose+0.15 M NaCl was 1.18 Osm kg^{-1}. Different concentrations of glycerol and sucrose were chosen to obtain the osmolality in the range reported in the literature. The glycerol-sucrose mixtures were used in the presence and absence of Asymptote nucleating beads in order to study the effect of early ice initiation on post-thaw cell survival.

5.2.2 Studying transition events of CPAs

To attain maximum survival, cells must be stored below their glass transition temperatures. Studying the transition events of the mixture of cryoprotectants will help to optimise the cryo storage protocols for LAB starter cultures when complex mixtures of cryoprotectants are used. Impedance monitoring system (TMS 2) was used to measure the ice initiation temperature and glass transition temperature of glycerol-sucrose mixtures. 0.5 ml of a cell suspension was required for Tg assessment. The cells were preserved for 3 days in liquid nitrogen vapour after undergoing cooling cycle of 5 °C min^{-1} from 0 °C to -90 °C, followed by liquid

nitrogen plunge. The selected cooling rate was identified from previous experiments (this chapter, Section 1) and treated as a standard cooling protocol in the following experiments.

After storage for 3 days in liquid nitrogen, cells were thawed in air at room temperature. The revived cells were cultured for 19 h and pH change and O.D. was monitored by means of spectrophotometer and conventional glass pH electrode.

The changes in pH and optical density were measured to determine the post-thaw activity of *L. delbrueckii* subsp. *bulgaricus* CFL1. The cells were incubated at 42 ℃ for 19 h in MRS broth (without agitation). The operating conditions for cell culturing were kept constant. (Brashears and Gilliland, 1995, Morice et al., 1992) have reported that in order to obtain the cells in the same growth phase (preferably stationary phase) and to observe metabolic activity in similar operating conditions, the timing and temperature of incubation must be kept constant. Similarity in operating conditions allowed the limiting factors affecting metabolic activity to be identified and helped to improve the resistance to freezing and frozen storage of bacteria (Fonseca et al., 2001). Several factors have been described in the literature that cause favourable or unfavourable effects on LAB preservation. However, interactions between influential factors have not been clearly understood. For example, ice nucleators have been used in the past to obtain equilibrium ice formation during cryopreservation. Yet, its effect on glass transition temperatures and cell survival has not been explored.

The purpose of the present work was to explore the interaction between mixture of cryoprotectants, ice initiation (in the presence or absence of nucleating beads) and glass transition temperatures on post-thaw cell survival of lactic acid bacterium.

5.2.3 5% Glycerol+5% Sucrose

Six replicates of the cells were preserved in 5% glycerol+ 5% sucrose solutions with the absence (Table 5.3) and presence (Table 5.4) of nucleating beads. The cells were preserved in liquid nitrogen vapour for three days. After cold-storage, cells were post-thawed in air at room temperatures and cultured in six replicates containing MRS broth, for 19 h at 42 °C. After post-thaw incubation, the replicates were stored in the fridge (to reduce their metabolic activity) during pH and O.D measurements. pH and O.D. change of each sample was observed at room temperature sequentially.

Table 5.3: Post-thaw metabolic activity of LAB (cooled in the absence of nucleator) after culturing for 19 h at 42 °C. The cells were stored in liquid N_2 vapour for 3 days in 5% Glycerol+5% Sucrose+0.15 M NaCl. Cell density (O.D.) and pH change were the parameters of metabolic assessment. Calculated values of pH (pH^{calc}) were obtained after calibrating the glass probe with standard buffers of pH 4.00, 7.00 and MRS buffer of pH 5.5.

Sample	pH^{calc}	$O.D.^{490nm}$
1	4.28	1.94
2	4.3	1.786
3	4.27	1.847
4	4.2	1.992
5	4.25	1.933
6	4.3	1.744
Control	4.05±0.16	2.21±0.23

Table 5.4: Post-thaw metabolic activity of LAB (cooled in the presence of nucleator) after culturing for 19 h at 42 °C. The cells were stored in liquid N_2 vapour for 3 days in 5% Glycerol+5% Sucrose+0.15 M NaCl+nucleator. Cell density (O.D.) and pH change were the parameters of metabolic assessment. Calculated values of pH (pH^{calc}) were obtained after calibrating the glass probe with standard buffers of pH 4.00, 7.00 and MRS buffer of pH 5.5.

Sample	pH^{calc}	$O.D.^{490nm}$
1	4.07	1.88
2	3.98	2.15
3	3.98	2.17
4	4.02	2.02
5	4.00	2.05
6	3.97	2.06
Control	4.05±0.16	2.21±0.23

In Table 5.3 the replicates have shown average pH change from 5.5 (set pH of culture medium before culturing) to 4.2 (after 19 h of culturing), whilst the cells preserved with nucleating beads (Table 5.4) have changed the pH from 5.5 to 3.9 with the average O.D. of 2.00 in six samples.

The comparative analysis shows that whilst decrease in pH (due to the production of lactic acid by LAB in the culture medium) has indicated the LAB metabolic activity in both cases, cells cryopreserved in the presence of nucleating beads show higher metabolic activity in contrast to the cells cryopreserved in the absence of nucleating beads. Conversely, mixture of glycerol and sucrose did not cause osmotic imbalance to the cells during cryopreservation as the cells were metabolically active after post thaw incubation. Its results have determined the post-thaw metabolic activity of cells after overnight incubation in MRS broth. Experiments have also demonstrated a better post-thaw recovery in the samples stored in liquid nitrogen temperatures for 3 days after cryopreservation in the presence and absence of nucleating beads (Table 5.3 and 5.4).

5.2.4 7.5% Glycerol + 2.5% Sucrose

Post-thaw metabolic activity of LAB in 7.5% glycerol + 2.5% sucrose in the absence and presence of nucleator are given in table 5.5 and 5.6. Starter cultures were harvested and preserved in the presence of cryoprotectant mixture and held for three days in liquid nitrogen vapour. 12 replicates for CPA+LAB were held in liquid nitrogen vapour. To undergo post-thaw checks, cells were thawed in air at room temperature and cultured in flasks containing the culture medium. Six replicates were prepared from 12 set of cryotubes (stored in nitrogen vapour). The cells were cultured for 19 h at 42 °C in an incubator. pH reduction and increase in optical density was monitored to determine post-thaw survival.

Table 5.5: Post-thaw metabolic activity of LAB (cooled in the absence of nucleator) after culturing for 19 h at 42 °C. The cells were stored in liquid N_2 vapour for 3 days in 7.5% Glycerol+2.5% Sucrose+0.15 M NaCl. Calculated values of pH (pH^{calc}) and potential change (glass/mV^{calc}) were obtained after calibrating the glass probe with standard buffers of pH 4.00, 7.00 and MRS buffer of pH 5.5.

Sample	pH^{calc}	$O.D^{490nm}$
1	4.19	2.09
2	4.17	2.04
3	4.18	1.97
4	4.19	1.9
5	4.19	2.05
6	4.16	1.99
Control	4.05±0.16	2.21±0.23

Table 5.6: Post-thaw metabolic activity of LAB (cooled in the presence of nucleator) after culturing for 19 h at 42 °C. The cells were stored in liquid N_2 vapours for 3 days in 7.5% Glycerol + 2.5% Sucrose + 0.15 M NaCl + nucleator. Calculated values of pH (pH^{calc}) and potential change (glass/mV^{calc}) were obtained after calibrating the glass probe with standard buffers of pH 4.00, 7.00 and MRS buffer of pH 5.5.

Sample	pH^{calc}	$O.D^{490nm}$
1	3.99	2.08
2	4	2.06
3	3.98	2.1
4	3.97	2.07
5	3.99	2.13
6	3.99	2.13
Control	4.05±0.16	2.21±0.23

The average change in pH and cell density in the absence and presence of nucleating beads was 4.18 (Table 5.5) and 2.00 (Table 5.6). In the presence of a nucleator, pH was reduced from 5.5 (adjusted pH of culture medium before cell incubation) to 3.98 and cell density was increased to 2.09 after post-thaw incubation. Significant decrease in the pH was observed in the cells stored with the presence of nucleator concluding that cells were in metabolically active state after post-thaw recovery. The cells have shown evidence of metabolic activity and cell density in the absence and presence of nucleating beads.

The results of post thaw metabolic activity after cryopreservation in two different % mixtures of CPAs in the absence and presence of nucleators (mentioned in sections 5.6.1 and 5.6.2) have shown post thaw metabolic activity after overnight incubation in MRS broth. Results have determined that LAB could be cryopreserved in the combined mixtures of penetrating and non-penetrating CPAs.

5.2.5 Impedance results

Ice-initiation temperature and glass transition temperature of the mixture of glycerol-sucrose was monitored using transition monitoring system 2. The reason for monitoring transition temperatures was to evaluate the effect of ice nucleators and different % mixtures of cryoprotectants on LAB post-thaw metabolic activity. Depression in Tg (in the presence of nucleators) have slightly increased the post-thaw metabolic activity of the cells as compared to the cells stored without nucleatores (Table 5.7). Although post-thaw metabolic activity was observed after culturing cells cryopreserved in the presence of different % mixtures of glycerol-sucrose (without or with nucleator) but, the control cultures (starter

cultures) were more active as compared to the cryopreserved cells post-thawed and incubated overnight in MRS broth (Tables 5.3, 5.4, 5.5 and 5.6).

Table 5.7: θ^i (ice-initiation temperatures), Tg^c (glass transition during cooling event) and Tg^w (glass transition during warming event) of 5% Glycerol + 5% Sucrose 0.15 M NaCl + LAB + and 7.5% Glycerol+2.5% Sucrose +0.15 M NaCl + LAB, without (-) and with (+) nucleator at cooling rate of 5 °C min^{-1} from 0 to -90 °C followed by liquid nitrogen plunge. Tg of 3 replicates of following CPA mixtures was monitored.

Sample+ cells	$\theta^{i\ n-}$ (℃)	$\theta^{i\ n+}$ (℃)	Tg^{c-}	Tg^{c+}	Tg^{w-}	Tg^{w+}
5% Glycerol+5 % Sucrose	-2.45 ±0.06	1.92 ± 0.02	-39.58 ± 0.14	-42.91±0.05	-41.74 ± 0.07	-42.3±0.23
7.5% Glycerol+2.5 % Sucrose	-3.99 ± 0.03	-1.81 ± 0.12	-37.78 ± 0.27	-44 ± 0.19	-39.79 ±0.17	-45.7±0.33

Glass transition temperatures of described % mixtures of glycerol-sucrose-H_2O is not reported in the literature. Transition temperatures of glycerol and sucrose seperately have been reported, i.e. Tg of 5% sucrose is -37.7 °C to -39 °C (Nesariker et al., 2007) and 10% Glycerol is -62.7 °C (Morris et al., 2006). Nucleators tend to lower the Tg temperaratures compared to Tg observed in the absence of nucleating beads. It has been illustrated that glycerol has a plasticizing effect due to lower molecular weight and liquid nature (Roos, 2010, Bhandari and Roos, 2003) combination of lower and higher molecular weight solutions might have changed the physical properties and plasticizing effect of the solution resulted in changes to transition temperatues.

The Tg of % mixtures of CPA was studied in the absence of cells as well to observe weather the cells also influence the Tg temperature of cryoprotectant mixtures (Chapter 4).

5.3 Conclusion

The results indicate that when designing cryo-protocols it is helpful to analyse the interaction of biological system (cells) with cryoprotectants, the composition and concentration of CPAs effect of ice nucleation temperature, glass transition temperature, and the influence of cryopreservation protocols on their post-thaw metabolic activity.

The results draw the attention to the steps that might be taken to improve the cryopreservation protocols and storage temperatures for cryoprotectants + cell suspension in the presence and absence of nucleating beads.

Change in post–thaw pH and O.D. results have shown metabolic activity in both mixtures of glycerol and sucrose (in the presence and absence of nucleating beads). The cells did not face osmotic shock or toxicity effects in the presence of different percentage mixtures of penetrating and non-penetrating cryoprotectant mixtures as they have shown post-thaw metabolic activity after overnight incubation in MRS broth (see Tables 5.3 to 5.6).

An interaction of ice nucleation and glass transition during moderate cooling regime was observed as well. The results have shown that initiation of ice nucleation at higher temperatures cause a lowering in glass transition temperatures. As a consequence, the diffusion of ions become limited (prevention of cell dehydration) due to the formation of freeze-concentrated matrix having solid

properties (Morris et al., 2006). Slow cooling and rapid warming in air at room temperature in the presence of nucleating beads have protected LAB from mechanical damage (caused by extracellular ice formation) during cooling and osmotic shock (due to rapid diffusion of ions across the cells) during warming (Appelbaum et al., 2004, Rall et al., 1980, Sherman 1962, Whittingham et al., 1979).

The impedance results obtained using TMS 2 in this study have determined the influence of nucleating beads and different CPA mixtures on Tg shifts and post thaw metabolic activity of LAB. Results have indicated that ice initiation at lower temperatures and very slow rate of cooling in the absence of nucleator were detrimental to the post thaw metabolic activity of cells. Additionally, it is required to improve the response of TMS 2 to obtain Tg results in line with the Tg values described in literature using conventional glass transition monitoring methods e.g. DSC.

Chapter 6

Conclusion

6.1 Reiteration of aims and objectives

Cryopreservation is an established technique to preserve biological samples at low temperatures in the presence of suitable concentrations of cryoprotectants. Cryoprotectants undergo thermodynamic changes during cooling and warming altering the state of the solution from liquid to solid (ice) or amorphous solid (glass). These changes alter with the rate of cooling and warming, addition of additives and ice-initiation temperatures. Studying changes in phase transition temperatures with different rates of cooling and concentration of cryoprotectant agents (CPA) mixtures would allow their effect to be studied on post-thaw survival of biological samples.

Current techniques used to monitor phase change events are expensive and time consuming, and cannot be applied widely for routine laboratory based analysis. However, an understanding of the effects of CPA systems, cooling rates and phase transition temperatures on survival is important.

Lactobacillus delbrueckii subsp*. bulgaricus* CFL1 is a cold-sensitive strain and was chosen as a model organism due to its sensitivity towards freezing and frozen storage. Several studies have been undertaken to improve the preservation and storage of LAB starter cultures.

Screen-printed sensors are widely used in the field of biosensors, medical diagnostics, pharmaceutics, etc. for potentiometric and electrochemical analysis. In this study, two kinds of disposable sensors were produced using screen- printed technology: a) impedance electrodes to monitor phase-change events in cryoprotectant samples during cooling and warming regimes; and b) pH electrodes to study the metabolic activity of post-thawed *Lactobacillus delbrueckii* subsp *bulgaricus* CFL1. In addition, initial studies were carried out on the design and response of screen-printed temperature probes

6.1.1 Aims

The aim of the work described was to develop sensor systems to inform the process of cryopreservation of *Lactobacillus sp.* cultures and their post-thaw recovery.

6.1.2 Objectives

- To design, develop and evaluate instrumentation to allow monitoring of phase transitions during cooling and warming of cryoprotectant mixtures in cryotubes and cryostraws;

- to explore the use of screen-printed impedance and temperature sensors to monitor phase changes and temperature profiles during cooling and warming of cryoprotectant mixtures;

- to investigate the potential of screen-printed pH sensors to monitor post-thaw activity of cryopreserved *Lactobacillus sp.* and;

- to demonstrate how the sensor systems could be used to optimise the cryopreservation of *Lactobacillus.*

6.1.2.1 Design and development of sensor systems to monitor phase change events of CPA mixtures during cooling and warming in cryotubes and cryostraws

The aim was to develop a system which was cheap, robust and able to determine transition temperatures in small volume samples. Two types of impedance based instrumentation were designed and developed to determine the phase change events in cryoprotectant systems during cooling and warming events.

The first of these was a bread-board based single-channel transition monitoring system while the other was a multi-channel transition monitoring system fabricated as a printed-circuit board. The monitoring systems were connected to a data logger and sensors to determine phase change events with respect to the change in the temperature.

An Asymptote EF600 was used to control the slow cooling protocols. The warming event was performed either by switching ON the EF600 after (completion of cooling cycle) returning the temperature to 20 ℃ or was simply undertaken in air at room temperature. Screen-printed impedance and commercial platinum resistance temperature detector (Pt-RTD) probes were used in combination to determine changes in phase transition temperatures during different cryo-regimes. The data was collected and analysed using 1^{st} and 2^{nd} order derivatisation to determine the

glass transition temperatures during both cooling and warming events in cryotubes and cryostraws.

Three types of impedance electrodes were screen-printed to monitor transition events in cryotubes and straws (see Chapter 2). Electrodes were tested with the two sensor systems to monitor their response towards changes in the states of CPA solutions during cooling and warming regimes. The different types of impedance electrodes were used to determine the most suitable design for use in cryotubes and cryostraws to monitor transition events in 0.5 ml of sample.

6.1.2.2 Exploring the use of screen-printed temperature sensors along with the impedance and temperature sensors to monitor phase changes and temperature profiles during cooling and warming events

The use of a commercial the Pt-RTD temperature probe in small volume of CPA appeared to compromise the cooling profiles since a significant difference in transition temperatures was observed between vials with and without nucleator. There is a need for an alternative system to monitor the temperature change in multiple channels. Screen-printed temperature probes appear to offer a useful approach since these would have a lower thermal mass and would be incorporated onto the same stature as the impedance sensors. Initial experiments were carried out for screen-printing temperature probes and the results were promising. However, the screen-printed temperature probe needs further refinement and possible printing in combination with the impedance sensor.

Whilst phase transition temperatures obtained using the single-channel transition monitoring system (TMS 1) were close to the literature values, the full achievement of the objectives for phase transition monitoring was compromised by the problems met in the application of the multichannel impedance monitoring system. The

cause of this problem need to identified and corrected. Phase transition temperature monitoring would be helped by using screen-printed temperature probes in combination with the impedance sensors.

6.1.2.3 Development of screen-printed pH sensors to investigate post-thaw metabolic activity of Lactic Acid Bacteria (LAB)

Different CPA systems have been successfully used to preserve LAB however, effect of quaternary CPA system (water+CPA+NaCl+nucleator) on LAB post-thaw cell recovery have not been described in detail. Application of different cryo-regimes in the presence of different CPA concentrations, presence or absence of additives and ice-nucleators would allow: a) to determine their effect of LAB post-thaw metabolic activity; and b) to develop a cooling and warming profile for LAB cryopreservation with maximum post-thaw metabolic activity.

Ruthenium and antimony metals were used to manufacture the working element of screen-printed pH sensors. Metal powders were mixed separately with graphite-carbon and different percentage concentrations of metal powders were screen-printed over the working area of electrodes and tested to determine their potentiometric response. 54.5% of antimony-carbon electrode was sensitive towards pH change as compared to ruthenium-carbon screen-printed pH electrode.

Selection of reference elements

The working electrode could not work without a suitable reference for electrochemical measurements. Five different kinds of reference electrodes were tested with the working (carbon-metal) and conventional glass pH electrodes to determine the most suitable reference element to determine post-thaw recovery of LAB.

a) Conventional glass silver/silver chloride;
b) conventional glass pH electrode (old)
c) conventional glass pH electrode (new)
d) screen-printed Ag/AgCl electrode and;
e) screen-printed and salt-bridged Ag/AgCl reference electrode.

The aim was to select a reference element that could easily incorporate into cryotubes, give potentiometric response nearest to Nernst's value, practicable for post-thaw recovery assessment in laboratories, disposable, cheap, robust and able to monitor metabolic activity in small volume samples. To achieve these aims, electrodes were tested with different reference solutions. Standard measurements were taken alongside with the experimental measurements to compare the linearity of the designed and conventional pH reference and working electrodes.

The results demonstrated that screen-printed antimony (working) sensor works well with screen-printed and salt-bridged Ag/AgCl (reference) electrode and Ag/AgCl reference element of conventional glass pH electrode. The ideal combination for pH measurements of LAB cultures in small volume samples and with less health risks (due to disposable and non-fragile nature of screen-printed electrodes) would be a combined screen-printed working + screen-printed, salt-

bridged Ag/AgCl reference. The initial objective was achieved; however the reference electrode requires further improvements in terms of its design and integration with the working electrode.

6.1.2.4 The use of sensors and sensor systems to optimise the cryopreservation of *Lactobacillus sp*.

In this study two kinds of sensor systems, screen-printed impedance and screen-printed pH probes were designed, validated and used to determine phase transition temperatures and post-thaw metabolic activity of lactic acid bacteria. Three different cooling rates and different concentrations of ternary and quaternary CPA mixtures in the presence and absence of ice-nucleator were studied for LAB cryopreservation. The results obtained in the presence and absence of ice-nucleators at different cooling profiles was compared with the set of controls to study the influence of cryopreservation and CPA's on post-thaw cell metabolic activity by monitoring pH change after overnight incubation in MRS broth.

Studies showed that the moderate cooling profile (5 ℃ min^{-1}) gave the best survival in the presence and absence of nucleating beads and was chosen to be the best protocol for LAB cryopreservation. Conversely the post-thaw survival of LAB stored at very slow rate of cooling (0.1 ℃ min^{-1}) was recovered in the presence of nucleator. It was concluded that best post-thaw cell survival was achieved in the presence of nucleating beads. Therefore, the favourable and adaptive approach of LAB cryopreservation is by addition of nucleating beads to the CPA mixtures.

The sensors and sensor systems have determined the transition temperatures during cooling and warming events of CPA+cells (with or without nucleator). The shifts in ice-initiation and glass transition temperatures due to the presence or

absence of ice-nucleating beads have indicated the effect of three different cooling profiles and early or delayed ice-initiation temperatures on post-thaw cell recovery. Assessment of post-thaw metabolic activity was undertaken with screen-printed pH or conventional glass pH probes after LAB incubation in MRS broth. The results have determined the effect of cooling profiles and ice nucleators on post-thaw cell viability.

The main objective of this study was fulfilled in parts as multichannel transition monitoring system (TMS 2) and screen-printed impedance probes require further refinements in their circuitry, probe design and fabrication.

6.2 Achievement of aims and objectives

The objectives have partially been achieved as desired due to problems in the signalling response of some devices and time limitation. Different phase transition temperature values were obtained with the two devices (single and multi-channel transition monitoring systems). Moreover, whilst the Tg values obtained by the single channel system were close to those reported in the literature, the values from the multichannel instrument were not.

Screen-printed temperature probes would offer a real advantage in multichannel monitoring, but they require more testing to ensure their response to temperature change. The pH screen-printed salt-bridged reference probes require further work to minimise the solution leakage from the capillary and better contact with antimony working electrode during pH measurements.

The main aims of the project have been largely met, with proof of principle of the potential for screen-printed impedance, temperature and pH sensors and the application in cryo-protocol design.

6.3 Future work

To overcome the problems in achieving aims and objectives in this study, the screen-printed pH sensors and multichannel phase transition monitoring systems need refinement.

In order to obtain Tg events from more than one samples using impedance monitoring system, multiple screen-printed temperature probes are required for the measurements. Initial tests were promising however, additional development in the sensors is required to improve its design and signalling response.

Although Tg temperatures were described by both devices designed in this project however, multi-channelled transition monitoring system needs to be modified in order to obtain transition temperatures closer to Tg values of CPAs described in the literature.

Screen-printed salt bridges Ag/AgCl reference electrodes need to be re-fabricated and used in combination with the carbon-antimony working electrode to obtain robust pH results from biological samples after post-thaw incubation. Instead of adding 0.1M KCl solution to the capillary chamber of salt-bridged electrode a gel (e.g. carrageenan gel) could be introduced to obtain potentiometric response from the outer solution without the formation of air bubbles in the KCl solution or its leakage from the chamber.

Improvements in the screen-printed pH sensor design would allow manufacturing a non-fragile and disposable sensor for sensing the metabolic activity of starter cultures of LAB at laboratory or industrial scale. It would help to assess a highly metabolically active sample from batch cultures without some health and safety issues (due to its disposable and non-fragile nature) and enable to improve the quality of dairy products.

6.4 Application of the present study

The devices designed and used in this project would have a commercial application in future if their performance could be improved. Modification of impedance monitoring system, screen-printed temperature and pH probes would enable real-time monitoring of the transition temperatures and post-thaw metabolic activity. They would be cheap, robust, disposable and portable alternatives to the current methodologies.

This study suggests that two combined sensor systems (i) a screen-printed impedance+screen-printed temperature sensor: and (ii) a screen-printed pH working+screen-printed salt-bridged Ag/AgCl reference, would offer real advantages in the monitoring of phase transition events during cryopreservation, and post-thaw activity of lactic acid bacteria.

6.5 Finally

To conclude:-

Phase change monitoring screen-printed interdigitated electrodes were designed for cryotubes and cryostraws. Later electrode design was further improved for use in cryotubes as cryostraws proved difficult for Tg assessment due to probe adjustment and solution leakage problems.

TMS1 system was initially developed for phase change monitoring of CPA mixtures. However, this was capable of monitoring phase change in only one sample at a time. Later an improved system, TMS2, allowed monitoring phase change events in more than one sample at a time, but due to the limitation of having only one temperature probe the experiments could still only be done using a single channel. The results obtained from TMS1 were not significantly different from the literature. However TMS2 gave values significantly different from those in the literature. In future TMS2 will require improvements in its signalling response and also require a combined temperature and impedance sensor system to exploit six channels for phase change monitoring.

For post-thaw metabolic assessment of LAB, screen-printed pH probes were designed and manufactured to adopt an alternative non-fragile technique for pH measurement in fresh and post-thawed cell samples. Both working and reference electrodes were fabricated in a single device and a salt-bridge was used to ensure good functioning of the reference electrode for better pH monitoring in MRS broth containing cells. Results have indicated that sensors were responding to the pH change, however further developments are required for improved sensor construction.

Chapter 7

References

Convert between times gravity (xg) and centrifuge rotor speed (RPM) [Online]. Rockford: Thermo Fisher Scientific. Available: http://www.piercenet.com/files/TR0040-Centrifuge-speed.pdf [Accessed TECH TIP 40.

ADAMBERG, K., KASK, S., LAHT, T.-M. & PAALME, T. 2003. The effect of temperature and pH on the growth of lactic acid bacteria: a pH-auxostat study. *International Journal of Food Microbiology,* 85**,** 171-183.

APPELBAUM, F. R., BLUME, K. G. & FORMAN, S. J. 2004. *Thomas' hematopoietic cell transplantation,* Malden, Mass. [u.a.], Blackwell.

ARCHER, D. L. 2004. Freezing: an underutilized food safety technology? *International Journal of Food Microbiology,* 90**,** 127-138.

AXELSSON, L. 2009. Lactic acid bacteria: Classification and physiology. *Lactic acid bacteria: microbiological and functional aspects,* 139**,** 1.

BAKER, B. 1998. Precision Temperature Sensing with RTD Circuits. *AN687, Microchip Technology Inc*.

BEAL, C. & CORRIEU, G. 1991. Influence of pH, temperature, and inoculum composition on mixed cultures of Streptococcus thermophilus 404 and Lactobacillus bulgaricus 398. *Biotechnology and bioengineering,* 38**,** 90-98.

BEAL, C., LOUVET, P. & CORRIEU, G. 1989. Influence of controlled pH and temperature on the growth and acidification of pure cultures of Streptococcus thermophilus 404 and Lactobacillus bulgaricus 398. *Applied Microbiology and Biotechnology,* 32**,** 148-154.

BÉAL, C., MARIN, M., FONTAINE, E., FONSECA, F. & OBERT, J. 2008. Production et conservation des ferments lactiques et probiotiques. *Bactéries lactiques, de la génétique aux ferments. Tec&Doc Lavoisier, Paris, France***,** 661-785.

BHANDARI, B. R. & ROOS, Y. H. 2003. Dissolution of sucrose crystals in the anhydrous sorbitol melt. *Carbohydrate research,* 338**,** 361-367.

BLOND, G. & SIMATOS, D. 1991. Glass transition of the amorphous phase in frozen aqueous systems. *Thermochimica Acta,* 175**,** 239-247.

BRASHEARS, M. & GILLILAND, S. 1995. Survival During Frozen and Subsequent Refrigerated Storage of *Lactobacillus acidophilus* Cells as Influenced by the Growth Phase. *Journal of Dairy Science,* 78**,** 2326-2335.

BUCK, R., RONDININI, S., COVINGTON, A., BAUCKE, F., BRETT, C., CAMOES, M., MILTON, M., MUSSINI, T., NAUMANN, R. & PRATT, K. 2002. Measurement of pH. Definition, standards, and procedures (IUPAC Recommendations 2002). *Pure and applied chemistry,* 74**,** 2169-2200.

CACHON, R., ANTÉRIEUX, P. & DIVIÈS, C. 1998. The comparative behavior of< i> Lactococcus lactis</i> in free and immobilized culture processes. *Journal of biotechnology,* 63**,** 211-218.

CARRINGTON, A. K., GOFF, H. D. & STANLEY, D. W. 1996. Structure and stability of the glassy state in rapidly and slowly cooled carbohydrate solutions. *Food Research International,* 29**,** 207-213.

CARVALHO, A. S., SILVA, J., HO, P., TEIXEIRA, P., MALCATA, F. X. & GIBBS, P. 2003. Protective effect of sorbitol and monosodium glutamate during storage of freeze-dried lactic acid bacteria. *Lait,* 83**,** 203-210.

CHAMPAGNE, C. P., GARDNER, N., BROCHU, E., BEAULIEU, Y. 1991. The freeze-drying of lactic acid bacteria. A review. *Canadian Institute of Food Science and Technology journal :Journal de l'Institut canadien de science et technologie alimentaire.,* 24**,** p. 118-128.

CHANG, J.-L. & ZEN, J.-M. 2006. Fabrication of disposable ultramicroelectrodes: Characterization and applications. *Electrochemistry Communications,* 8**,** 571-576.

CHEN, N., MORIKAWA, J. & HASHIMOTO, T. 2005. Effect of cryoprotectants on eutectics of NaCl·2H2O/ice and KCl/ice studied by temperature wave analysis and differential scanning calorimetry. *Thermochimica Acta,* 431**,** 106-112.

CHOI, J. H. & BISCHOF, J. C. 2008. A quantitative analysis of the thermal properties of porcine liver with glycerol at subzero and cryogenic temperatures. *Cryobiology,* 57**,** 79-83.

COCKS, F., HILDEBRANDT, W. & SHEPARD, M. 1975. Comparison of the low-temperature crystallization of glasses in the ternary systems H2O-NaCl-dimethyl sulfoxide and H2O-NaCl-glycerol. *Journal of Applied Physics,* 46**,** 3444-3448.

COOK, I., WARD, K., MALIK, K. & MATEJTSCHUK, P. The use of impedance analysis for the study of critical events in the frozen state, for formulation and lyo-cycle development. Journal of Pharmacy and Pharmacology, 2009. Pharmaceutical press-royal pharmaceutical soc great britian 1 lambeth high st, london se1 7jn, england, A103-A104.

DALY, C., FITZGERALD, G. F., O'CONNOR, L. & DAVIS, R. 1998. Technological and health benefits of dairy starter cultures. *International Dairy Journal,* 8**,** 195-205.

DELUCA, P. & LACHMAN, L. 1965. Lyophilization of pharmaceuticals I. Effect of certain physical-chemical properties. *Journal of Pharmaceutical Sciences,* 54**,** 617-624.

DOMÍNGUEZ RENEDO, O. & ARCOS MARTÍNEZ, M. J. 2007. Anodic stripping voltammetry of antimony using gold nanoparticle-modified carbon screen-printed electrodes. *Analytica chimica acta,* 589**,** 255-260.

EVEN, S., LINDLEY, N. D., LOUBIÈRE, P. & COCAIGN-BOUSQUET, M. 2002. Dynamic response of catabolic pathways to autoacidification in Lactococcus lactis: transcript profiling and stability in relation to metabolic and energetic constraints. *Molecular microbiology,* 45**,** 1143-1152.

FAHY, G. M. 1986. The relevance of cryoprotectant "toxicity" to cryobiology. *Cryobiology,* 23**,** 1-13.

FASZER, K., DRAPER, D., GREEN, J., MORRIS, G. & GROUT, B. 2006. Cryopreservation of horse semen under laboratory and field conditions using a stirling cycle freezer. *CryoLetters,* 27**,** 179-184.

FERNANDA MOZZI, R. R. R., GRACIELA M. VIGNOLO. 2010. Biotechnology of Lactic Acid Bacteria: Novel Applications. Willey-Blackwell Publishing.

FERREIRA, V. N., SOARES, V. N., SANTOS, C., SILVA, J., GIBBS, P. A. & TEIXEIRA, P. 2005. Survival of Lactobacillus sakei during heating, drying

and storage in the dried state when growth has occurred in the presence of sucrose or monosodium glutamate. *Biotechnology Letters,* 27**,** 249-252.

FONSECA, F., BÉAL, C. & CORRIEU, G. 2001. Operating Conditions That Affect the Resistance of Lactic Acid Bacteria to Freezing and Frozen Storage. *Cryobiology,* 43**,** 189-198.

FONSECA, F., BÉAL, C., MIHOUB, F., MARIN, M. & CORRIEU, G. 2003a. Improvement of cryopreservation of Lactobacillus delbrueckii subsp. bulgaricus CFL1 with additives displaying different protective effects. *International Dairy Journal,* 13**,** 917-926.

FONSECA, F., BÉAL, C., MIHOUB, F., MARIN, M. & CORRIEU, G. 2003b. Improvement of cryopreservation of *Lactobacillus delbrueckii* subsp.*bulgaricus* CFL1 with additives displaying different protective effects. *International dairy journal,* 13**,** 917-926.

FONSECA, F., BEALL, C. & CORRIEU, G. 2000. Method of quantifying the loss of acidification activity of lactic acid starters during freezing and frozen storage. *Journal of Dairy Research,* 67**,** 83-90.

FONSECA, F., MARIN, M. & MORRIS, G. J. 2006a. Stabilization of Frozen Lactobacillus delbrueckii subsp. bulgaricus in Glycerol Suspensions: Freezing Kinetics and Storage Temperature Effects. *Appl. Environ. Microbiol.,* 72**,** 6474-6482.

FONSECA, F., MARIN, M. & MORRIS, G. J. 2006b. Stabilization of frozen Lactobacillus delbrueckii subsp. bulgaricus in glycerol suspensions: Freezing kinetics and storage temperature effects. *Applied and environmental microbiology,* 72**,** 6474-6482.

FRANKS, F. 1985. *Biophysics and biochemistry at low temperatures,* Cambridge, Cambridge University press.

FRANKS, F., MATHIAS, S. F., GALFRE, P., WEBSTER, S. D. & BROWN, D. 1983. Ice nucleation and freezing in undercooled cells. *Cryobiology,* 20**,** 298-309.

FUJIWARA, S. & NISHIMOTO, Y. 1998. Nonbiological Complete Differentiation of the Enantiomeric Isomers of Amino Acids and Sugars by the Complexes of Gases with the Eutectic Compounds of Alkali Chlorides and Water. *Analytical Sciences,* 14**,** 507-514.

GAO, D. & CRITSER, J. 2000. Mechanisms of cryoinjury in living cells. *ILAR journal,* 41**,** 187-196.

GERMOND, J. E., LAPIERRE, L., DELLEY, M., MOLLET, B., FELIS, G. E. & DELLAGLIO, F. 2003. Evolution of the bacterial species Lactobacillus delbrueckii: A partial genomic study with reflections on prokaryotic species concept. *Molecular Biology and Evolution,* 20**,** 93-104.

GLANC-GOSTKIEWICZ, M., SOPHOCLEOUS, M., ATKINSON, J. K. & GARCIA-BREIJO, E. 2013. Performance of miniaturised thick-film solid state pH sensors. *Sensors and Actuators A: Physical,* 202**,** 2-7.

GLANC, M., SOPHOCLEOUS, M., ATKINSON, J. & GARCIA-BREIJO, E. 2013. The effect on performance of fabrication parameter variations of thick-film screen printed silver/silver chloride potentiometric reference electrodes. *Sensors and Actuators A: Physical,* 197**,** 1-8.

GLEASON, K. 2012. *How to convert Centrifuge RPM to RCF or G-force?* [Online]. Cambridge: Clinfield Limited. Available: http://clinfield.com/2012/07/how-to-convert-centrifuge-rpm-to-rcf-or-g-force/ [Accessed July 15 2012].

GONÇALVES, L., RAMOS, A., ALMEIDA, J., XAVIER, A. & CARRONDO, M. 1997. Elucidation of the mechanism of lactic acid growth inhibition and production in batch cultures of Lactobacillus rhamnosus. *Applied Microbiology and Biotechnology,* 48**,** 346-350.

GRATTEPANCHE, F., MIESCHER-SCHWENNINGER, S., MEILE, L. & LACROIX, C. 2008. Recent developments in cheese cultures with protective and probiotic functionalities. *Dairy Science and Technology,* 88**,** 421-444.

GREAVES, R. 1954. Theoretical aspects of drying by vacuum sublimation. *Biological Applications of Freezing and Drying***,** 87-127.

GURIAN-SHERMAN, D. & LINDOW, S. E. 1993. Bacterial ice nucleation: significance and molecular basis. *Faseb j,* 7**,** 1338-43.

HALÁSZ, A. 2009. Lactic acid bacteria. *Food Quality and Standards,* 3**,** 70-82.

HARRISON JR, A. P. 1956. Causes of death of bacteria in frozen suspensions. *Antonie van Leeuwenhoek,* 22**,** 407-418.

HEIDEBACH, T., FÖRST, P. & KULOZIK, U. 2010. Influence of casein-based microencapsulation on freeze-drying and storage of probiotic cells. *Journal of Food Engineering,* 98**,** 309-316.

HER, L. M., JEFFERIS, R. P., GATLIN, L. A., BRAXTON, B. & NAIL, S. L. 1994. Measurement of glass transition temperatures in freeze concentrated solutions of non-electrolytes by electrical thermal analysis. *Pharm Res,* 11**,** 1023-9.

HUBALEK, Z. 2003. Protectants used in the cryopreservation of microorganisms. *Cryobiology,* 46**,** 205-229.

JACOBS, P., VARLAN, A. & SANSEN, W. 1995. Design optimisation of planar electrolytic conductivity sensors. *Medical and Biological Engineering and Computing,* 33**,** 802-810.

JOCHEM, M. & KÖRBER, C. 1987. Extended phase diagrams for the ternary solutions H< sub> 2</sub> O-NaCl-glycerol and H< sub> 2</sub> O-NaCl-hydroxyethylstarch (HES) determined by DSC. *Cryobiology,* 24**,** 513-536.

JOHN MORRIS, G. & ACTON, E. 2013. Controlled ice nucleation in cryopreservation – A review. *Cryobiology,* 66**,** 85-92.

KADARA, R. O., JENKINSON, N. & BANKS, C. E. 2009. Characterization and fabrication of disposable screen printed microelectrodes. *Electrochemistry Communications,* 11**,** 1377-1380.

KAKIUCHI, T. 2014. Ionic liquid salt bridge—Current stage and perspectives: A mini review. *Electrochemistry Communications,* 45**,** 37-39.

KALICHEVSKY, M. T., JAROSZKIEWICZ, E. M., ABLETT, S., BLANSHARD, J. M. V. & LILLFORD, P. J. 1992. The glass transition of amylopectin measured by DSC, DMTA and NMR. *Carbohydrate Polymers,* 18**,** 77-88.

KAWAHARA, H. 2013. Characterizations of Functions of Biological Materials Having Controlling-Ability Against Ice Crystal Growth. *In:* FERREIRA, D. S. (ed.) *Advanced Topics on Crystal Growth.* InTech.

KHALID, K. 2011. An overview of lactic acid bacteria. *Int J Biosci,* 1**,** 1-13.

KILMARTIN, P. A., REID, D. S. & SAMSON, I. 2000. The measurement of the glass transition temperature of sucrose and maltose solutions with added NaCl. *Journal of the Science of Food and Agriculture,* 80**,** 2196-2202.

LAAKSONEN, T. J. & ROOS, Y. H. 2000. Thermal, Dynamic-mechanical, and Dielectric Analysis of Phase and State Transitions ofFrozen Wheat Doughs. *Journal of Cereal Science,* 32**,** 281-292.

LANGEREIS, G., OLTHUIS, W. & BERGVELD, P. Measuring conductivity, temperature and hydrogen peroxide concentration using a single sensor structure. Solid State Sensors and Actuators, 1997. TRANSDUCERS'97 Chicago., 1997 International Conference on, 1997. IEEE, 543-546.

LAWN, R. E. & PRICHARD, E. 2003. *Measurement of PH*, Royal Society of Chemistry.

LE MARREC, C., BON, E. & LONVAUD-FUNEL, A. 2007. Tolerance to high osmolality of the lactic acid bacterium< i> Oenococcus oeni</i> and

identification of potential osmoprotectants. *International journal of food microbiology,* 115**,** 335-342.
LINDNER, E. 2014. Konstantin N. Mikhelson: Ion-selective electrodes. *Analytical and Bioanalytical Chemistry,* 406**,** 373-374.
LOUIS REY, J. C. M. 2004. *Freeze-Drying/Lyopilization of Pharmaceutical and Biological Products,* New York, USA, Marcel Dekker, Inc.
LOVELOCK, J. 1953a. The haemolysis of human red blood-cells by freezing and thawing. *Biochimica et Biophysica Acta,* 10**,** 414-426.
LOVELOCK, J. 1953b. Het mechanism of the protective action of glycerol against haemolysis by freezing and thawing. *Biochimica et biophysica acta,* 11**,** 28-36.
LOVELOCK, J. 1954. The protective action of neutral solutes against haemolysis by freezing and thawing. *Biochemical Journal,* 56**,** 265.
LUYET, B. & RASMUSSEN, D. 1967. Study by differential thermal analysis of the temperatures of instability of rapidly cooled solutions of glycerol, ethylene glycol, sucrose and glucose. *Biodynamica,* 10**,** 167-191.
LUYET, B., RASMUSSEN, D. & KROENER, C. 1966. Successive crystallization and recrystallization, during rewarming, of rapidly cooled solutions of glycerol and ethylene glycol. *Biodynamica,* 10**,** 53.
MACKENZIE, A. 1985. Changes in electrical resistance during freezing and their application to the control of the freeze-drying process. *Science et Technique du Froid*.
MAGNUSSON, K. E. & EDEBO, L. 1976. Influence of salts and gelatin on disintegration of Saccharomyces cerevisiae by freeze-pressing. *Biotechnology and bioengineering,* 18**,** 449-463.
MATTOCK, G., TAYLOR, G. R. & PAUL, M. A. 1963. pH measurement and titration. *Journal of The Electrochemical Society,* 110**,** 31C-31C.
MAURYA, D., SARDARINEJAD, A. & ALAMEH, K. 2013. High-sensitivity pH sensor employing a sub-micron ruthenium oxide thin-film in conjunction with a thick reference electrode. *Sensors and Actuators A: Physical,* 203**,** 300-303.
MAZUR, P. 1960. PHYSICAL FACTORS IMPLICATED IN THE DEATH OF MICROORGANISMS AT SUBZERO TEMPERATURES*. *Annals of the New York Academy of Sciences,* 85**,** 610-629.
MAZUR, P. 1963a. Kinetics of water loss from cells at subzero temperatures and the likelihood of intracellular freezing. *The Journal of General Physiology,* 47**,** 347-369.
MAZUR, P. 1963b. Studies on rapidly frozen suspensions of yeast cells by differential thermal analysis and conductometry. *Biophysical journal,* 3**,** 323-353.
MAZUR, P. 1965. The role of cell membranes in the freezing of yeast and other single cells*. *Annals of the New York Academy of Sciences,* 125**,** 658-676.
MAZUR, P. 1970. Cryobiology: The Freezing of Biological Systems. *Science,* 168**,** 939-949.
MAZUR, P. 1977. The role of intracellular freezing in the death of cells cooled at supraoptimal rates. *Cryobiology,* 14**,** 251-272.
MERYMAN, H., WILLIAMS, R. & DOUGLAS, M. S. J. 1977. Freezing injury from "solution effects" and its prevention by natural or artificial cryoprotection. *Cryobiology,* 14**,** 287-302.
MERYMAN, H. T. The exceeding of a minimum tolerable cell volume in hypertonic suspension as a cause of freezing injury. Ciba Foundation Symposium-The Frozen Cell, 1970. Wiley Online Library, 51-67.

MERYMAN, H. T. 1974. Freezing injury and its prevention in living cells. *Annual Review of Biophysics and Bioengineering,* 3**,** 341-363.

MIZRAHY, O., BAR-DOLEV, M., GUY, S. & BRASLAVSKY, I. 2013. Inhibition of Ice Growth and Recrystallization by Zirconium Acetate and Zirconium Acetate Hydroxide. *PloS one,* 8**,** e59540.

MORICE, M., BRACQUART, P. & LINDEN, G. 1992. Colonial Variation and Freeze-Thaw Resistance of *Streptococcus thermophilus*. *Journal of Dairy Science,* 75**,** 1197-1203.

MORRIS, G. J., GOODRICH, M., ACTON, E. & FONSECA, F. 2006a. The high viscosity encountered during freezing in glycerol solutions: effects on cryopreservation. *Cryobiology,* 52**,** 323-34.

MORRIS, G. J., GOODRICH, M., ACTON, E. & FONSECA, F. 2006b. The high viscosity encountered during freezing in glycerol solutions: effects on cryopreservation. *Cryobiology,* 52**,** 323-334.

MULDREW, K., ACKER, J. & WAN, R. 2000. Investigations into quantitative post-hypertonic lysis theory using cultured fibroblasts. *Cryobiology,* 41**,** 337.

NAKAMURA, L. K. 1996. Chapter 4 - Preservation and Maintenance of Eubacteria. *In:* JENNIE, C. H.-C. & ANGELA, B. (eds.) *Maintaining Cultures for Biotechnology and Industry.* San Diego: Academic Press.

NASCIMENTO, V. B. & ANGNES, L. 1998. Screen-printed electrodes. *Química Nova,* 21**,** 614-629.

NESARIKAR, V. V. & NASSAR, M. N. 2007. Effect of cations and anions on glass transition temperatures in excipient solutions. *Pharm Dev Technol,* 12**,** 259-64.

NESARIKER, V., V., NASSAR & N., M. 2007. *Effect of cations and anions on glass transition temperatures in excipient solutions,* New York, NY, ETATS-UNIS, Informa Healthcare.

NICOLAS, P., BESSIÈRES, P., EHRLICH, S. D., MAGUIN, E. & VAN DE GUCHTE, M. 2007. Extensive horizontal transfer of core genome genes between two Lactobacillus species found in the gastrointestinal tract. *BMC evolutionary biology,* 7**,** 141.

OLDENHOF, H., WOLKERS, W. F., FONSECA, F., PASSOT, S. & MARIN, M. 2005. Effect of Sucrose and Maltodextrin on the Physical Properties and Survival of Air-Dried Lactobacillus bulgaricus: An in Situ Fourier Transform Infrared Spectroscopy Study. *Biotechnology Progress,* 21**,** 885-892.

ORLA-JENSEN, S. 1919. *The Lactic Acid Bacteria*, E. Munksgaard.

PANOFF, J. M., THAMMAVONGS, B. & GUEGUEN, M. 2000. Cryoprotectants lead to phenotypic adaptation to freeze-thaw stress in Lactobacillus delbrueckii ssp. bulgaricus CIP 101027T. *Cryobiology,* 40**,** 264-9.

PARKS, J. E. & GRAHAM, J. K. 1992. Effects of cryopreservation procedures on sperm membranes. *Theriogenology,* 38**,** 209-222.

PEIGHAMBARDOUST, S. H., GOLSHAN TAFTI, A. & HESARI, J. 2011. Application of spray drying for preservation of lactic acid starter cultures: a review. *Trends in Food Science & Technology,* 22**,** 215-224.

QINGWEN, L., GUOAN, L. & YOUQIN, S. 2000. Response of nanosized cobalt oxide electrodes as pH sensors. *Analytica chimica acta,* 409**,** 137-142.

RALL, W. F., REID, D. S. & FARRANT, J. 1980. Innocuous biological freezing during warming. *Nature,* 286**,** 511-514.

RAULT, A., BOUIX, M. & BÉAL, C. 2008. Dynamic analysis of Lactobacillus delbrueckii subsp. bulgaricus CFL1 physiological characteristics during fermentation. *Applied Microbiology and Biotechnology,* 81**,** 559-570.

RAULT, A., BOUIX, M. & BÉAL, C. 2009. Fermentation pH influences the physiological-state dynamics of Lactobacillus bulgaricus CFL1 during pH-controlled culture. *Applied and environmental microbiology,* 75**,** 4374-4381.

RENEDO, O. D., ALONSO-LOMILLO, M. & MARTINEZ, M. 2007. Recent developments in the field of screen-printed electrodes and their related applications. *Talanta,* 73**,** 202-219.

REY, L. 1999. Glimpses into the realm of freeze-drying: classical issues and new ventures. *Drugs and the pharmaceutical sciences,* 96**,** 1-30.

REY, L. R. 1960. THERMAL ANALYSIS OF EUTECTICS IN FREEZING SOLUTIONS. *Annals of the New York Academy of Sciences,* 85**,** 510-534.

RHEE, S. & PACK, M. 1980. Effect of environmental pH on chain length of lactobacillus bulgaricus. *Journal of bacteriology,* 144**,** 865-868.

ROOS, Y. & KAREL, M. 1991a. Amorphous state and delayed ice formation in sucrose solutions. *International journal of food science & technology,* 26**,** 553-566.

ROOS, Y. & KAREL, M. 1991b. Nonequilibrium ice formation in carbohydrate solutions. *Cryo-Letters,* 12**,** 367-376.

ROOS, Y. H. 2010. Glass transition temperature and its relevance in food processing. *Annual Review of Food Science and Technology,* 1**,** 469-496.

ROOZEN, M. J. G. W., HEMMINGA, M. A. & WALSTRA, P. 1991. Molecular-Motion in Glassy Water Maltooligosaccharide (Maltodextrin) Mixtures as Studied by Conventional and Saturation-Transfer Spin-Probe Esr Spectroscopy. *Carbohydrate Research,* 215**,** 229-237.

SALMINEN, S., VON WRIGHT, A. & OUWEHAND, A. 2004. *Lactic acid bacteria: microbiology and functional aspects*, Marcel Dekker.

SANDERS, J. W., VENEMA, G. & KOK, J. 1999. Environmental stress responses in Lactococcus lactis. *FEMS Microbiology Reviews,* 23**,** 483-501.

SAVOIE, S., CHAMPAGNE, C., CHIASSON, S. & AUDET, P. 2007. Media and process parameters affecting the growth, strain ratios and specific acidifying activities of a mixed lactic starter containing aroma-producing and probiotic strains. *Journal of Applied Microbiology,* 103**,** 163-174.

SCHILDER, G. 2003. The possibilities of electrical resistance measurements to determine freeze-drying process data compared with data from the cryomicroscope. *ISL-FD Lyophilization Conference.*

SCHOUG, A., OLSSON, J., CARLFORS, J., SCHNÜRER, J. & HÅKANSSON, S. 2006. Freeze-drying of Lactobacillus coryniformis Si3--effects of sucrose concentration, cell density, and freezing rate on cell survival and thermophysical properties. *Cryobiology,* 53**,** 119-127.

SHERMAN, J. K. 1962. Survival of higher animal cells after the formation and dissolution of intracellular ice. *The Anatomical Record,* 144**,** 171-189.

SMITH, G., POLYGALOV, E., ARSHAD, M. S., PAGE, T., TAYLOR, J. & ERMOLINA, I. 2013. An impedance-based process analytical technology for monitoring the lyophilisation process. *International Journal of Pharmaceutics,* 449**,** 72-83.

SMITH, G. D., SERAFINI, P. C., FIORAVANTI, J., YADID, I., COSLOVSKY, M., HASSUN, P., ALEGRETTI, J. R. & MOTTA, E. L. 2010. Prospective randomized comparison of human oocyte cryopreservation with slow-rate freezing or vitrification. *Fertility and Sterility,* 94**,** 2088-2095.

SMITTLE, R. B., GILLILAND, S. E. & SPECK, M. L. 1972. Death of Lactobacillus bulgaricus Resulting from Liquid Nitrogen Freezing. *Applied microbiology,* 24**,** 551-4.

SOLEIMANI, M., SOPHOCLEOUS, M., GLANC, M., ATKINSON, J., WANG, L., WOOD, R. & TAYLOR, R. 2013. Engine oil acidity detection using solid state ion selective electrodes. *Tribology International,* 65**,** 48-56.

STIEGLMEIER, M., WIRTH, R., KMINEK, G. & MOISSL-EICHINGER, C. 2009. Cultivation of anaerobic and facultatively anaerobic bacteria from spacecraft-associated clean rooms. *Applied and environmental microbiology,* 75**,** 3484-3491.

TEIXEIRA, P., CASTRO, H., MOHÁCSI-FARKAS, C. & KIRBY, R. 1997. Identification of sites of injury in Lactobacillus bulgaricus during heat stress. *Journal of Applied Microbiology,* 83**,** 219-226.

TYMCZYSZYN, E., GÓMEZ-ZAVAGLIA, A. & DISALVO, E. 2007. Effect of sugars and growth media on the dehydration of Lactobacillus delbrueckii ssp. bulgaricus. *Journal of Applied Microbiology,* 102**,** 845-851.

VAN REENEN, C. A. & DICKS, L. M. 2011. Horizontal gene transfer amongst probiotic lactic acid bacteria and other intestinal microbiota: what are the possibilities? A review. *Archives of microbiology,* 193**,** 157-168.

VONAU, W. & GUTH, U. 2006. pH Monitoring: a review. *Journal of Solid State Electrochemistry,* 10**,** 746-752.

WANG, H.-Y., LU, S.-S. & LUN, Z.-R. 2009. Glass transition behavior of the vitrification solutions containing propanediol, dimethyl sulfoxide and polyvinyl alcohol. *Cryobiology,* 58**,** 115-117.

WANG, J. 2002. Real-Time Electrochemical Monitoring: Toward Green Analytical Chemistry. *Accounts of Chemical Research,* 35**,** 811-816.

WARD, K. R. & MATEIJTSCHUK, P. 2010. The use of microscopy, thermal analysis, and impedance measurements to establish critical formulation parameters for freeze-drying cycle development. *Freeze drying/lyophilization of pharmaceutical and biological products, 3rd edn. Informa Healthcare, New York, NY*.

WHITTINGHAM, D. G., WOOD, M., FARRANT, J., LEE, H. & HALSEY, J. A. 1979. SURVIVAL OF FROZEN MOUSE EMBRYOS AFTER RAPID THAWING FROM -196-DEGREES-C. *Journal of Reproduction and Fertility,* 56**,** 11-21.

WIEST, S. C. & STEPONKUS, P. L. 1978. Freeze-thaw injury to isolated spinach protoplasts and its simulation at above freezing temperatures. *Plant physiology,* 62**,** 699-705.

Appendix I

Table IA: Calibration of painted temperature probe at different temperatures

	Temperature/ ° C							
	20	**-10**	**-20**	**-40**	**-60**	**-80**	**-100**	**20**
Resistivity/ MΩ	102.8	097.91	092.41	089.17				103.33
	105.2	099.28	97.185	093.62	091.69			104.86
	104.86				090.75			105.36
	105.65	099.82	098.79	094.10	092.24			105.86
	105.83	100.78	098.76	093.79	091.76	090.66		106.38
	106.44	100.76	099.67	095.05	092.32	091.03		106.83
	106.83	101.80	099.76	094.91	092.37	091.13		106.97
	108.70	104.16	100.65	097.24	095.22	093.7	092.92	108.75
	108.76	103.75	100.51	096.37	094.44	093.14	092.54	108.85
	108.89	103.37	100.54	095.90	093.83	092.50	091.85	108.09
	Mean							
	106.41 ± 1.9	**101.3 ± 2.16**	**98.7 ± 2.6**	**94.5 ± 2.3**	**92.74 ± 1.4**	**92.0 ± 1.3**	**92.4 ± 0.5**	**106.5 ± 1.7**

Table IB: Change in potential (mV) of Ruthenium IV oxide before/after CV treatment. The potential alteration was entirely different in before/after CV treatment. It verifies ruthenium IV oxide was less sensitive towards pH change.

pH	**Potential before CV (mV)**	**Potential after CV (mV)**
6.4	-7.68	40.05
5.6	-7.4	46.36
4.7	-5.04	45.11
3.6	-1.22	60.76
1.9	12.61	94.31
1.8	21.57	60.24

Table IC: Three day data collection to obtain long term response of probes

i) Day 0, ii) Day 1, iii) Day 2

Number of days	*MRS+ cells pH*	*glass (mV)*	*Indicated Glass+glass Ag/AgCl (mV)*	*∆E/mVglassAg/AgCl vs glass pH sensor*	*Indicated pH Glass+glass Ag/AgCl*	*Calculated pH*	*Indicated Glas+ Antimony (mV)*	*∆E antimony/mV vs glass pH sensor*	*Indicated Glass+Antimony (pH)*
D0	7.22	5.1	24.3	24.24	6.604	6.52	-342.6	-342.66	12.8
	7.22		24.1	24.04	6.604	6.52	-340.7	-340.76	12.80
	7.22		24.6	24.54	6.604	6.52	-341.2	-341.26	12.80
	5.514	105.5	23.3	23.25	6.618	6.53	-269.4	-269.46	11.55
	5.514		21.6	21.5	6.616	6.53	-269.3	-269.36	11.55
	5.514		22.1	22.05	6.617	6.53	-269.5	-269.56	11.55
	4.65	190.5	25.6	25.56	6.573	4.60	-187.2	-187.259	10.16
	4.65		26.4	26.36	6.561	4.60	-187.3	-187.359	0.16

Number of days	*MRS+ cells pH*	*glass (mV)*	*Indicated Glass+glass Ag/AgCl (mV)*	*ΔE/mVglassAg/AgCl vs glass pH sensor*	*Indicated pH Glass+glass Ag/AgCl*	*Calculated pH*	*Indicated Glas+ Antimony (mV)*	*ΔE antimony/mV vs glass pH sensor*	*Indicated Glass+Antimony (pH)*
D1	7.022		18.4	25.1	25.04	6.58	6.97	-330.5	-330.56
	7.022		24.3	24.24			-330.4	-330.46	12.808
	7.022		22.8	22.74	6.604	6.97	-330.6	-330.66	12.806
	5.523	106.3	23	22.95	6.581	5.48	-267.7	-267.76	11.559
	5.523		22.7	22.65	6.601	5.48	-268.1	-268.16	11.558
	5.523		24.6	24.55	6.604	5.48	-268	-268.06	11.555
	4.053	191.2	24.9	24.86	6.567	4.01	-186.8	-186.85	10.166
	4.053		26.3	26.26	6.568	4.01	-186.4	-186.45	10.167
	4.053		25.3	25.26	6.57	4.01		-0.059	10.169
D2	7.029		27.9	24.6	24.54	6.57	6.98	-325.3	-325.36
	5.576		108.6	22.1	22.05	6.62	5.53	-265.6	-265.66
	4.072		192.9	27.8	27.76	6.53	4.02	-185.4	-185.45
	4.072	192.9	27.8	27.76	6.534	4.029	-185.4	-185.45	

Appendix II

Table II A: t-test result of 0.15 M NaCl (straw). Data was collected from Table 4.4.

0.15 M NaCl (straw)	*Eutectic calculated*	*Eutectic Literature*
Mean	-19.5	-22
Variance	5.25	0
Observations	3	3
Hypothesized Mean Difference	0	
df	2	
t Stat	1.889822365	
P(T<=t) one-tail	0.099679615	
t Critical one-tail	2.91998558	
P(T<=t) two-tail	0.199359231	
t Critical two-tail	4.30265273	

Table II B: t-test result of 0.85% NaCl (straw). Data was collected from Table 4.4.

0.85% NaCl (straw)	*Eutectic calculated*	*Eutectic Literature*
Mean	-23.1087	-21.5
Variance	88.12257	0
Observations	3	3
Hypothesized Mean Difference	0	
df	2	
t Stat	-0.29681	
P(T<=t) one-tail	0.397298	
t Critical one-tail	2.919986	
P(T<=t) two-tail	0.794597	
t Critical two-tail	4.302653	

Table II C: t-test result of 0.15 M NaCl (tube). Data was collected from Table 4.5.

0.15 NaCl (tube)	*Eutectic calculated*	*Eutectic Literature*
Mean	-28.5	-22
Variance	2.25	0
Observations	3	3
Hypothesized Mean Difference	0	
df	2	
t Stat	-7.505553499	
P(T<=t) one-tail	0.008646185	
t Critical one-tail	2.91998558	
P(T<=t) two-tail	0.01729237	
t Critical two-tail	4.30265273	

Table II D: t-test result of 0.15M NaCl (tube). Data was collected from Table 4.5.

0.85% NaCl (tube)	*Eutectic calculated*
diff between means	2.03
degrees of freedom (df)	3
denominator	0.557997
t-critical	3.182
t-calculated	3.63801
P (two-tail)	0.765

Appendix III

Table III A: t-test results of glycerol in the absence of NaCl. Tests were performed in cryostraws (see Table 4.6).

Glycerol	*Tg exp*	*Tg Literature*
Mean	-32.5	-41
Variance	12.5	2
Observations	2	2
Hypothesized Mean Difference	0	
df	1	
t Stat	3.156821	
P(T<=t) one-tail	0.097649	
t Critical one-tail	6.313752	
P(T<=t) two-tail	0.195299	
t Critical two-tail	12.7062	

Table III B: t-test results of Me_2SOin the absence of NaCl. Tests were performed in cryostraws (see Table 4.6).

Me_2SO	*Tg exp*	*Tg Literature*
Mean	-24.5	-93.5
Variance	0.5	4.5
Observations	2	2
Hypothesized Mean Difference	0	
df	1	
t Stat	43.63943	
P(T<=t) one-tail	0.007293	
t Critical one-tail	6.313752	
P(T<=t) two-tail	0.014586	
t Critical two-tail	12.7062	

Table III C: t-test results of sucrose in the absence of NaCl. Tests were performed in cryostraws (see Table 4.6).

Sucrose	*Tg exp*	*Tg Literature*
Mean	-22	-42.5
Variance	2	60.5
Observations	2	2
Hypothesized Mean Difference	0	
df	1	
t Stat	3.667151	
P(T<=t) one-tail	0.08474	
t Critical one-tail	6.313752	
P(T<=t) two-tail	0.16948	
t Critical two-tail	12.7062	

Table III D: t-test results of glycerol in the presence of NaCl. Tests were performed in cryostraws (see Table 4.7).

Glycerol	*Tg exp*	*Tg Literature*
Mean	-51	62.7
Variance	18	0
Observations	2	2
Hypothesized Mean Difference	0	
df	1	
t Stat	-37.9	
P(T<=t) one-tail	0.008397	
t Critical one-tail	6.313752	
P(T<=t) two-tail	0.016793	
t Critical two-tail	12.7062	

Table III E: t-test results of sucrose in the presence of NaCl. Tests were performed in cryostraws (see Table 4.7).

Sucrose	*Tg exp*	*Tg Literature*
Mean	-35.15	-42.5
Variance	6.845	60.5
Observations	2	2
Hypothesized Mean Difference	0	
df	1	
s	1.26663	
P(T<=t) one-tail	0.212728	
t Critical one-tail	6.313752	
P(T<=t) two-tail	0.425455	
t Critical two-tail	12.7062	

Table III F: t-test results of Me_2SO in the presence of NaCl. Tests were performed in cryostraws (see Table 4.7).

Me_2SO	*Tg exp*	*Tg Literature*
Mean	-63.5	-93.5
Variance	12.5	4.5
Observations	2	2
Hypothesized Mean Difference	0	
df	2	
t Stat	10.28992	
P(T<=t) one-tail	0.004656	
t Critical one-tail	2.919986	
P(T<=t) two-tail	0.009313	
t Critical two-tail	4.302653	

Table III G: t-test results of glycerol in the absence of NaCl. Tests were performed in cryotubes (see Table 4.8).

Glycerol	*Tg exp*	*Tg Literature*
Mean	-35.5	-41
Variance	12.5	2
Observations	2	2
Hypothesized Mean Difference	0	
df	1	
t Stat	2.042649	
P(T<=t) one-tail	0.144914	
t Critical one-tail	6.313752	
P(T<=t) two-tail	0.289828	
t Critical two-tail	12.7062	

Table III H: t-test results of sucrose in the absence of NaCl. Tests were performed in cryotubes (see Table 4.8).

Sucrose	*Tg exp*	*Tg Literature*
Mean	-19	-42.5
Variance	2	60.5
Observations	2	2
Hypothesized Mean Difference	0	
df	1	
t Stat	4.203808	
P(T<=t) one-tail	0.074338	
t Critical one-tail	6.313752	
P(T<=t) two-tail	0.148676	
t Critical two-tail	12.7062	

Table III I: t-test results of Me_2SO in the absence of NaCl. Tests were performed in cryotubes (see Table 4.8).

Me_2SO	*Tg exp*	*Tg Literature*
Mean	-48.5	-93.5
Variance	4.5	4.5
Observations	2	2
Hypothesized Mean Difference	0	
df	2	
t Stat	21.2132	
P(T<=t) one-tail	0.001107	
t Critical one-tail	2.919986	
P(T<=t) two-tail	0.002215	
t Critical two-tail	4.302653	

Table III J: t-test results of glycerol in the presence of NaCl. Tests were performed in cryotubes (see Table 4.9).

Glycerol	*Tg exp*	*Tg Literature*
Mean	-56.5	-62.7
Variance	12.5	0
Observations	2	2
Hypothesized Mean Difference	0	
df	1	
t Stat	2.48	
P(T<=t) one-tail	0.12200313	
t Critical one-tail	6.31375151	
P(T<=t) two-tail	0.24400627	
t Critical two-tail	12.7062047	

Table III K: t-test results of sucrose in the presence of NaCl. Tests were performed in cryotubes (see Table 4.9).

Sucrose	*Tg exp*	*Tg Literature*
Mean	-35.45	-42.5
Variance	6.125	60.5
Observations	2	2
Hypothesized Mean Difference	0	
df	1	
t Stat	1.221478	
P(T<=t) one-tail	0.21837	
t Critical one-tail	6.313752	
P(T<=t) two-tail	0.436739	
t Critical two-tail	12.7062	

Table III L: t-test results of Me_2SO in the presence of NaCl. Tests were performed in cryotubes (see Table 4.9).

Me_2SO	*Tg exp*	*Tg Literature*
Mean	-76.5	-93.5
Variance	12.5	4.5
Observations	2	2
Hypothesized Mean Difference	0	
df	2	
t Stat	5.830952	
P(T<=t) one-tail	0.014087	
t Critical one-tail	2.919986	
P(T<=t) two-tail	0.028175	
t Critical two-tail	4.302653	

Appendix IV

Table VV A: t-test results of Protocol a (see Table 4.11).

Protocol a	*Tg Experimental*	*Tg Literature*
Mean	-66.35	-62.7
Variance	276.125	7.57E-29
Observations	2	3
Hypothesized Mean Difference	0	
df	1	
t Stat	-0.310638298	
P(T<=t) one-tail	0.404128914	
t Critical one-tail	6.313751515	
P(T<=t) two-tail	0.808257827	
t Critical two-tail	12.70620474	

Table IV B: t-test results of Protocol b (see Table 4.11).

Protocol b	*Tg Experimental*	*Tg Literature*
Mean	-61.7	-62.7
Variance	264.5	7.57306E-29
Observations	2	3
Hypothesized Mean Difference	0	
df	1	
t Stat	0.086956522	
P(T<=t) one-tail	0.472390329	
t Critical one-tail	6.313751515	
P(T<=t) two-tail	0.944780659	
t Critical two-tail	12.70620474	

Table IV C: t-test results of Protocol c (see Table 4.11).

Protocol c	*Tg Experimental*	*Tg Literature value*
Mean	-55.65	-62.7
Variance	3.645	7.57306E-29
Observations	2	3
Hypothesized Mean Difference	0	
df	1	
t Stat	5.22222222	
P(T<=t) one-tail	0.06022392	
t Critical one-tail	6.31375151	
P(T<=t) two-tail	0.12044784	
t Critical two-tail	12.7062047	

Publication

Jahangir, J., Andres, R., Morris, J., Haggett, B., & Rawson, D. M. (2013). 128 **Development of a low cost sensor system for determination of glass transition temperatures during cooling and warming**. *Cryobiology*, *67*(3).